Optimization of functional electrical stimulation (FES) parameters for FES cycling

Petar Kajganic

THESE

en vue de l'obtention du grade de Docteur, délivré par

l'ECOLE NORMALE SUPERIEURE DE LYON

Ecole Doctorale N° 52
Physique et Astrophysique de Lyon (PHAST)

Discipline : Physique

Soutenue publiquement le 21/09/2023, par:

Petar KAJGANIĆ

Optimization of functional electrical stimulation (FES) parameters for FES cycling

Optimisation des paramètres de stimulation électrique fonctionnelle (SEF) pour le cyclisme SEF

Devant le jury composé de :

AZEVEDO COSTE, Christine	DR	Université de Montpellier	Rapporteure
HUNT, Kenneth	Prof.	Bern University of Applied Sciences	Rapporteur
GIRAUX, Pascal	Prof.	Université Jean Monnet	Examinateur
METANI, Amine	IR	ENS de Lyon	Examinateur
BERGERON, Vance	DR	ENS de Lyon	Directeur de thèse

Acknowledgements

First and foremost, I need to express my deepest gratitude to my thesis director Vance Bergeron for his professional and emotional support. Vance showed me how to be a researcher, how to write and present, how to work on multiple projects, study different fields, etc. He has always provided honest opinions of my work and was incredibly generous with his time in helping me improve – especially showcased in the present manuscript. Working together, what I have enjoyed the most is his infectious enthusiasm when discussing new ideas and forming future projects and studies during our countless brainstorming sessions. Furthermore, during the toughest times, he and his family cared for me and invited me into their home for which I will always be grateful. A big thank you to Danièle, Marine and Théo!

I am very grateful to my supervisor Dr. Amine Metani who has helped me settle in the lab and France. Amine co-wrote my first journal paper and taught me many things throughout the years. One of the quotes that I will never forget is: “It doesn’t *matter* what we think”. I had a lot of fun working together!

I would also like to thank Dr. Efe Anil Aksöz who was a joy to work with. Despite only briefly working together, I have countless memories. Things that I learned from Anil will impact every study I design. Hopefully, we will have an opportunity to work together again.

I want to thank my fellow Ph.D. student Ehsan Jafari not only for his help with developing protocols, setting up studies, working with subjects, processing the data and discussing the results but also for his company and friendly chats.

A special thanks goes to Prof. Dejan Popović without whom I most certainly wouldn’t be where I am. He believed in me, encouraged me to pursue an academic career and opened a door into the world of electrical stimulation. I would also like to express my gratitude to Dr. Lana Popović-Maneski with whom I went from building stimulators to setting up clinical studies in, what felt like, a blink of an eye. Working together, I took my first FES steps (both figuratively and literally), during the thesis her advice was always priceless, and I am sure we will continue to work together in the years to come.

I have been incredibly lucky, as all of the people mentioned above, I don’t consider directors, supervisors or colleagues but good friends.

Thank you to the whole physics lab and the students that helped us carry out the studies. Thank you to the staff at the ANTs association who have helped us recruit subjects for our studies and, of course, a big thank you to the subjects who graciously gave us their time and trust. A special thank you to Julien Jouffroy for his patience, advice and chess lessons.

Outside of the lab, I had many friends who kept me happy. I would like to thank my first and dearest friends from Lyon: Vera and Mila with her family for helping me adjust to life in France. Back home, many thanks to Sofija, Tamara and Adam for their love and support. A special thanks to Adam for enriching my work with his illustrations. Thank you to Luka, Milos and Jovana for our long talks and short trips. I would also like to thank my friends Aleksa, Vladimir, Andrijana, Ruzica and Aleksandra whom I miss very much.

There are no words to express what I feel for my parents Biljana and Velibor Kajganić who have always given me unconditional and unwavering love and support. I am who I am because of them and this thesis is theirs as much as mine. I am also eternally grateful to my grandparents for always believing in me.

Thank you all,

Petar

Contents

Abstract – Executive summary

By applying surface electrodes on the skin in specific areas that cover motor neurons, or by using implanted electrodes over individual muscles, we can induce contractions of the skeletal muscles located within the electric field that is generated when the electrodes are activated with an electrical pulse. By synchronizing these muscle contractions, functional movements such as cycling, rowing and walking can be achieved. This technique is termed functional electrical stimulation (**FES**).

FES is a useful rehabilitation tool as it can reduce the secondary medical complications that stem from muscle paralysis after having a spinal cord injury (SCI). The most commonly used form of FES is FES cycling which is achieved by stimulating lower-limb muscle groups, notably the quadriceps, hamstrings and gluteal muscle groups. Some of the benefits of the prolonged use of FES cycling are: an increase in muscle mass, bone density and cardiovascular fitness, better peripheral blood circulation, improved metabolic response and reduced possibility of pressure sores. Despite the benefits, because of the high price and certain inherent limitations of the technology, FES cycling and FES in general, are not commonly used. The most prevalent limitations encountered when using FES cycling are the rapid onset of fatigue and low power output from the stimulated muscles. This leads to limiting the exercise time and level of cardiovascular intensity. These factors, coupled with the high price of these devices have led to a scarcity of FES cycling equipment and further difficulty for users to regularly exercise enough to acquire significant health benefits.

The overall aim of this thesis is to ***develop and assess novel electrical stimulation strategies*** to address the limitations of FES cycling in people with SCI, i.e., to ***postpone the onset of muscle fatigue, augment the power produced by the paralyzed muscles*** and offer options for ***universal home-use low-cost FES cycling equipment***.

For assessing the efficacy of electrical stimulation strategies, a novel instrumented cycling ergometer platform (ICEP) was developed. This platform consists of highly sensitive force-torque measuring pedals, a precise magnetic ring crank encoder and a motorized controller system that assists the cyclist by maintaining a constant and smooth cycling cadence. Different electrical stimulation parameters and strategies are provided by an 8-channel electrical stimulator synchronized with the various components of the platform. The capabilities of the platform were showcased in an experimental study that allowed us to quantitatively evaluate new electrostimulation strategies that, maximize the cycling performance in SCI subjects by meticulously analyzing the forces produced by their stimulated quadriceps muscles while simultaneously limiting the muscle fatigue induced by stimulation.

Our preliminary studies used isometric force conditions of lower-limb paralyzed individuals, to study *spatially distributed sequential stimulation* (SDSS). These tests revealed reduced muscle fatigue and augmentation of the output power compared to the state-of-the-art *single electrode stimulation* (SES). The results concur with similar conclusions that investigated SDSS for performing a *dynamic* knee extension task. We revealed that the electrical stimulation intensity has an influence on the comparative performance when using SDSS or SES configurations.

Experimental studies comparing the fatigue-reducing ability of SDSS at high and moderate stimulation intensities in subjects with lower-limb motor-complete SCI were designed and conducted. In four sessions, SDSS and SES were used to produce isometric contractions in paralyzed quadriceps muscles of seven subjects with an SCI while continuously recording the force produced by the stimulated muscle group. The fatigue-reducing ability and force produced by quadriceps muscles stimulated with SDSS and SES were compared to evaluate the effectiveness of SDSS at different intensities. This study showed that, when applied to the quadricep muscle group, moderate-intensity SDSS is significantly more effective than high-intensity SDSS. The results confirmed the hypothesis that at high intensities, more muscle fibers are activated by multiple SDSS electrodes reducing their rest time and thus diminishing the benefits of SDSS.

In this thesis, we also extended our understanding of using SDSS to stimulate muscles for FES applications by assessing the efficacy of SDSS versus SES when performing FES cycling. Similar to the isometric investigations, we determined the effect that SDSS stimulation has on muscle fatigue and the power produced when muscles are stimulated to perform a *dynamic repetitive* cycling task.

In a case series conducted on the ICEP, the muscle fatigue and power produced while performing FES cycling using SDSS versus SES were compared. Four subjects without lower-limb motor function participated in two multiday sessions. Each session consisted of both SES and SDSS stimulation, the order of which was chosen at random for the first session and in the opposite order for the second session. Based on the conclusions of the previous isometric study, quadriceps muscle groups were stimulated using moderate stimulation parameters to optimize any effects of SDSS. The power output during the first and last 30 seconds of stimulation showed better fatigue resistance of SDSS compared to SES in three of the subjects while all four subjects produced greater mean power with SDSS than SES. The results of this case series showed that SDSS is more effective than SES when performing a cycling task, however, more subjects are needed for statistical significance.

Finally, the possibility of using a stretch sensor (a sensor that changes conductive properties when stretched) instead of the crank encoder for controlling FES cycling was examined. This study was motivated by the desire to develop lower-cost, more flexible FES cycling equipment. A prototype of a knee-angle-based FES cycling system was developed and tested. Using custom-made stimulator firmware, the output of the stretch sensor, placed over the knee, was acquired and used to control the stimulation pattern. One subject with a lower-limb motor-complete SCI used the system while cycling on the ICEP with a constant cycling cadence. The output of the stretch sensor was similar (RMSE < 3º) to the output of the high-cost sensitive magnetic crank encoder. Forces produced by the stimulated quadriceps and hamstrings muscles showed that muscle contraction timing was identical for each rotation of the crank cycle. The results of the study serve as a proof of concept for using a stretch sensor for controlling FES cycling, thus allowing for the development of simple and cheaper FES cycling equipment.

Stimulation strategies studied in this work will improve future FES cycling by optimizing the cyclist's output power while postponing the onset of muscle fatigue. Furthermore, the ICEP developed to study FES cycling will help contribute to discovering novel stimulation strategies that will further push the limitations of FES technologies for both leg and arm cycling. Contributions made in this work will hopefully make FES cycling a more effective rehabilitation tool available to a larger population.

Résumé

En appliquant des électrodes sur la surface de la peau ou en utilisant des électrodes implantées sur des muscles individuels, nous pouvons induire des contractions des muscles squelettiques situés dans le champ électrique qui est généré lorsque les électrodes sont activées. En synchronisant les contractions musculaires, il est possible de réaliser des mouvements fonctionnels tels que le cyclisme, l'aviron et la marche. Cette technique est appelée stimulation électrique fonctionnelle (SEF).

La stimulation électrique fonctionnelle est un outil de rééducation utile car elle peut réduire les complications médicales secondaires qui découlent de la paralysie musculaire après une lésion médullaire (SCI). La forme de SEF la plus utilisée est le cyclisme SEF, qui est réalisé en stimulant les groupes musculaires des membres inférieurs, notamment les quadriceps, les tendons du jarret et les groupes musculaires fessiers. Certains avantages de l'utilisation prolongée du cyclisme SEF sont: une augmentation de la masse musculaire, de la densité osseuse et de la capacité cardiovasculaire, une meilleure circulation sanguine périphérique, une amélioration de la réponse métabolique et une réduction du risque d'escarres. Malgré ses avantages, le cyclisme SEF et le SEF en général ne sont pas couramment utilisés en raison de son prix élevé et de certaines limitations inhérentes à la technologie. Les limitations les plus courantes rencontrées lors de l'utilisation du cyclisme SEF sont l'apparition rapide de la fatigue et la faible puissance de sortie des muscles stimulés. Cela conduit à limiter la durée de l'exercice et le niveau d'intensité cardiovasculaire. Ces facteurs, associés au prix élevé, entraînent une pénurie d'équipements de cyclisme SEF et une difficulté supplémentaire pour les utilisateurs à s'exercer régulièrement et suffisamment pour en tirer des avantages significatifs.

L'objectif global de cette thèse est de développer et d'évaluer de nouvelles stratégies de stimulation électrique afin de répondre aux limites du cyclisme SEF chez les personnes atteintes de lésions médullaires, c'est-à-dire de retarder l'apparition de la fatigue musculaire et d'augmenter la puissance produite par les muscles paralysés. En outre, une nouvelle méthode de contrôle pour le cyclisme SEF basée sur le genou est proposée afin de rendre l'équipement de cyclisme SEF plus accessible et moins coûteux.

Afin de pouvoir évaluer l'efficacité des stratégies de stimulation électrique, une nouvelle plateforme de vélo ergomètre instrumenté (ICEP) a été mise au point. La plateforme se compose de pédales mesurant la force-couple, d'un encodeur à manivelle à anneau magnétique et d'un système d'actionneur motorisé capable d'aider le cycliste à maintenir une cadence de pédalage constante. Différentes stratégies de stimulation sont réalisées par un stimulateur à 8 canaux synchronisé avec la plateforme. Les capacités de la plateforme ont été démontrées dans un exemple déterminant les schémas de stimulation nécessaires pour reproduire le mouvement cycliste chez un sujet atteint d'une lésion médullaire en analysant les forces produites lors de la stimulation du groupe musculaire des quadriceps.

Dans les études isométriques, il a été démontré que la stimulation séquentielle répartie dans l'espace (SDSS) réduisait la fatigue musculaire et augmentait la puissance de sortie par rapport à la configuration la plus moderne à électrode unique (SES). Une conclusion similaire a été obtenue dans les études utilisant la SDSS pour effectuer la tâche d'extension dynamique du genou. Dans cette thèse, l'efficacité de la SDSS par rapport à la SES lors de la pratique du cyclisme SEF a été évaluée en deux étapes : 1) en déterminant l'influence des paramètres de

stimulation sur l'efficacité de la SDSS 2) en comparant la fatigue musculaire et la puissance produite par les muscles quadriceps paralysés stimulés avec la SDSS par rapport à la SES lors de la réalisation d'une activité de cyclisme fonctionnel.

Une étude expérimentale a été menée pour comparer la capacité de réduction de la fatigue de la SDSS à des intensités élevées et modérées chez des sujets souffrant d'une lésion médullaire complète des membres inférieurs. En quatre sessions, la SDSS et la SES ont été utilisées pour produire des contractions isométriques dans les muscles quadriceps paralysés de sept sujets atteints d'une lésion médullaire, tout en enregistrant en continu la force produite par le groupe musculaire stimulé. La capacité de réduction de la fatigue et la force produite avec les SDSS et SES ont été comparées pour évaluer l'efficacité de la SDSS à une intensité choisie. Cette étude a montré que, lorsqu'elle est appliquée au groupe musculaire du quadriceps, la SDSS d'intensité modérée est significativement plus efficace que la SDSS d'intensité élevée. Les résultats ont confirmé l'hypothèse selon laquelle, à des intensités élevées, davantage de fibres musculaires sont activées par plusieurs électrodes SDSS, ce qui réduit leur temps de repos et diminue donc les avantages de la SDSS.

Nous avons également réalisé une étude de cas sur la plateforme de vélo ergomètre instrumenté afin de comparer la puissance et la fatigue produites lors de la pratique du cyclisme SEF en utilisant la SDSS par rapport à la SES. Trois sujets atteints d'une lésion médullaire complète des membres inférieurs ont participé à deux sessions de plusieurs jours. Chaque session consistait en une stimulation SES et une SDSS, dont l'ordre était choisi au hasard pour la première session et l'ordre inverse pour la deuxième session. Sur la base des conclusions de l'étude isométrique précédente, les groupes de muscles quadriceps ont été stimulés en utilisant des paramètres de stimulation modérés. Pour deux sujets, la puissance de sortie pendant les 30 premières et 30 dernières secondes de stimulation a montré une meilleure résistance à la fatigue dans le cas de la SDSS par rapport à la SES, tandis que tous les trois sujets ont produit une puissance moyenne plus importante avec la SDSS qu'avec la SES. Les résultats de l'étude de cas ont montré que la SDSS est plus efficace que la SES lors de la réalisation d'une activité de cyclisme, mais un plus grand nombre de sujets est nécessaire pour obtenir une importance statistique.

Dans une autre étude, la possibilité d'utiliser un capteur étirable (un capteur qui change de propriétés conductives lorsqu'il est étiré) à la place de l'encodeur à manivelle pour contrôler le cyclisme SEF a été examinée. Un prototype de système de cyclisme SEF basé sur l'angle du genou a été développé et testé. À l'aide d'un firmware personnalisé pour le stimulateur, la sortie du capteur étirable, placé sur le genou, a été acquise et utilisée pour contrôler la stimulation. Un sujet atteint d'une lésion médullaire complète des membres inférieurs a utilisé le système en faisant du vélo sur la plateforme de vélo ergomètre instrumenté avec une cadence de pédalage constante. La sortie du capteur étirable (RMSE < 3º) était similaire à la sortie de l'encodeur à manivelle. Les forces produites par les muscles quadriceps et tendons du jarret stimulés ont montré que le timing de la contraction musculaire était identique pour chaque cycle. Les résultats de l'étude peuvent servir de preuve de concept pour l'utilisation d'un capteur étirable pour contrôler le cyclisme SEF, permettant ainsi le développement d'un équipement de cyclisme SEF simple et moins onéreux.

Les stratégies de stimulation étudiées dans ce document permettront d'améliorer le futur cyclisme SEF, c'est-à-dire d'augmenter la puissance de sortie et de retarder l'apparition de la fatigue. Par ailleurs, la plateforme de vélo ergomètre instrumenté développée pour étudier le cyclisme SEF contribuera à la découverte de nouvelles

stratégies de stimulation qui permettront de repousser les limites des technologies SEF. Les contributions apportées dans le cadre de ce travail permettront, nous l'espérons, de faire du cyclisme SEF un outil de rééducation plus efficace, accessible à une population plus large.

List of Figures

List of Tables

1 Introduction

Abstract

In this chapter, fundamental mechanisms of human movement are presented, from the nervous system and neurons to the skeletal muscle contractions. The role of the spinal cord and the impact of spinal cord injury on body functions and quality of life are provided in order to explain the purpose of functional electrical stimulation (FES). FES and FES cycling are presented along with the parameters, benefits and limitations of the technology. Subsequently, the overall objective and the outline of this thesis are provided.

1.1 Nervous system

The nervous system is the most complex body system that monitors and controls the entire body. It consists of the central nervous system (CNS), composed of the brain and the spinal cord, and the peripheral nervous system (PNS) divided into sensory and motor divisions. Sensory divisions carry signals from the sensory receptors, which detect changes in the external or internal environment, to the spinal cord. Signals ascend the spinal cord to the brain which is in charge of processing the received signals and producing responses. Responses travel down the spinal cord, through motor divisions to the effectors (muscles and glands). Responses that are normally not under conscious control travel through autonomic nerves to activate smooth muscles, cardiac muscles and glands. In contrast, skeletal muscles are often consciously controlled through somatic nerves that convey the motor output from the CNS to the skeletal muscles causing voluntary contractions [1].

The functional unit of a nervous system is called a neuron (nerve cell). Neurons are conducting cells with the ability to produce an electrical impulse in response to outside stimuli. They communicate with other cells via synapses - specialized connections that commonly use minute amounts of chemical neurotransmitters to pass the electric signal from the presynaptic neuron to the target cell through the synaptic gap. A typical neuron consists of a cell body (soma), a nucleus, multiple dendrites and a single axon with axon terminals on the end (Figure 1.1). Dendrites are short branches emerging from the cell body that represent the input of a neuron. Dendrites typically branch profusely and extend a few hundred micrometers from the soma. They are equipped with reception sites (synapses) for receiving stimuli from other cells which change the electrical potential of the cell membrane via chemical ions. When the membrane potential reaches a threshold, the cell generates an electrical impulse called an action potential. The axon propagates the action potential from the cell body to the axon terminals from where it continues to another neuron, muscle fiber or gland cell. Axons and dendrites in the central nervous system are typically only about one micrometer thick, while some in the peripheral nervous system are much thicker. The soma is usually about 10–25 micrometers in diameter and often is not much larger than the cell nucleus it contains. The longest axon of a human motor neuron can be over a meter long, reaching from the base of the spine to the toes.

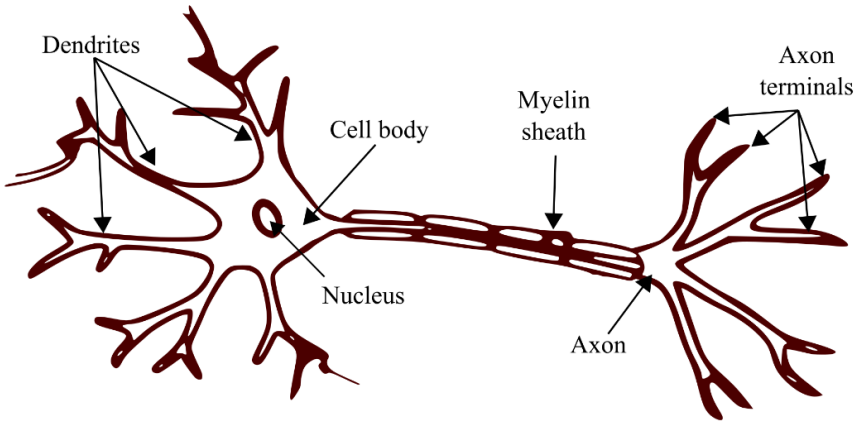

Figure 1.1: Structure of a motor neuron.

The number and the position of dendrites and axons in a neuron can vary based on the neuron's function. Figure 1.1 represents a typical motor neuron that propagates action potential from the CNS toward skeletal muscle fibers. Most neurons in the brain and the spinal cord have the same structure. The areas in the CNS with high numbers of neuron cell bodies are called gray matter while axon dominated regions are called white matter.

The action potential is an electrical signal generated by the excitation of the neuron and occurs when the cell membrane's electrical potential rapidly rises and falls. The action potential is the primary communication means of the nervous system as it is the signal conveyed from the sensory receptors to the brain and the response sent from the brain to muscles and glands. In muscle cells, for example, the action potential is the first step in the chain of events leading to a muscle contraction.

Relative to the extracellular environment, almost all cells are polarized having a permanent membrane potential. However, the membrane potential of nerve and muscle cells varies in time due to the ion channels that open and close in response to specific stimuli. A neuron is surrounded by a high concentration of sodium ions (Na^+) while a high concentration of potassium ions (K^+) is inside the cell. The membrane potential of a resting neuron is around -70 mV and is kept constant by sodium-potassium pumps. The sodium-potassium pump, discovered in 1957 by the Danish scientist Jens Christian Skou, is an enzyme (e.g., protein that acts as a biological catalyst) found in the membrane of the cell.

Stimuli arriving at the dendrites of the neuron temperately change the membrane potential. If the membrane potential reaches the threshold of -55 mV, an action potential is generated in three phases (Figure 1.2). Subthreshold stimuli do not trigger an action potential and the cell eventually returns to the resting potential. When the membrane depolarizes to the threshold, voltage-gated sodium channels located in the cell membrane open. As the cell is negatively charged, in reference to the Na^+-rich extracellular environment, the Na^+ ions rush into the cell causing rapid depolarization of the cell. This is referred to as the Depolarization phase. When the membrane potential reaches a value of around 40 mV, the voltage-gated sodium channels close and voltage-gated potassium channels open causing the outflow of K^+ ions from the now positively charged cell. This is called the Repolarization phase. The outflow of K^+ ions often creates an overshoot lowering the membrane potential under the resting value of -70 mV. This is called the After-hyperpolarization phase. The voltage-gated potassium channels close and the membrane potential is slowly restored to the resting value. During this period, termed the refractory period, a new action potential can only be initiated by strong stimuli as the membrane potential is further from the threshold than when the cell is in the resting state [1], [2].

The action potential travels from the initial trigger zone to the axon terminals without any loss in signal strength. In fact, the action potential does not travel down the axon but instead generates identical action potentials in the surrounding zones. As a consequence of the refractory period of the action potential, new action potentials can only be generated in the direction leading to the axon terminals, away from the trigger zone. Because the signal can propagate without any loss, it is capable of communicating over long distances, for example, from the brain to the muscles.

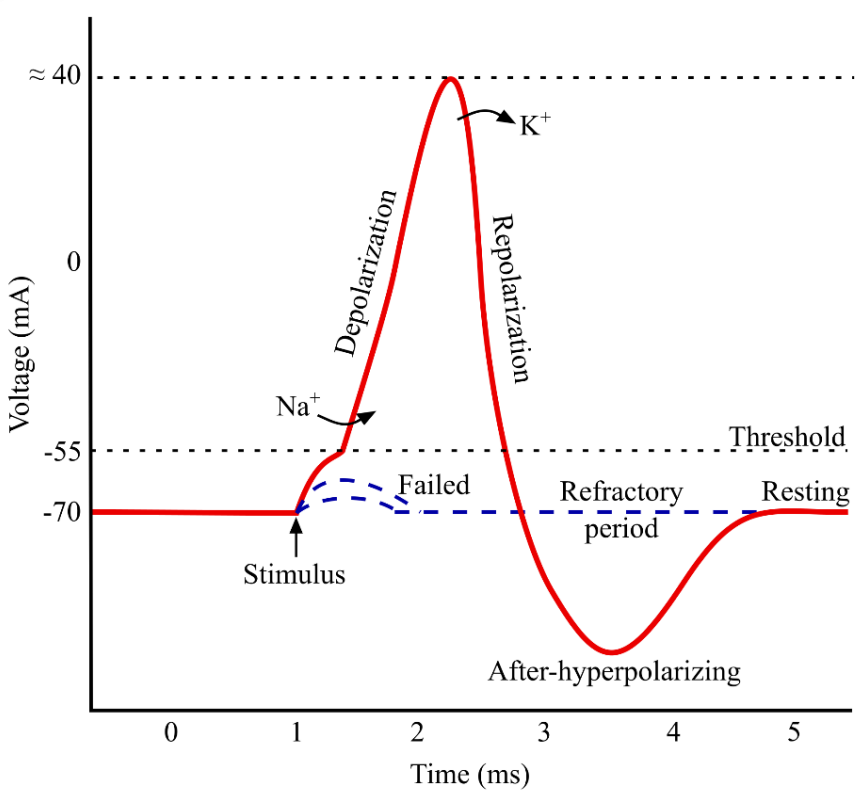

Figure 1.2: Illustration of an action potential (Adapted from [3]).

1.2 Skeletal muscles

The primary function of a muscle is the transformation of chemical energy into mechanical energy. By contacting and relaxing, muscles stabilize the body, produce body movements, generate heat and move substances within the body. There are three types of muscular tissue: skeletal, cardiac and smooth. They differ in their anatomy, position and method of activation. Cardiac and smooth muscles are controlled by the autonomic nervous system while skeletal muscles are often continuously (voluntary) contracted by the somatic nervous system. Henceforth, this work will focus on the structure and function of skeletal muscles.

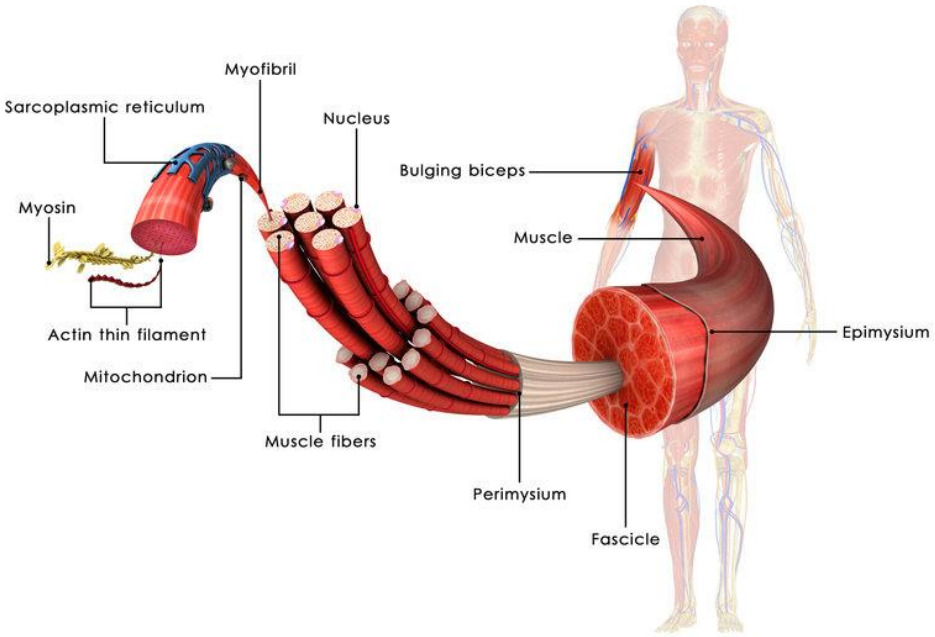

Figure 1.3: Structure of a skeletal muscle (Adapted from [4]).

Each muscle is a separate organ made up of thousands of rope-like structures called muscle fibers (Figure 1.3). Muscle fibers are muscle cells surrounded by blood vessels and nerves. Groups of muscle fibers wrapped in a layer of connective tissue (perimysium) form muscle fiber bundles (fascicles). Each muscle fiber consists of thousands of parallel strands called myofibrils separated by the sarcoplasmic reticulum, an internal membrane storing high concentrations of calcium ions (Ca^{2+}). Myofibrils are contractile fibers made out of actin thin filaments and myosin thick filaments which are the origin of the muscular function. By using adenosine triphosphate (ATP) (note: ATP acts as a portable energy molecule that fuels cellular activities by undergoing a cycle of conversion between ATP and adenosine diphosphate (ADP), releasing and storing energy as needed), myosin heads can bind to the actin filament and slide it resulting in a contraction of the muscle fibers, thus converting ATP (chemical energy) into motion (mechanical energy). However, myosin can bind to actin only in a calcium-rich environment, meaning that Ca^{2+} ions trigger muscle skeletal contractions.

However, myosin can bind to actin only in a calcium-rich environment meaning that skeletal muscle contractions are controlled through the release of Ca^{2+} ions stored in the sarcoplasmic reticulum. The action potential, generated by the CNS and propagated by the motor neurons, travels through the muscle cells to the sarcoplasmic reticulum opening the voltage-gated channels, releasing Ca^{2+} ions. Eventually, the concentration of Ca^{2+} ions rises allowing for the muscle cells to contract [5]. The presented process is called the sliding filament model of the muscle (a video showing the animation of the sliding filament model is available at [6]).

In healthy muscles, multiple muscle fibers are supplied by one motor neuron forming a motor unit. Depending on the size and function, each muscle has a range of motor unit sizes, from 10 fibers in small muscles to several thousands of fibers in quadriceps muscles. When triggered, this motor neuron delivers an action potential to all muscle fibers in the motor unit causing them to simultaneously contract resulting in a muscle contraction [7].

A muscle contraction caused by a single action potential is called a twitch (Figure 1.4). The muscle does not contract immediately after the arrival of an action potential. Instead, there is a latent period during which the concentration of calcium ions is raised. During the contraction period, the Ca^{2+} ions and ATP are used to produce increased muscle tension. After the Ca^{2+} ions are expended, the muscle starts to relax causing the tension to drop.

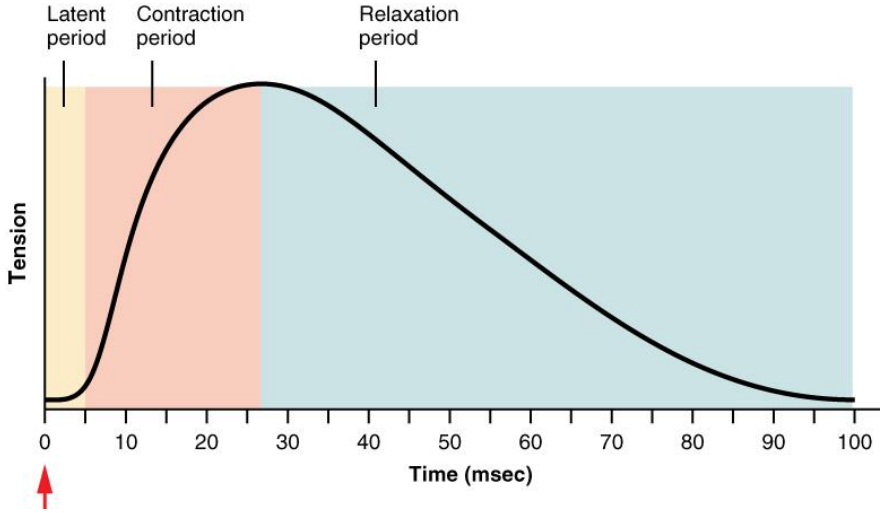

Figure 1.4: Muscle contraction in response to a single action potential (Adapted from [8]).

However, if an additional action potential arrived at the muscle before the muscle had completely relaxed from the previous contraction, the generated force would increase, surpassing the force created by the initial twitch. This effect is termed summation (Figure 1.5). The force produced by the muscle is controlled by the number of muscle fibers activated and by altering the frequency of action potentials sent to the muscle.

If action potentials are repeatedly sent with an adequate frequency (i.e., before the force from the previous action potential subsides), the force produced by the muscle would reach a maximal level. Such a muscle response

is known as tetanus or tetanic contraction. The level of force is maintained until the muscle fatigue occurs causing a decline in force [9].

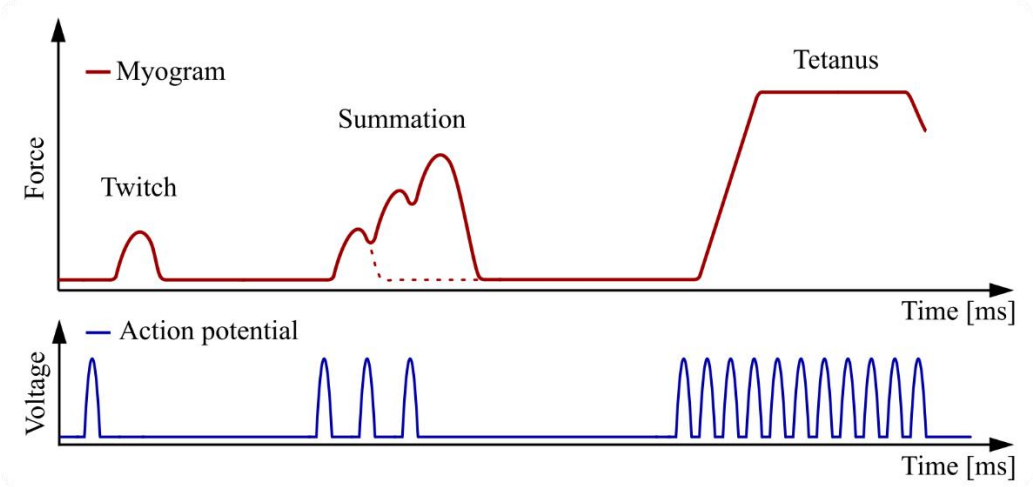

Figure 1.5: Development of the force produced by muscle contractions.

1.3 Spinal cord injury

As described in Sections 1.1 and 1.2, if, for example, someone wants to stand up, the brain sends action potentials down the spinal cord to the PNS from where action potentials are propagated to the leg muscles, releasing calcium ions into the muscle cells allowing the muscles to contract. Conversely, when the foot touches the ground, sensory receptors detect a certain change and send this information through the sensory divisions, up the spinal cord, to the brain where the information is processed.

The spinal cord can be seen as a pathway connecting the brain with the rest of the body. Sensory information is carried through ascending (afferent) nerve tracts located in the posterior region of the spinal cord. Motor output traverses the descending (efferent) nerve tracts running through the anterior region of the spinal cord [10]. These nerve tracks, composed of about 100 million neurons, are protected by the vertebral column. There are 8 cervical (C), 12 thoracic (T), 5 lumbar (L) and 5 sacral (S) spinal cord segments (shown in Figure 1.6) named after the matching vertebrae [11]. Each muscle in the body is typically innervated by nerve fibers originating from several spinal cord segments.

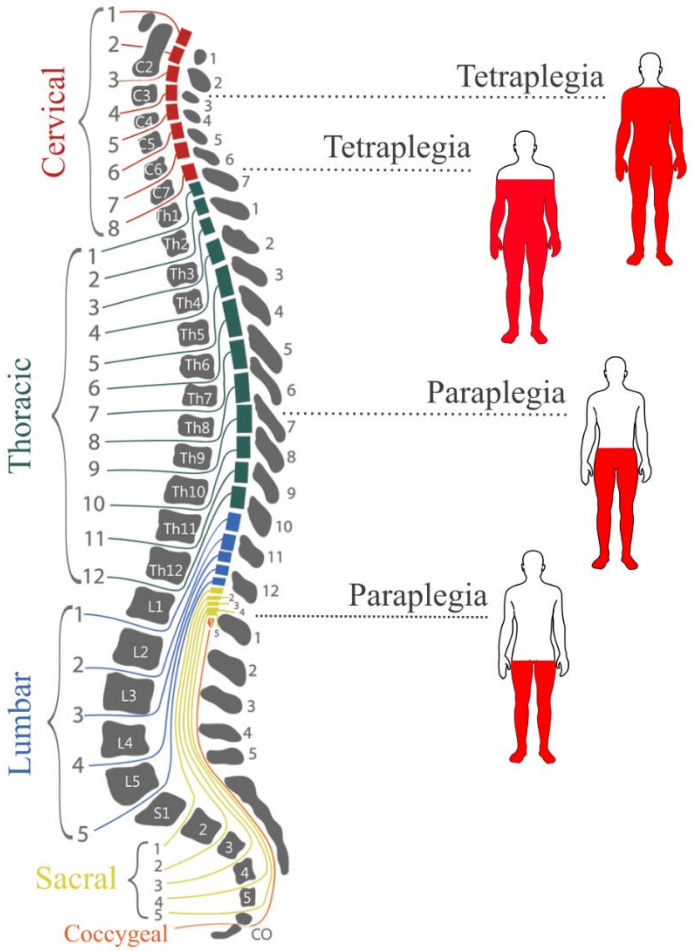

Figure 1.6: Spinal cord segments and spinal cord injury (Adapted from [12]).

An injury of the spinal cord can cause an interruption of the neurological pathways leading to the loss of some or all motor and sensory functions in the regions controlled by the spinal cord segments located below the injury point (displayed in red in Figure 1.6). Spinal cord injury (SCI), depending on the level, may cause paraplegia or tetraplegia. Paraplegia is an impairment or loss of motor and/or sensory function in thoracic, lumbar or sacral segments of the spinal cord affecting lower limbs and the abdomen. Tetraplegia refers to impairment or loss of motor and/or sensory function in the cervical segments of the spinal cord affecting all limbs (Illustrated in Figure 1.6).

Depending on the severity, the SCI can be complete or incomplete. Complete SCI is defined as the loss of all conscious sensory and voluntary motor functions in the lowest sacral segment of the spinal cord (S4-S5). Incomplete SCI means that some information can travel past the injury site, i.e., some sensory and/or motor functions at the injury site are preserved. Most spinal cord injuries are considered incomplete [9]. To classify the severity of SCI, the American Spinal Injury Association (ASIA) Impairment scale is used to categorize the patients with SCI into 5 categories shown in Table 1.1.

Table 1.1. ASIA Impairment scale.

A	Complete	No sensory or motor function is preserved in the sacral segments S4-S5.
B	Incomplete	Sensory but not motor function is preserved below the neurological level including sacral segments S4-S5.
C	Incomplete	Motor function is below the neurological level and more than half key muscles below the neurological level have a muscle grade less than 3.
D	Incomplete	Motor function is below the neurological level and more than half key muscles below the neurological level have a muscle grade greater than 3.
E	None	Normal motor and sensory function.

There are few reliable statistics on the incidence or prevalence of spinal cord injury. However, according to a report of the European Assembly [13], it is estimated that there are at least 330000 people living with some form of SCI (paraplegia or tetraplegia) in the European Union (EU). Every year, around 14 people per million sustain a spinal cord injury (around 11000 people), 40% to 50% of which are a result of a road accident, mostly at a young age (20- to 30-year-olds).

The quality of life for people with tetraplegia or paraplegia can vary depending on a range of factors, including the individual's personal circumstances, available support systems, access to healthcare and rehabilitation services, and societal attitudes towards disability. It is important to note that each person's experience is unique, and generalizations may not capture the full complexity of their lives. However, here are some points that can provide insights into the quality of life considerations for individuals with tetraplegia or paraplegia:

1. Physical Health: Tetraplegia and paraplegia often result in physical challenges, such as mobility limitations, sensory impairments, and secondary health issues. Access to appropriate medical care, assistive devices, and rehabilitation services can significantly impact an individual's physical well-being.
2. Independence and Functional Abilities: Maintaining independence and functional abilities are crucial for the quality of life of individuals with tetraplegia or paraplegia. Assistive technologies, home modifications, and access to personal care assistance can support independence in activities of daily living.
3. Psychological and Emotional Well-being: Adjusting to life with tetraplegia or paraplegia can involve emotional and psychological challenges. Mental health support, counseling, and peer support networks can play a vital role in promoting psychological well-being and a positive outlook on life.
4. Social Support and Inclusion: Social support from family, friends, and the broader community is essential for individuals with tetraplegia or paraplegia. Inclusive environments, accessibility, and opportunities for participation in social, recreational, and employment activities can contribute to a higher quality of life.
5. Accessibility and Inclusion: The level of accessibility in society, including physical infrastructure, transportation, and public spaces, greatly affects the quality of life for people with tetraplegia or paraplegia. Inclusive policies, laws, and societal attitudes towards disability can promote equal opportunities and full participation.

It is crucial to recognize that advancements in medical care, rehabilitation practices, assistive technologies, and societal attitudes towards disability have the potential to improve the quality of life for individuals with tetraplegia or paraplegia. However, challenges and disparities in access to resources and support can still exist, highlighting the need for continued efforts to enhance the quality of life for people with these conditions and this is one of the primary motivations for this thesis.

1.4 Functional Electrical Stimulation (FES)

Spinal cord injury can lead to the paralysis of the muscles controlled by the spinal cord segments located under the injury site. The action potentials from the brain cannot reach the affected muscles but muscles themselves retain the ability to contract (see Section 1.3). Externally generated electrical pulses can substitute the missing action potentials and cause paralyzed muscles to contract. The electrical field generated by the electrical pulses triggers the adjacent motor neurons to produce action potentials that cause the muscle to contact. Functional electrical stimulation (FES) is a method utilizing trains of electrical pulses to induce contractions in paralyzed muscles in order to produce a functional movement.

Electrical pulses are transmitted to the muscles either through implanted or surface electrodes (transcutaneously). Implanted electrodes are surgically inserted in close proximity to the targeted nerve bundles allowing for the isolation of the specific muscles. Stimulation with the implanted electrodes is very efficient but it comes with the inherent risks of infection and the electrode positions cannot be changed after the fact. Self-adhesive surface electrodes are placed on the skin above the motor points of the targeted muscles. As they are further from the nerve bundles, the stimulation with the surface electrodes is less efficient, and the deeper muscles cannot be isolated but it is easy to reposition the electrodes and activate different muscles. In this thesis, we focused on the use of surface electrodes.

Electrical pulses are created by an electrical stimulator. Most modern stimulators generate current-controlled pulses that are defined by their shape, amplitude (mA), pulse width (μs) and frequency (Hz) or inter-pulse interval (ms) (Figure 1.7). Stimulation intensity affects the type of nerve fibers that are stimulated while the pulse width represents the duration of the pulse. The product of the pulse width and amplitude defines the amount of charge delivered to the stimulated tissue. Most pulses have an asymmetrical or a symmetrical bipolar shape (Figure 1.7) with an equal amount of charge delivered and removed from the body ensuring the long-term safety of the stimulated tissues [14]. The stimulation frequency affects the type of achieved muscle contraction, similar to the action potential induced contraction shown in Figure 1.5.

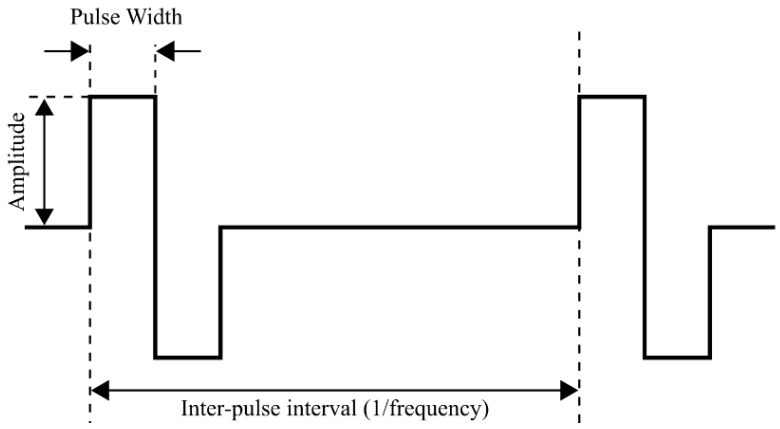

Figure 1.7: Functional electrical stimulation pulse train parameters.

Even though FES is used as a rehabilitation tool for multiple types of motor disabilities such as stroke [15] and multiple sclerosis [16], in this work we focus exclusively on the SCI population. Common applications of FES in rehabilitation are: cycling (see Section 1.5), rowing [17], [18] and grasping [19], [20]. When utilized in the early stages of rehabilitation therapy, FES can increase the quality of life by mitigating the secondary medical complications associated with SCI. The current evidence indicates that regular lower-limb FES exercise improves muscle health (specifically muscle mass and a shift to more fatigue-resistant fiber types), increases aerobic fitness and augments the power produced by the stimulated muscles. An increase in muscle mass may reduce the risk of pressure sores and augment the low resting metabolic rates which typically contribute to obesity [21]. Furthermore, FES exercise has positive psychological effects, especially when performed outdoors. New emerging applications for FES include swimming [22] and novel orthotic devices to help SCI individuals perform activities in daily life (ADL).

1.5 FES Cycling

FES cycling was first used in the 1980s [23], and today, it is one of the most widely utilized applications of FES. Besides the benefits of lower-limb FES exercise listed in Section 1.4, the appeal of FES cycling specifically to the SCI population is that it can be safely performed on stationary bicycles or ergometers while remaining seated in their wheelchairs. As the feet are attached to the pedals using orthoses, the risk of losing balance is minimal. Perhaps the most alluring aspect of FES cycling is the possibility to perform cycling outdoors which has the added benefit of a positive impact on mental health. Outdoor FES cycling is performed in recumbent tricycles fitted with sensors and controls required for the stimulation. These devices typically include an electric motor for assistance to help overcome difficult obstacles and prevent excessive muscle fatigue.

Key muscle groups for FES cycling are quadriceps, hamstrings and gluteal muscles which are made up of sub-muscles that can be activated separately (shown in Table 1.2). However, it is possible to achieve cycling movement by stimulating only quadriceps muscles [24]. The quadriceps muscle group is the most frequently stimulated muscle group when performing FES cycling exercise, and it is the main focus of the present work (along with the quadriceps sub-muscles). That said there exists a potential to stimulate additional muscles such as the grand dorsal (Latissimus dorsi) and tibialis anterior for additional cardiovascular exercise, muscle strengthening, and cycling performance.

Table 1.2. Muscles typically stimulated during FES cycling.

Muscle Group	Muscles	Abb.
Quadriceps	Rectus Femoris	RF
	Vastus Lateralis	VL
	Vastus Medialis	VM
Hamstrings	Biceps Femoris	BF
	Semitendinosus	ST
	Semimembranosus	SM
Gluteal muscles	Gluteus Maximus	GMax
	Gluteus Medius	GMed

In most FES cycling systems, muscle activation timing is based on the crank angle. The crank angle is typically acquired by an encoder sensor placed in the crank of the cycling device. As the legs are secured to the pedals, the crank angle corresponds to the position of the legs. Muscles are activated based on the stimulation pattern which is a set of crank angle intervals defined for when each muscle group should be stimulated, in order to produce a functional cycling movement. However, new methods of controlling the stimulation based on the thigh inclination or knee angle, have recently been developed, as we show in Chapter 5. Many factors must be considered when determining the stimulation pattern including the seating position, cycling cadence, the physiology and condition of the pilot. Determining the optimal stimulation pattern is key to achieving smooth and efficient cycling movement and is discussed in Chapter 2.

1.6 Limitations of FES

Despite the health benefits and quality of life improvement resulting from regular lower-limb FES exercise (Section 1.4), FES cycling, and FES in general, are not widespread. This is a consequence of the unresolved limitations of the technology, mainly low power output produced by the stimulated muscles and rapid onset of muscle fatigue, in addition to the high cost of the stimulation devices.

Low power output can be attributed to the relatively crude control of the muscle activation patterns employed by FES. Volitional cycling is performed by synergistic activation of multiple surface and deep muscles. Muscle contractions are achieved by trains of action potentials with varying frequency. In contrast, electrical stimulation cannot activate deeper muscles, only partial recruitment of surface muscles can be reliably achieved due to poor determination of the location of the different motor points which change as the muscle moves and overlap of the electric fields causing antagonistic muscle contraction. By increasing the stimulation intensity, larger portions of muscles can be recruited but this increases the likelihood of co-activation of antagonistic muscle groups. Usually, stimulation frequency is constant and stimulation patterns are set regardless of the changes in power production level and the cycling cadence. Additionally, autonomic factors such as the lack of sensory feedback, vasomotor control and muscle atrophy stemming from chronic SCI contribute to the low power output and poor efficiency of FES cycling.

Rapid onset of muscle fatigue results in the decline in power produced by the stimulated muscles. Voluntary muscle contractions are achieved by recruiting motor units based on their size, from smaller axons that innervate slow, fatigue-resistant muscle fibers to larger axons innervating fast, easily fatigable muscle fibers [25]. In contrast, electrical stimulation is localized without the ability to select the motor unit type. Motor units found in the electric field generated between the electrodes can all be triggered. However, as the size of an axon defines the axon's activation threshold, larger axons are more likely to be triggered resulting in a faster onset of muscle fatigue (Illustrated in Figure 1.8). Additionally, as the stimulation is localized, the same motor units are repeatedly activated whereas, during voluntary contractions, motor units are randomly activated resulting in the possibility of rest periods for each motor unit.

Another factor contributing to the scarcity of FES is the high price and the complexity of the FES equipment. FES equipment is typically not designed for home use as it requires aid from a medical practitioner to set up the stimulation parameters and locate the motor points for each muscle group. As a consequence of the complexity and the high price, coupled with the technical limitations, FES systems can only be found in some hospitals and rehabilitation centers. This poses a major challenge to the SCI population as it is often difficult for them to access FES equipment, and ideally, exercise should be performed several times a week to obtain optimal results.

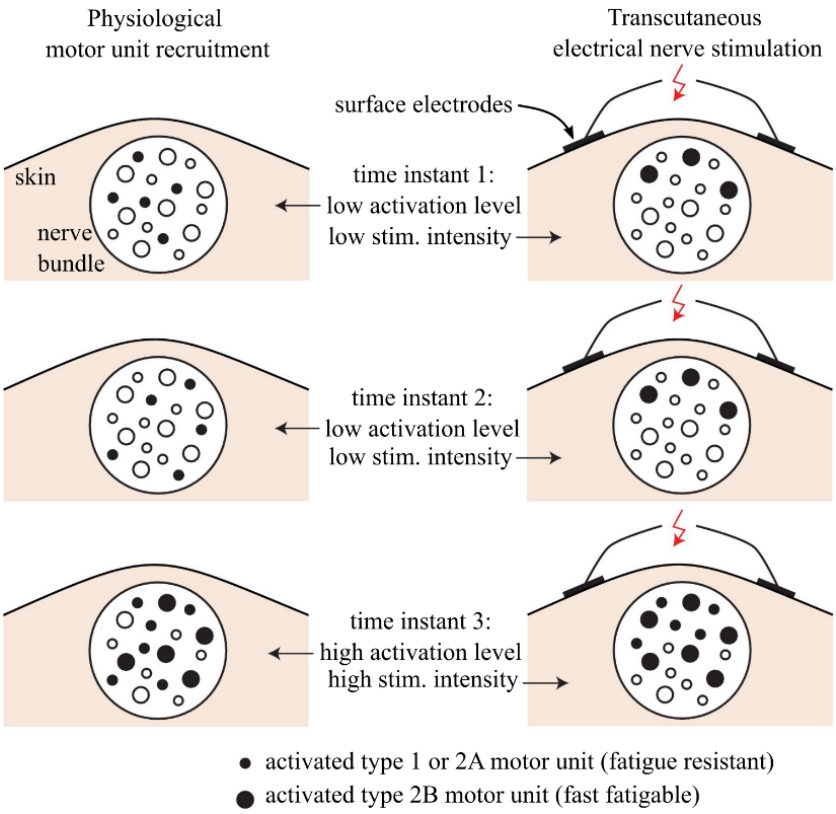

Figure 1.8: Physiological and FES induced motor unit recruitment (Appropriated from [26]).

1.7 Objective of the thesis

The primary aim of the present work is to systematically assess novel electrical stimulation strategies in order to address the limitations of FES cycling in people with spinal cord injury, i.e., to postpone the onset of muscle fatigue and augment the power produced by the paralyzed muscles. An additional goal is to simplify FES cycling systems in order to make them a more affordable and a viable option for home use. Achieving these goals will make FES cycling a more effective rehabilitation tool available to a larger population for clinical, home or outdoor use.

This thesis is separated into three distinct categories:

1. Development of an instrumented cycling ergometer;

   This is a laboratory tool that allows us to measure quantitatively the force exerted on the pedals in every direction (x-y-z) and correlate these forces to the different muscles that are stimulated. The device is arranged to accept different types of tricycles and wheelchairs, moreover, it can be adjusted for people with different morphologies and outfitted to be used for hand cycling as well as lower limb cycling.

2. Assessment of novel FES cycling strategies;

   Here the objective is to address the two major limitations of FES cycling, muscle fatigue and power produced during lower limb cycling. The muscle fatigue studies are centered around different electrical stimulation configurations that include electrode placement, size and stimulation sequencing.

3. Development of a simplified FES cycling system.

   In an effort to make FES cycling more available to a wide of range of individuals, we have designed a system that is cost affordable, limited in size, easy to use and constructed with components that can be obtained from many different manufacturers to tailor the device to the user's needs.

1.8 Outline of the thesis

Following this introduction, the present work is structured into the following chapters:

Chapter 2 presents an instrumented cycling ergometer platform developed for the assessment of the efficacy of novel electrical stimulation strategies.

- Kajganic, P.; Bergeron, V.; Metani, A., ICEP: An Instrumented Cycling Ergometer Platform for the Assessment of Advanced FES Strategies. Sensors 2023, 23, 3522. https://doi.org/10.3390/s23073522

Chapter 3 reports the findings of the study comparing the fatigue-reducing ability of high-intensity SDSS versus moderate-intensity SDSS in subjects with SCI performing *isometric contractions* of the quadriceps muscle group.

- Jafari, E.; Kajganic, P.; Popović-Maneski, L.; Mollà Casanova, S.; Metani, A.; Bergeron, V., Efficacy of High versus Moderate-Intensity SDSS in Subjects with Spinal Cord Injury – an Isometric study, *In preparation.*

Chapter 4 reports the results of the case series assessing the efficacy of SDSS versus SES applied to the paralyzed quadriceps muscles of four subjects while performing a *functional cycling task.*

- Kajganic, P.; Jafari, E.; Popović-Maneski, L.; Metani, A.; Bergeron, V., SDSS Applied to the Paralyzed Quadriceps Muscles while Performing Motor-assisted FES Cycling – a Case series, *In preparation.*

Chapter 5 presents a prototype of a knee-angle-based FES cycling system using a stretch sensor. The purpose of the prototype was to serve as proof-of-concept for the development of simple and cheaper FES cycling equipment.

- Kajganic, P.; Bergeron, M.; Bergeron, V., Knee-angle-based FES cycling control, *In preparation.*

Chapter 6 provides a summary and a discussion of the work presented in this thesis and the avenues that can be further explored in order to expand on the present work.

2 An Instrumented Cycling Ergometer Platform for the Assessment of Advanced FES Strategies

Abstract

The aim of the present work was to develop a novel instrumented cycling ergometer platform designed to assess the efficacy of electrical stimulation strategies. The capabilities of the platform are showcased in an example determining the adequate stimulation patterns for reproducing a cycling movement of the paralyzed legs of a spinal cord injury (SCI) subject. Two procedures have been followed to determine the stimulation patterns: (1) using the EMG recordings of the able-bodied subject; (2) using the recordings of the forces produced by the SCI subject's stimulated muscles. The stimulation pattern derived from the SCI subject's force output was found to produce 14% more power than the EMG-derived stimulation pattern. The cycling platform proved useful for determining and assessing stimulation patterns, and it will be used to further investigate advanced stimulation strategies.

2.1 Introduction

Lower-limb cycling devices are among the most globally available human-powered mechanical devices and are used for locomotor, sport or leisure activities. They come in numerous designs (bicycles, tricycles, recumbent bikes, etc.) – the most important variations being the number of riders, their position on the device (i.e., upright or reclined) and the number of wheels, depending on the specific functional needs [27], [28].

As a result, cycling is one of the most widely used forms of exercise to increase cardiovascular health and build lower-limb muscle strength. For these reasons, this type of activity is ideal for individuals with lower-limb deficiencies, such as paralysis after a spinal cord injury (SCI), stroke [29] or multiple sclerosis [30], [31]. When these conditions are present, the muscles may not respond fully to voluntary commands but can be activated using electrical stimulation. When electrical stimulation is used for functional outcomes, such as cycling, it is referred to as functional electrical stimulation (FES). FES uses weak electrical fields to trigger action potentials, which provoke nerve impulses, leading to muscle contractions. These contractions can then be sequentially activated to complete a movement. When used with cycling for individuals with motor disabilities, it provides an excellent tool for rehabilitation or recreational activity [32]–[34]. A more detailed explanation of FES can be found in Section 1.4.

Although invented in the 1980s [23], over the last decade, FES cycling has seen an upsurge in interest, in large part due to international sporting events such as the Cybathlon [35], [36] and Lyon Cyberdays [37]. This is reflected in the increase in the number of articles published on the topic of FES cycling since 2016: 101 articles in the year 2022, which is more than double the number of articles published any year prior to the Lyon Cyberdays and the first Cybathlon in 2016. The increase in the number of FES cyclists, which include individuals with various types of motor disabilities, has created a growing need for assessment tools in order to determine the most efficient electrical stimulation strategies to adapt to the different needs, such as optimizing the stimulation patterns (the timing in which the cyclist's leg muscles are activated) in order to achieve a smooth and powerful cycling movement. Furthermore, selecting the stimulation parameters, such as electrical pulse shape and charge density, that will maximize the torque generated by the muscle contraction while minimizing the subsequent muscular fatigue will have a major influence on the cycling efficacy and its potential health benefits [38]–[43].

Despite the growing popularity of FES cycling, instrumented cycling devices for the assessment of FES-cycling strategies are not common. The existing devices are mainly designed around commercially available cycling ergometers or recumbent tricycles. Cadence-controlled cycling ergometers that provide motor and crank position data can be adapted for FES cycling, and the torque produced by the cyclist can be derived from the motor current [44]. Another approach is utilizing the recumbent tricycle by replacing the crankset with a crank power meter [42], [45]. Hunt et al. [46] have expanded on this by motorizing the recumbent tricycle and integrating the power meter into the crank, allowing the system to be cadence- and output-power-controlled. Alternatively,

an isokinetic knee joint torque measurement system with integrated electrical stimulation can be used to assess FES-cycling strategies by mimicking the knee joint motion during cycling movement [47].

The main limitation of the mentioned devices is versatility. The seating position is predefined and requires a transfer which is often difficult for individuals with certain disabilities. In addition, most of the mentioned devices do not record the torque produced by each leg separately. The torque recorded is one-dimensional, and it corresponds to the component which is perpendicular to the crank arm and contributes to the cycling motion. Thus, the only possible optimization method is to maximize that component. Recording three-dimensional torque allows for optimization techniques that would, in addition, try to minimize the power lost in forces exerted onto the pedals that do not contribute to the cycling motion.

In order to optimize FES-cycling movements and protocols, we developed a novel instrumented cycling ergometer platform (ICEP) designed to evaluate the effectiveness of various FES-cycling strategies. The platform is adaptable to different reclined cycling positions and is outfitted with highly sensitive force sensors to directly measure the effects of different FES-cycling parameters. In addition, subjects can also be tested while seated in their wheelchair, so a transfer is not required.

The purpose of the present article is to describe and assess the ICEP. Furthermore, the capabilities of the ICEP are demonstrated through the example of determining and optimizing stimulation patterns. The platform described in this work can be easily reproduced and will hopefully motivate future in-depth specific studies to further progress the number of applications and designs of new FES-cycling devices.

2.2 Materials and Methods

2.2.1 Description of the Equipment

The platform consists of a modified bicycle frame fitted with pedal force/torque sensors, a crank encoder and a motor (Figure 2.1). The frame rests on two wall-mounted rails, allowing the ergometer to slide up and down, changing the height of the crank in order to make the system suitable for hand or foot pedaling in a seated or standing position. It is additionally stiffened with tension wires to increase sturdiness, hence limiting the shaking and deformation of the frame caused by cycling.

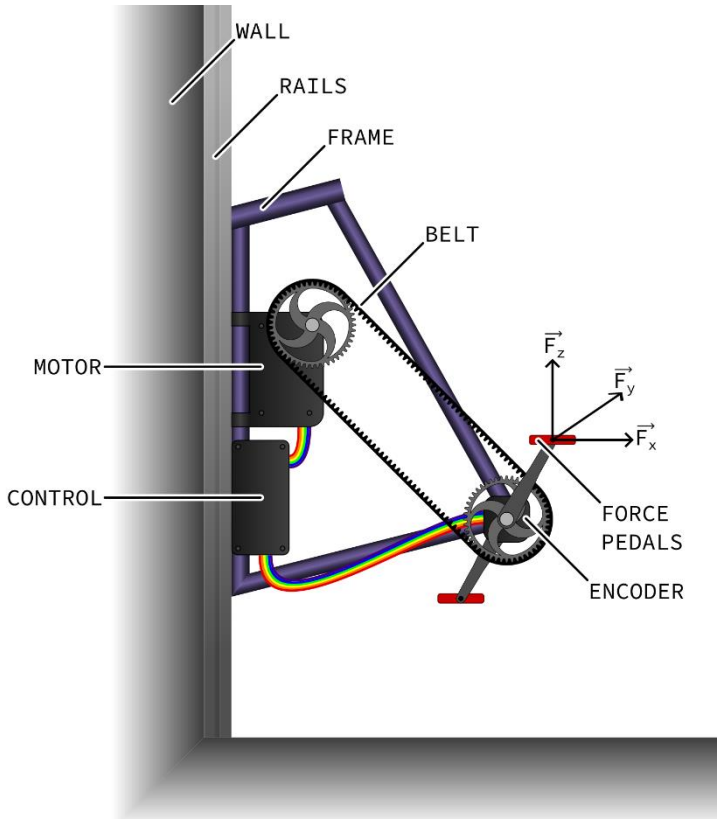

Figure 2.1: Sketch of the wall-mounted instrumented cycling ergometer platform. Details concerning the components of the ICEP are provided in the text of the manuscript.

The actuator system, consisting of a brushless motor (EC60 Flat, Maxon Motor AG, Switzerland) associated with a planetary 53:1 ratio gear-head (GP52C, Maxon, Switzerland), can produce a maximum torque of 228 Nm. It is connected to the crankset through a pulley and belt system (A9-H075, A8-H, Michaud-Chailly, Saint-Priest, France). The motor rotational speed is controlled by a servo controller, and the power is supplied through a shunt regulator (ESCON 70/10, DSR 70/30, Maxon, Sachseln, Switzerland). It is set up to assist the cyclist with producing the cycling movement while maintaining a constant cycling cadence, which can be set from within a custom-made LabVIEW (National Instruments, Austin, TX, USA) graphical interface, with values ranging from 1 rpm to 100 rpm.

Each pedal independently measures all three components of the force and torque applied to their surface, as well as the inclination angle of the pedal in reference to the crank arm (ICS-RM, Sensix, Poitiers, France). Force values up to 2.8 kN can be measured while the inclination angle is measured with a resolution of 0.072°. A magnetic ring encoder (LM13, RLS, Ljubljana, Slovenia) placed around the spindle of the crankset acquires the crank angle with a resolution of 0.06°. Data are acquired at a 1 kHz sampling rate and displayed in real-time, as well as recorded in a text file for later analysis.

Leg orthoses (Hase Bikes, Waltrop, Germany) were modified to attach the legs to the force-measuring pedals. To ensure that there are zero degrees of movement between the leg orthosis and the pedal, custom connecting metal plates were manufactured (Figure 2.2) and attached to the pedals, providing a grooved surface to which the orthosis can be attached. The grooves in the metal plates allow for the adjustment of the position of the orthosis, and therefore the foot, in reference to the pedal. The platform was designed to be used from a wheelchair; therefore, it does not have a built-in seat. Cycling from their wheelchairs allows pilots to avoid transfer and provides more comfort in general. The platform can also be used while seated on a recumbent tricycle, from which the boom (the part of the trike carrying the crankset that slides in and out of the frame to adjust for leg length) has been removed in order to reproduce accurate cycling positions (Figure 2.3). We used the Carbontrike (Carbontrikes, Bandhagen, Sweden), a custom-made carbon recumbent trike used by the ENS de Lyon team for the 2016 and 2020 editions of Cybathlon's FES-cycling races. The trike, or the wheelchair, is secured to the ergometer with a retractor system attached to the ergometer frame and hooked to the wheels (Q'straint, Oakland Park, FL, USA).

Figure 2.2: A custom connecting plate attached to the force/torque measuring pedal.

A current-controlled electrical stimulator (MotiMove, 3F—Fit Fabricando Faber, Belgrade, Serbia) is synchronized with the force-measuring pedals through the custom-made LabVIEW graphical interface. This 8-

channel stimulator produces asymmetrical biphasic pulses with exponential compensation [48]. It can be controlled through a dedicated communication protocol, similar to Hasomed Rehastim's Science Mode, that allows for the following parameters to be preset or changed in real-time for each channel: stimulation mode (singlet or doublet), pulse amplitude (0–170 mA), pulse width (0–1000 µs), frequency (0–100 Hz) and inter-pulse interval in the doublet stimulation mode (2.7–10 ms).

A data acquisition card (PCI-6221, National Instruments, Austin, TX, USA) completes the platform and collects the data from the crank encoder, allowing for the synchronization of the stimulation with the pedaling cadence, as well as triggering the recording of the force measuring pedals, and setting up the motor cadence and stimulation parameters. Both the motor and the stimulator have an emergency stop button that disconnects them from the power supply.

The force-measuring pedals are factory-calibrated by the manufacturer, while the crank angle and pedal inclination encoders are calibrated before starting each new trial. A crank angle of 0° is achieved when the left crank arm is in the forward position and parallel to the ground. Motor rotational speed control was verified for cycling cadences ranging from 10 rpm to 50 rpm in steps of 10 rpm.

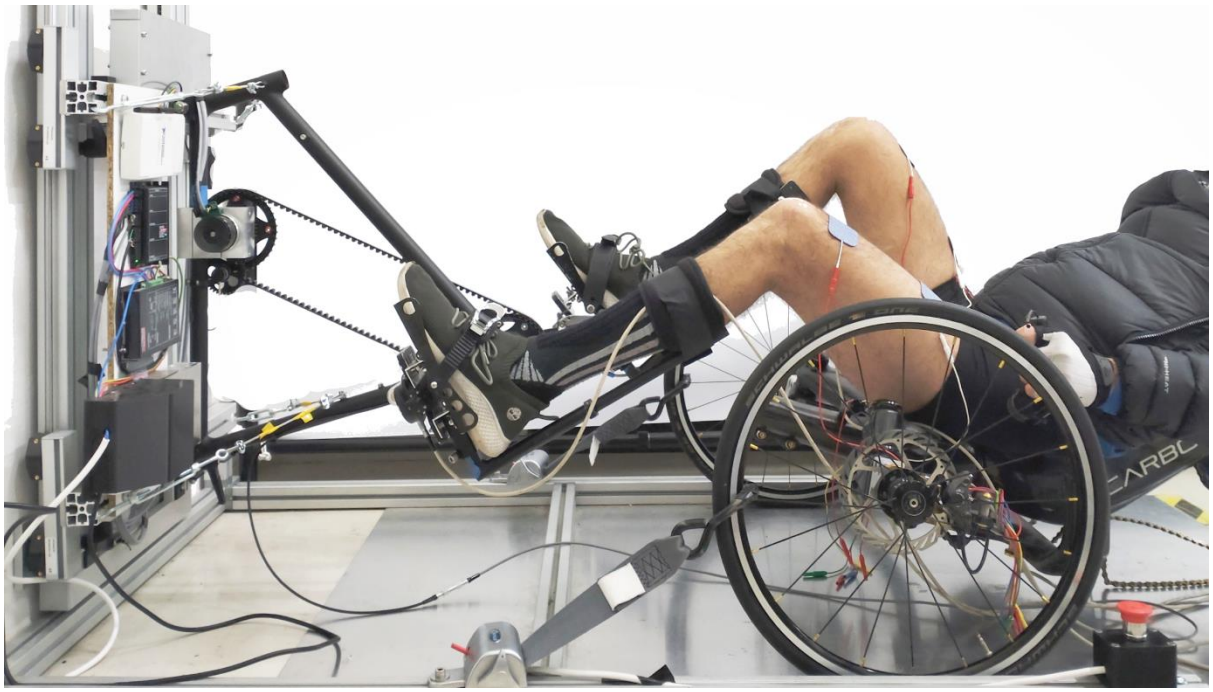

Figure 2.3: Photo of an SCI subject using the platform from the Carbontrike.

2.2.2 Determining Stimulation Patterns

In FES cycling, a stimulation pattern is a set of crank angle intervals defined for when each muscle group should be stimulated, in order to reproduce a functional cycling movement. Determining these suitable stimulation intervals can be a tedious process as it will vary according to the pilot's physical condition, morphology, seating position and the number of muscle groups used; moreover, it has to be optimized in relation to the type of exercise (endurance, interval, sprint, etc.) in order to achieve the best compromise between power and fatigue. As a result, determining and optimizing stimulation patterns served as an appropriate application for demonstrating the capabilities of the cycling platform.

In the following parts, we will describe two different methods for determining FES-cycling stimulation patterns: from EMG measurements on an able-bodied subject and from direct measurements of the forces produced by each SCI subject's muscle group during a crank revolution.

2.2.2.1 EMG Recording during Volitional Cycling

A straightforward procedure for reproducing an FES-induced cycling movement is to measure the activation timings of an able-bodied subject's muscle groups during cycling, through EMG recordings, then to apply these timings to the stimulation of the muscle groups of a paralyzed subject in order to try producing a similar motion [49], [50].

One able-bodied adult male (26 years old) subject was chosen on account of having a similar height (185 cm) and leg dimensions (50 cm calf and 50 cm thigh) to the SCI subject participating in the second part of the study. Similar leg dimensions are important for achieving the same cycling position, with the same basin versus pedalboard geometrical configuration.

EMG activities of five main muscles used in cycling (rectus femoris, vastus lateralis, vastus medialis, biceps femoris and semitendinosus) were acquired on the able-bodied subject, using a 6-channel EMG recorder (FreeEMG 100RT, BTS Bioengineering, Garbagnate Milanese, Italy). The electrodes were placed on shaved and cleaned skin, between 1.5 and 2 cm apart, parallel to the muscle fibers, in accordance with the surface electromyography for the non-invasive assessment of muscles (SENIAM) project guidelines [51].

The recordings were performed on the subject's dominant leg, during constant-cadence motor-assisted cycling i.e. the subject was cycling volitionally while the motor maintained a constant cadence. The subject cycled seated in the Carbontrike, legs attached to the force-measuring pedals using leg orthoses, at a cadence of 50 rpm.

The EMG recordings were processed and analyzed in Matlab (Mathworks, Natick, MA, USA). The raw signals were filtered with a [10 Hz, 30 Hz] 4th order band-pass Butterworth filter. The processed EMG signals were normalized for each revolution and subsequently averaged. The resulting signals were plotted against the crank angles on a 360° plot (Figure 2.4). They represent the mean EMG profile from where the muscle activation pattern will be determined.

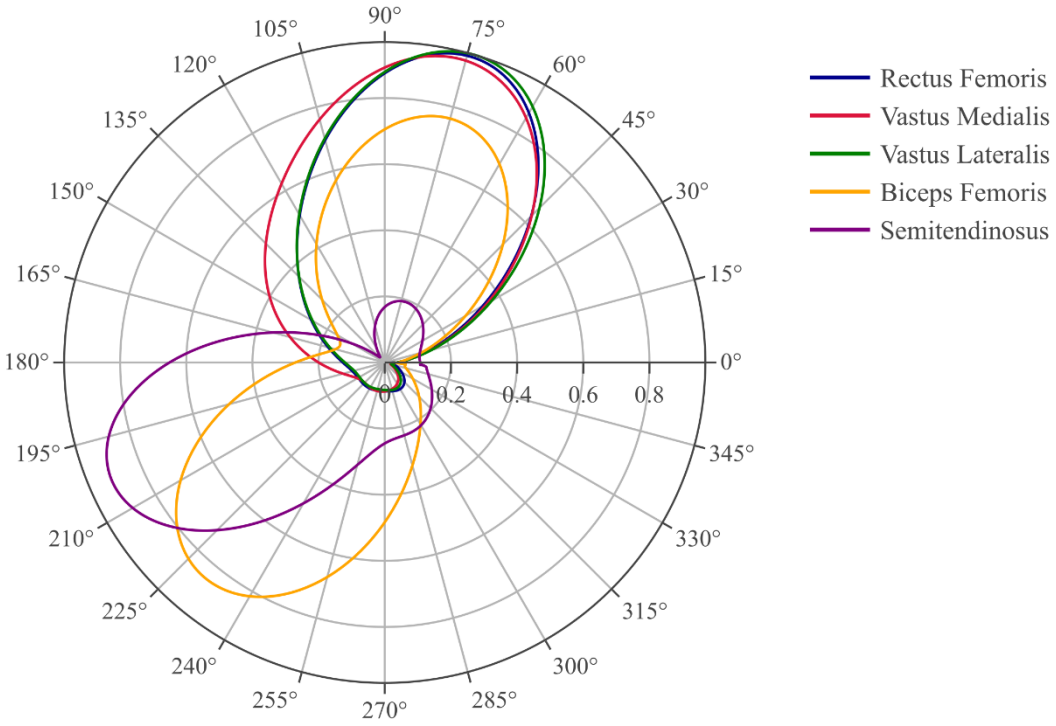

Figure 2.4: EMG recordings of the five main muscles used by the able-bodied subject.

2.2.2.2 Recording Force Profiles of the Muscle during FES Cycling

An obvious limitation of using an able-bodied cyclist's EMG recordings to set up a paralyzed pilot's FES-cycling pattern is that FES only allows for the stimulation of a limited number of muscles that are close to the skin's surface, whereas volitional cycling also engages deep muscles, such as the iliopsoas muscle, that cannot be reached using non-invasive electrical stimulation. Therefore, the optimal activation timings of a limited number of surface muscles, in order to achieve an effective cycling movement, might substantially differ from the activation timings measured on an able-bodied subject, who would use those surface muscles in combination with additional muscles that remain out of the reach of FES.

In order to take this limitation into account, a straightforward procedure is to record the tangential force (i.e., the force tangential to the cycling motion, by opposition to the normal force that is parallel to the crank and produces no motion, as illustrated in Figure 2.5) exerted by a pilot's foot on each pedal, while continuously stimulating one muscular group during at least one revolution of a motor-assisted cycling motion. In order to only take into account the force produced by the muscle contraction, we need to deduce the forces produced by the feet on the pedals when no muscle is stimulated and the pedaling motion only occurs through motor assistance. We refer to this as passive cycling, in opposition to active cycling when at least one muscle group is stimulated.

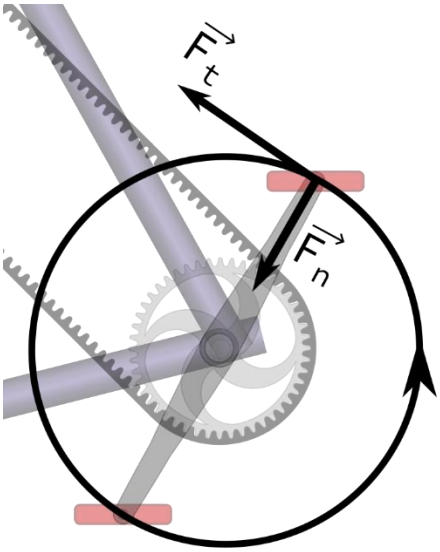

Figure 2.5: Tangential and normal forces Ft & Fn.

Other contributing forces, such as the weight of the legs and inertial forces, are similar if passive and active cycling are conducted consecutively in similar conditions (i.e., without changing the seating position or the cadence). By comparing the forces produced during active (stimulation-induced) and passive (motor-assisted) cycling over a complete revolution, we can evaluate the individual contributions of each single muscle group. The difference between active and passive cycling over one revolution (or several averaged revolutions) will be called the muscle's force profile (MFP) (Figure 2.6) and used to determine a stimulation pattern.

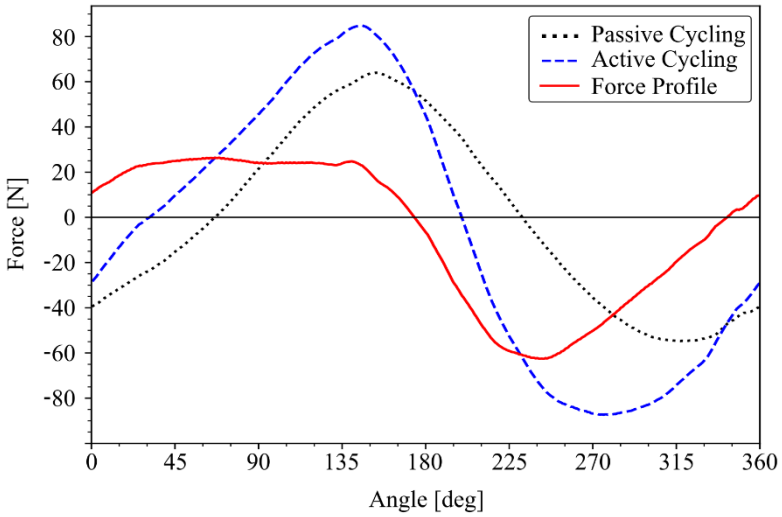

Figure 2.6: Passive cycling, active cycling and muscle force profile (active - passive) of the right quadricep recorded on the SCI subject.

A positive value of the MFP indicates that the stimulated muscle contributes to cycling in that specific angular range; while a negative value of the force profile indicates an angular range where the stimulated muscle is hindering the cycling motion.

2.2.3 Deriving Stimulation Patterns from EMG and MFP

To derive a stimulation pattern from the EMG recording from Figure 2.4, an EMG activation interval was defined as the crank angular range during which the mean EMG activation profile was greater than a 25% threshold in comparison to its maximal peak [41]. The activation interval of the quadriceps was then defined as the union of the activation intervals of the rectus femoris, vastus lateralis and vastus medialis. Analogously, the activation interval of the hamstring was defined as the union of the activation intervals of the biceps femoris and semitendinosus. This pattern will hereafter be referred to as the EMG pattern.

Based on Figure 2.6, if the force profile is positive, the muscle is contributing to the cycling motion; if the force profile is negative, the muscle is resisting the cycling motion. Therefore, the only range of positions suitable for electrical stimulation is where the force profile is positive. In order to derive a stimulation pattern, several procedures could be considered. One could, for instance, detect the maximal force and then set the start angle at the first zero transition before the maximum and the stop angle at the first zero transition after the maximum [40]. Such a range would likely maximize the power output, but also the muscular fatigue. From there, an arbitrary threshold could be defined as a percentage of maximum force, in order to limit the range of stimulation where the produced force is above a certain value. This would allow a compromise between power output and muscle fatigue, hence optimizing the pattern for a less intense but longer exercise.

In order to allow for a fair comparison of the measured power output with the EMG pattern, start and stop angles were chosen so as to have the same angular length as the EMG pattern (and therefore generate the same amount of muscle fatigue) and to maximize the area below the force profile. The resulting pattern will hereafter be referred to as the MFP pattern. Both EMG and MFP patterns are displayed in Figure 2.7.

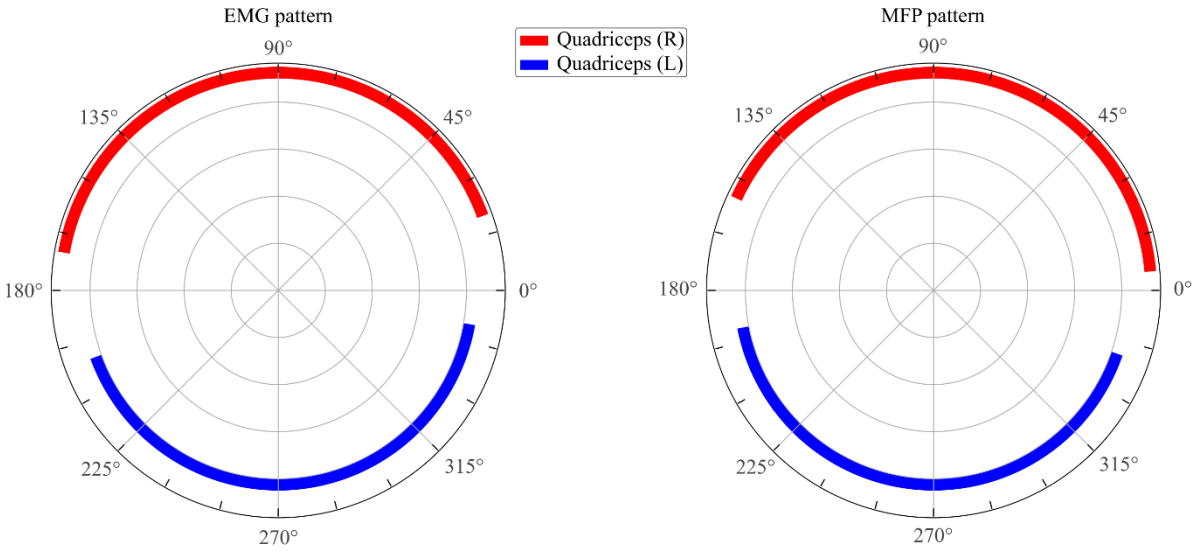

Figure 2.7: Stimulation patterns for left and right quadriceps derived from EMG recordings on the able-bodied subject (left) and from MFP measurement on the SCI subject (right).

2.2.4 Delay Compensation

Regardless of the method chosen to determine the stimulation pattern, various delays must be considered. The delays are a product of the stimulator (1), the measuring equipment (2) and the muscles themselves (3). Estimating or measuring them will allow for compensating for them.

1. The stimulator delay (D_S) is the internal stimulator delay and represents the time from the moment when the stimulator receives the command to generate a pulse (input signal), to the moment the generated pulse arrives at the electrode placed on the skin (output signal). By comparing the timings of the input and output signals using an oscilloscope, the stimulator delay can be measured and, in the case of the MotiMove stimulator, it amounts to 3.2 ms in the stimulation mode used in the present study.

2. The delay caused by the measuring equipment is a product of the acquisition and processing of the crank angle data. It amounts to 1 ms, which, when cycling at 50 rpm, is equivalent to 0.3° of the crank angle. We will thus consider it insignificant.

3. Muscle activation delay, also called electromechanical delay (EMD), is defined as the time it takes for the muscle to develop tension once the stimulation pulse reaches the motor nerve. Muscle delay is usually derived from literature, but it can also be measured.

When recording passive and active profiles in order to measure the MFP, the muscle groups of interest are continuously stimulated. Thus, they are not affected by either of these delays. The delays should be compensated for only when the muscle stimulation follows a specific intermittent pattern.

To ensure that the muscles are activated at the correct position, the angular ranges of the stimulation patterns have to be shifted. To compensate for the stimulator delay, both start and stop angles must be shifted by the same amount. To compensate for the EMD, only the start angle has to be shifted. The required angular shifts depend on the cycling cadence and can be calculated using the following equations:

$$\Delta\theta_{start} = \frac{(D_s + EMD) \times 360}{60}\omega \tag{2.1}$$

$$\Delta\theta_{stop} = \frac{D_s \times 360}{60}\omega \tag{2.2}$$

where $\Delta\theta$ represents the angular shift [°], D_S is the stimulator delay [s], EMD is the muscle activation delay [s] and ω is the cycling cadence [rpm].

Angular shifts, and therefore total delay, can also be directly measured by comparing the angle where the stimulation of the muscle begins and the angle where the muscle actually produces a noticeable change in force exerted on the pedals. In Figure 2.8, the SCI subject's quadriceps were stimulated at an arbitrary angle, within the first half of the angular range where the MFP is positive, at a cadence of 50 rpm. The "net-force" is the curve

obtained by subtracting passive forces from active forces when the muscle group of interest is stimulated only within the angular range defined by the chosen pattern. It represents the effect of the stimulated muscle group on the cycling motion and can be used to measure the total delay and also to calculate the power produced by that muscle group.

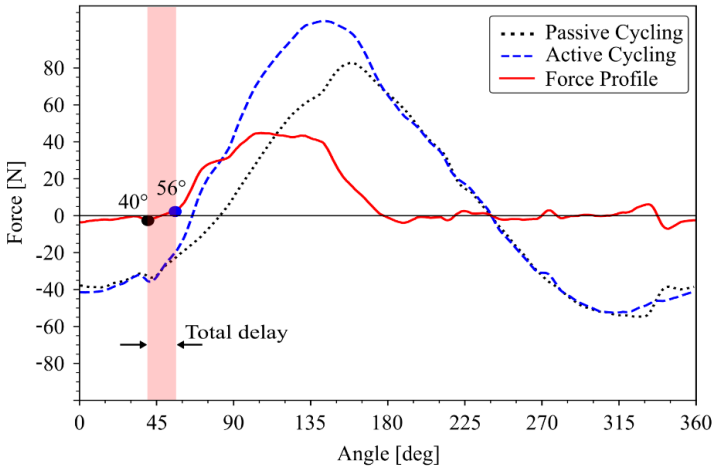

Figure 2.8: Direct measurement of the angular shift at 50 rpm for the SCI subject.

2.2.5 Experimental Protocol

One adult male (46 years old) with a motor-complete SCI (lesion level C7-C8, American Spinal Injury Association (ASIA) Impairment Scale (AIS) B) participated in the present case study. The injury occurred 11 years prior to the study. The subject is 184 cm tall, with 50 cm calf and 50 cm thigh lengths. The subject is experienced with FES cycling as he competed in the 2016 and 2020 editions of Cybathlon's FES-cycling races. He was asked to refrain from exercising at least for 24 h before the experiment as he was involved in the FES-cycling training program at the time of the study.

The medical device used (Motimove 8) was operated strictly following its intended use. As such, the present study does not require the approval of an ethical committee according to French regulations. All procedures followed the usual practices and guidelines regarding rehabilitation of motor function in adult SCI patients, and the subjects gave their written informed consent for study participation.

The experiment was conducted in one session. The session began with a two-minute passive cycling warm-up where the cycling cadence was gradually increased from 10 to 50 rpm. It was followed by four electro-stimulated phases respectively dedicated to:

1. determining the force profiles for each muscle of interest;
2. measuring the total delay;
3. cycling using the EMG pattern;
4. cycling with the MFP pattern.

Each of these four phases began with 5 to 10 passive cycles, followed by 2 active cycles and ended with a 5 min period of rest.

The subject was seated on the Carbontrike in a comfortable position with the legs secured to the ergometer. The trike was placed at the same distance from the pedals as for the EMG test with the able-bodied subject. Using one stimulation channel per leg, pulses were delivered through 9 × 5 cm electrodes (Dura-Stick Premium, Chattanooga, UK) located over the motor points of the quadriceps muscle groups. As the subject has issues with stimulating hamstring muscles, this muscle group was not used. The stimulation frequency was set to 40 Hz, the pulse width to 350 μs and the pulse amplitude to 70 mA. Stimulation parameters were chosen based on the prior experience with FES cycling of the subject, who usually trains 2 to 3 times a week, one-hour sessions on either RT300 (Restorative Therapies, Nottingham, MD, USA) or Motomed (Reck, Betzenweiler, Germany).

After the initial warm-up, the measuring began with obtaining the force profiles. As a compromise between the number of samples acquired and the muscle fatigue produced by the stimulation, the cadence was set to 30 rpm during the first phase. Throughout the other phases of the protocol, the cadence was set to 50 rpm. Following the rest period, the second phase of the protocol was carried out. During the break, recorded data were processed, and the MFP was analyzed using a custom-made Python script. The angular shift was measured to compensate for the delay, and the MFP pattern was set up. During the third and the fourth phases of the protocol, EMG and MFP patterns were respectively used.

The net-forces were calculated from the recorded cycling data. Angular velocity together with the net-forces was used to calculate the mean power produced during one cycle by muscles stimulated with the EMG pattern (P_{EMG}) and with the MFP pattern (P_{MFP}).

2.3 Results

The results of the motor cadence control test are presented in Table 2.1. The error of the cadence control system increased with the cadence, as shown in Figure 2.9.

Table 2.1: Measured and target cadences in the motor cadence control test.

Target Cadence [rpm]	Measured Cadence [rpm]	Delta Percentage [%]
10	10.003	0.03
20	19.86	0.7
30	29.70	1
40	39.47	1.34
50	49.18	1.66

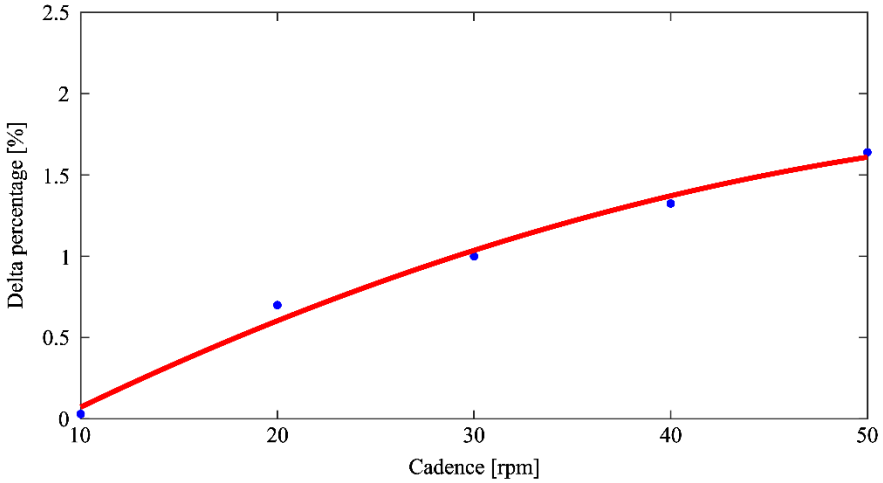

Figure 2.9: Difference between the target and measured cadence in percentage.

The angular shift was measured to be 16° (Figure 2.8), and it was applied to the start angle of the EMG and MFP patterns from Figure 2.7. The angle values for the delay-compensated stimulation patterns are shown in Table 2.2.

Table 2.2: Start and stop angles of delay-compensated stimulation patterns for left and right quadriceps.

	Left Quadriceps		Right Quadriceps	
	Start Angle [°]	Stop Angle [°]	Start Angle [°]	Stop Angle [°]
EMG pattern	184	350	4	170
MFP pattern	175	341	349	155

The calculated net-forces produced by the quadricep muscles stimulated with the EMG pattern are shown in Figure 2.10, and the net-forces produced by the quadricep muscles stimulated with the MFP pattern are shown

in Figure 2.11. The mean power produced by the MFP pattern (P_{MFP} = 10.1 W) was 14% greater than the mean power produced by the EMG pattern (P_{EMG} = 8.8 W).

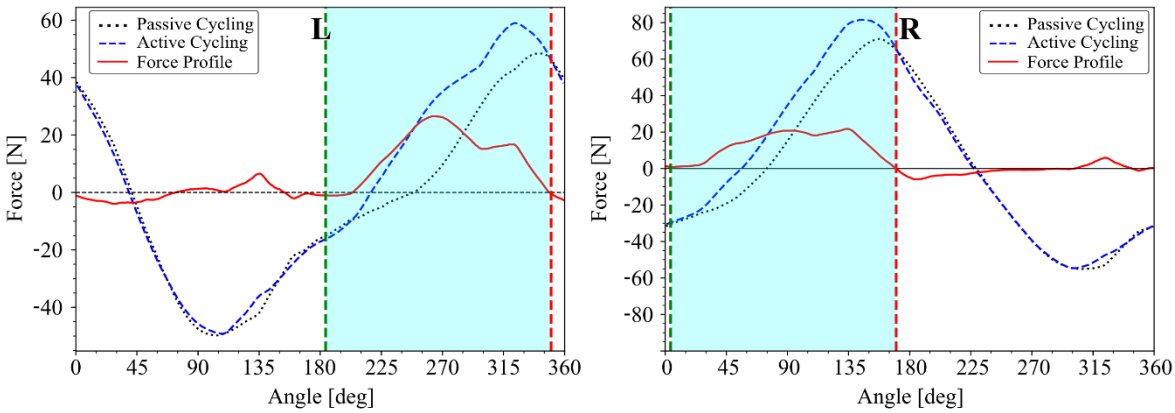

Figure 2.10: Passive, active and the net-force produced by the left and right quadriceps of the SCI subject stimulated by the EMG pattern. Green and red lines represent the start and stop angles of the delay-compensated EMG pattern, respectively.

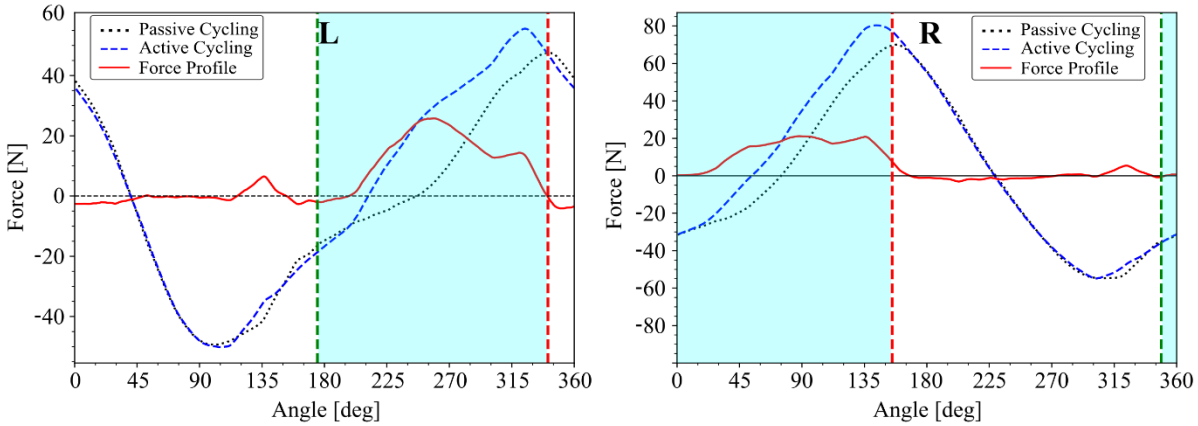

Figure 2.11: Passive, active and the net-force produced by the left and right quadriceps of the SCI subject stimulated by the MFP pattern. Green and red lines represent the start and stop angles of the delay-compensated MFP pattern, respectively.

2.4 Discussion

We built a wall-mounted instrumented cycling ergometer, designed to facilitate the assessment of advanced FES-cycling strategies. The motor cadence control accuracy was measured. As an example of the platform's capabilities, we demonstrated how to determine delay-compensated FES-cycling patterns following two different methods and how to compare their efficiencies.

In order to be able to make a fair comparison between EMG and MFP patterns, we determined the latter so as to generate the same amount of muscular fatigue as the first. This means that after determining the EMG pattern, the MFP pattern was determined by giving it the same angular range while maximizing the total amount of force produced. However, since the angular stimulation range of the EMG pattern was very wide (i.e., 166° which is almost half a revolution), there was little room for variation, and as a consequence, the variation of the power produced when shifting the pattern was limited. Despite the limitation, the increase in power was still substantial, which is consistent with the results of our previous study [38]. Although encouraging, the patterns need to be further assessed with more subjects in order to achieve statistical relevance. In addition, both patterns should be assessed during longer cycling sessions, specifically to verify the assumption that both patterns induce the same amount of muscle fatigue.

Regardless of the EMG pattern, in order to determine how to optimize the MFP pattern, we need to understand for what type of exercise this pattern is intended. It can be optimized for maximum power production, in which case it would also induce an early onset and rise of fatigue. In that case, the start angle would be set at the first zero transition before the maximum, and the stop angle at the first zero transition after the maximum, which we would call the "full-range" MFP pattern.

However, if the pilot needs to exercise for a substantially longer period of time, a compromise is needed between force and fatigue. In that case, using the full-range MFP pattern is most likely suboptimal. A threshold would need to be defined as a percentage of the maximum force to be exceeded in order to trigger the stimulation. Optimizing the value of that threshold and quantifying the efficacy of the resulting patterns is typically the type of investigation that this platform facilitates.

When measuring the angular shift with the fresh SCI subject, we found a 16° value which, at the cadence of 50 rpm, represents a total delay of 53.3 ms. Considering that the stimulator delay is constant (3.2 ms), we can deduce that the EMD equals 50.1 ms, which is in concordance with [52]. However, during the course of the experiment, we observed that the angular shift was rising, up to 24° (80 ms). This augmentation correlates with the increase in fatigue of the stimulated muscles. This observation is consistent with the findings of isometric and isokinetic studies measuring the relationship between EMD and muscle fatigue [52]–[54]. However, other factors, such as the amount of muscle stretching (thus the leg position) when the stimulation hits, might also contribute to the increase in the EMD. The relationship between induced muscle fatigue and EMD during longer FES-cycling sessions could be investigated using the platform.

One limitation of the present study is that only the quadriceps muscles were used for the SCI subject. The latter is a trained FES cyclist that has been using only quadriceps muscles and has never trained his gluteal or hamstring muscles. As a consequence, we were not able to get repeatable measurements from these muscles, probably because they were too weak and possibly spastic. They would need to be progressively trained with TENS prior to FES. The process of determining the stimulation patterns for additional muscle groups remains identical. However, combining the effects of multiple muscle groups might also introduce uncontrolled muscle synergies [24], which should be investigated in further experiments, along with including more subjects for statistical relevance.

In order to extend its capabilities, the platform is being continuously improved. For instance, although it was originally designed for FES cycling, the addition of a new motor position control system will allow for its use in isometric studies. A more powerful motor unit could also permit volitional cycling with able-bodied subjects producing higher torques. Additionally, as the platform is height adjustable, another possible expansion of its capacities is the inclusion of hand cycling. Adapting the pedals to the force-measuring system will introduce the possibility of performing upper-limb FES cycling studies.

2.5 Conclusion

An instrumented cycling ergometer platform for the assessment of advanced FES-cycling strategies was designed and presented in this work. The capabilities of the platform were demonstrated by determining stimulation patterns for the stimulation of paralyzed quadriceps muscles. The description of the platform provided in the present article will hopefully enable other research groups to replicate and improve upon this work and, thus, further contribute to the advancement of the assessment of novel stimulation strategies.

3 Efficacy of High versus Moderate-Intensity SDSS in Subjects with Spinal Cord Injury – an Isometric study

Abstract

For producing isometric contractions, spatially distributed sequential stimulation (SDSS) was proven to be better than the traditional FES that uses a single electrode stimulation (SES) in terms of fatigue-reducing ability and the power output produced by the muscle. However, the influence of the stimulation parameters (mainly stimulation intensity) on the effectiveness of SDSS is not well understood. The aim of this work is to scientifically compare the fatigue-reducing capabilities of SDSS at high and moderate electrical stimulation intensities in individuals with lower-limb motor-complete spinal cord injuries. Two experiments were conducted, involving isometric contractions of the quadriceps muscle group (Experiment 1) and the vastus lateralis muscles (Experiment 2). The effectiveness of high-intensity SDSS was compared to moderate-intensity SDSS, with SES serving as a reference. Seven SCI subjects took part in the study. Fatigue measurements, including time to fatigue (TTF) and force-time integral (FTI), were analyzed for both electrical stimulation intensity levels. Statistical analysis revealed that moderate-intensity SDSS applied to the quadriceps muscle group significantly increased TTF and force output compared to high-intensity SDSS. These findings offer valuable scientific insights into the practical applications of SDSS, such as FES cycling, and contribute to a better understanding of its mechanisms in reducing muscle fatigue. Further research is warranted to investigate the effect of stimulation parameters in order to optimize SDSS for various muscle groups and functional tasks.

3.1 Introduction

Functional electrical stimulation (FES) is a method used to activate paralyzed skeletal muscles to perform functional tasks. FES and the benefits of FES exercise are explained in greater detail in Section 1.4. In the following chapter, conventional functional electrical stimulation that employs one cathode electrode placed over the motor point of the stimulated muscle will be referred to as FES using a single electrode stimulation (SES).

Maintaining high output force levels for a prolonged period of time is necessary for performing functional tasks such as walking, cycling and rowing. However, a major limitation of SES is the rapid onset of muscle fatigue resulting in the decline in force produced by the stimulated muscles. Voluntary muscle contractions are achieved by recruiting motor units based on their size, from smaller axons that innervate slow fatigue-resistant muscle fibers, to larger axons innervating fast easily fatigable muscle fibers [25]. As the size of an axon defines the axon's activation threshold, low-level electrical stimulation is more likely to activate larger axons resulting in an earlier onset of muscle fatigue. Additionally, conventional electrical stimulation (SES) uses rather large transcutaneous electrodes (5x5 cm or larger) located over the same motor units activating them with every stimulation pulse whereas, during voluntary contractions, motor units are randomly activated resulting in longer periods of rest for each motor unit. A more detailed explanation of the limitations of the technology is provided in Section 1.6.

By mimicking voluntary contractions, SES-induced muscle fatigue can be reduced by distributing the stimulation across multiple smaller electrodes that cover different motor points. Each electrode activates different motor units at a lower frequency than standard SES activation while maintaining a strong fused contraction of the muscle. This method was shown to be effective at reducing muscle fatigue when the electrodes are placed over different synergistic muscle bellies (sum of muscle fibers) [55]–[58] or over the same muscle belly [59]–[68]. The latter approach, termed spatially distributed sequential stimulation (SDSS), delivers the pulses through four small closely spaced electrodes placed identically over the same location of the SES electrode setup. Individual electrodes stimulate at one-fourth of the typical SES frequency (10-15Hz) with an implemented 90º phase shift between the electrodes.

Higher fatigue resistance of SDSS compared to SES was shown when performing isometric contractions of the quadriceps muscle group in subjects with SCI [45], [60], [62]. A similar electrode setup was chosen in all three studies, a 2x2 matrix of 4.5 x 2.5 cm electrodes placed over the belly of the entire quadriceps muscle groups. Similar results were reached in the studies using SDSS to perform a dynamic knee extension task in able-bodied [64] and SCI subjects [67]. In both cases, the 2x2 matrixes of 4.5 x 2.5 cm electrodes were placed as close as possible to the motor points of m. vastus medialis and m. vastus lateralis. However, in two recent studies [69], [70], a significant difference in fatigue resistance of the SDSS was not observed. One of the possible reasons for this is the higher intensity used during the experiment. Although the fatigue-reducing ability of SDSS compared to SES was shown in paralyzed muscles with different electrode configurations, none of the studies have purposefully investigated the effect of the stimulation parameters, such as the higher stimulation intensity alluded

to above. One hypothesis is that since the electrodes are closely spaced with SDSS, it is reasonable to assume that with the increase of the stimulation intensity, electric fields created by each electrode overlap over a larger area activating a greater number of muscle fibers more frequently, and thus diminishing the intended effect of SDSS. This effect was also noticed in a theoretical computational analysis of the electric fields generated by SDSS in a Tibialis Anterior muscle [71]. An overlap of the activated muscle fibers parallel to the electrodes increased with the stimulation intensity. This case differed from the experimental studies in that the simulation was performed on a smaller muscle and the stimulation intensity was limited to 60 mA.

The present study compares the fatigue-reducing ability of SDSS at high and moderate electrical stimulation intensities in subjects with motor-complete SCI. The effects of the stimulation strategies were assessed during isometric contractions of the quadriceps muscle groups (Experiment 1) and isometric contractions of the vastus lateralis muscles (Experiment 2). The primary purpose of the study was to compare the effectiveness of high-intensity SDSS to moderate-intensity SDSS using SES as a reference. Although deduction can be made, the experiments were not designed to produce a direct comparison of SDSS and SES. The outcome of these experiments provides further insight into practical applications of SDSS (particularly FES-cycling due to the effect quadriceps muscles have on cycling performance) and hopefully a better understanding of the mechanisms behind SDSS.

3.2 Methods

3.2.1 Subjects

Seven adult male subjects with lower-limb motor-complete spinal cord injury participated in the study. Five subjects had previous experience with FES of the studied muscles, four of which were undergoing FES-cycling strength training at the time of the study. In an effort to mitigate the effects of residual fatigue, all subjects were asked to refrain from using FES for at least 48 hours before the experiments were conducted. One subject (P6) was excluded from the study due to experiencing intense spasms during the test, despite receiving antispasmodic medication (Baclofen). All subjects met the inclusion criteria, which required a spinal cord injury spanning from cervical 4 to thoracic 12 spinal segments, no voluntary movement or pain sensation in the legs (ASIA A or B), and at least 12 months having elapsed since the injury. The exclusion criteria stipulated that the subjects must not have sustained lower limb fractures within the past year or have open wounds or rashes on the skin surface where the electrodes would be placed. The study protocol was explained in detail to the subjects, and every subject gave informed consent to participate in the study. More information about the subjects is provided in Table 3.1.

Table 3.1. Study group demographics.

Subjects	Age	Injury	ASIA	Time after spinal cord injury (years)	Previous FES experience	Current FES training
P1	46	C7 - C8	B	11	Yes	Yes
P2	30	C5 - C6	B	14	Yes	Yes
P3	59	T9 - T10	B	6	Yes	Yes
P4	59	C6 - C7	A	6	Yes	Yes
P5	62	C6 - C7	B	10	Yes	No
P6	49	T5 - T6	B	30	No	No
P7	38	C5 - C6	A	20	No	No

3.2.2 Description of the Equipment

Subjects were seated on a height-adjustable mat table with the posterior of the knee (Popliteal Fossa) in contact with the edge of the table and their thigh parallel to the ground. The angle of the knee joint was set to 90° and a cushioned backrest was used to achieve the posterior inclination of 115°. In cases where trunk control was insufficient, straps were employed to stabilize the torso. The table height was adjusted such that the foot sole could not touch the ground.

An 8-channel MotiMove stimulator (3F-Fit Fabricando Faber, Belgrade, Serbia) [48], controlled with a custom-made LabVIEW program (National Instruments, Austin, TX, USA), was utilized to produce asymmetric biphasic electrical pulses at a frequency of 48 Hz and a pulse width of 400 μs. To distribute pulses in SDSS mode, an anti-fatigue unit (AFU) device (3F-Fit Fabricando Faber, Belgrade, Serbia) was connected to the cathode of

one of the stimulation channels. The force produced by the stimulated muscle was measured with a force meter (Chronojump-Boscosystem, Barcelona, Spain) secured to the shank of the stimulated leg. The height of the mat table and the position of the sensor on the shank were measured to ensure identical experimental conditions between sessions. Force measurements were acquired with a frequency of 80 Hz and recorded in a text file for subsequent data analysis. An illustration of the experimental setup is shown in Figure 3.1.

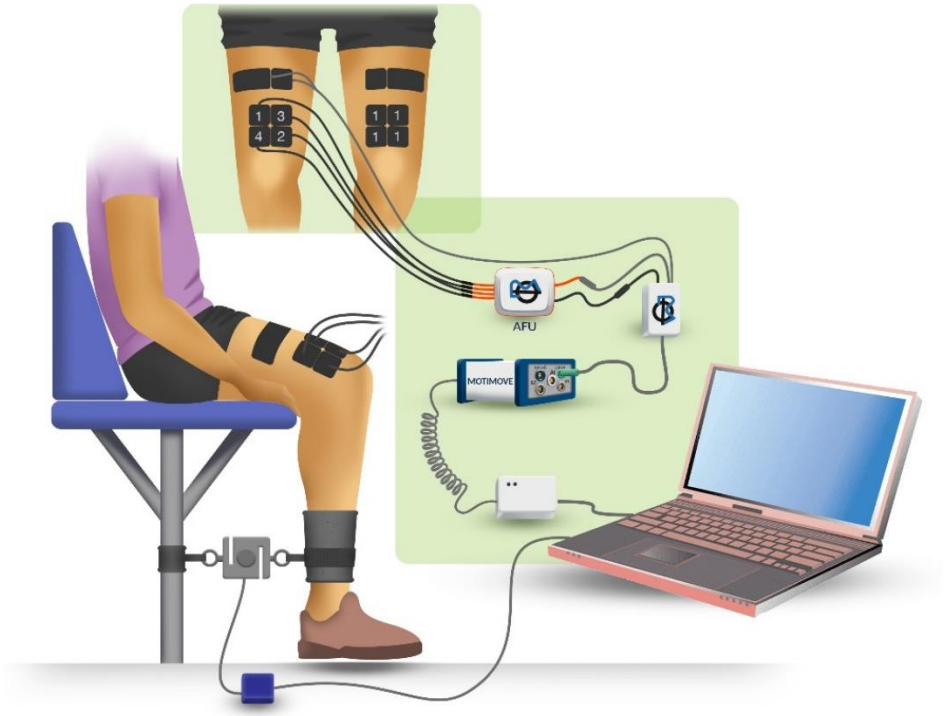

Figure 3.1: Illustration of the experimental setup for performing isometric muscle contractions to assess muscle fatigue using SDSS and SES electrode configurations. Details concerning the different components and procedures are provided in the text of the manuscript.

3.2.3 Electrode configuration

Two types of experiments with different electrode configurations were conducted to compare the fatigue-reducing ability of SDSS at moderate and high electrical stimulation intensities. What we refer to as “Experiment 1” was conducted on the quadriceps muscle group while “Experiment 2” was performed on the vastus lateralis muscle. In all experiments, four self-adhesive surface electrodes (Compex Dura-Stick plus) were placed distally (cathodes) while the reference electrode (anode) was placed proximally. This electrode configuration was chosen considering literature protocols [63] and the preliminary tests conducted during the study design phase. Before applying the electrodes, proximal and distal motor points of the rectus femoris (RF) and the vastus lateralis (VL) muscles were detected using the measured anatomic landmarks [72] and served as reference points for electrode placement. Motor points were marked with an indelible marker pen to ensure identical electrode placement across

the sessions. Prior to electrode placement, the thigh skin was sanitized with an antiseptic spray to prevent skin irritation and ensure a clean surface.

In Experiment 1, the proximal electrode was made by connecting two electrodes to the anode of the same stimulation channel and thus creating an electrode with an effective surface area of 5 x 14 cm^2. Electrodes used for the anode were a 5 x 5 cm electrode placed on the proximal motor point of the RF muscle and a 5 x 9 cm electrode placed laterally, between the proximal motor points of the RF and VL muscles, just to the side of the 5 x 5 cm electrode. Distal (cathode) electrodes, measuring 5 x 5 cm, were placed distally (cathodes) in close proximity to each other, forming a 2x2 matrix just below the distal motor point of the RF muscle (see Figure 3.2a). Positions of the electrodes were confirmed or modified based on visual observations and gentle touch of the muscle contraction resulting from a short train of pulses sent to each electrode separately. In order to minimize fatigue, the pulses used were slightly above the motor threshold. The electrode configuration for Experiment 1 is shown in Figure 3.2a.

In Experiment 2, the proximal (anode) electrode (5 x 9 cm) was placed on the motor point of the VL muscle. Four independent distal (cathode) electrodes, with a surface area of 2.5 x 4.5 cm^2 each, were placed around the distal motor point of the VL muscle. Similar to Experiment 1, the position of each electrode was tested separately and adjusted until the appropriate positioning was achieved. The electrode configuration for Experiment 2 is shown in Figure 3.2b.

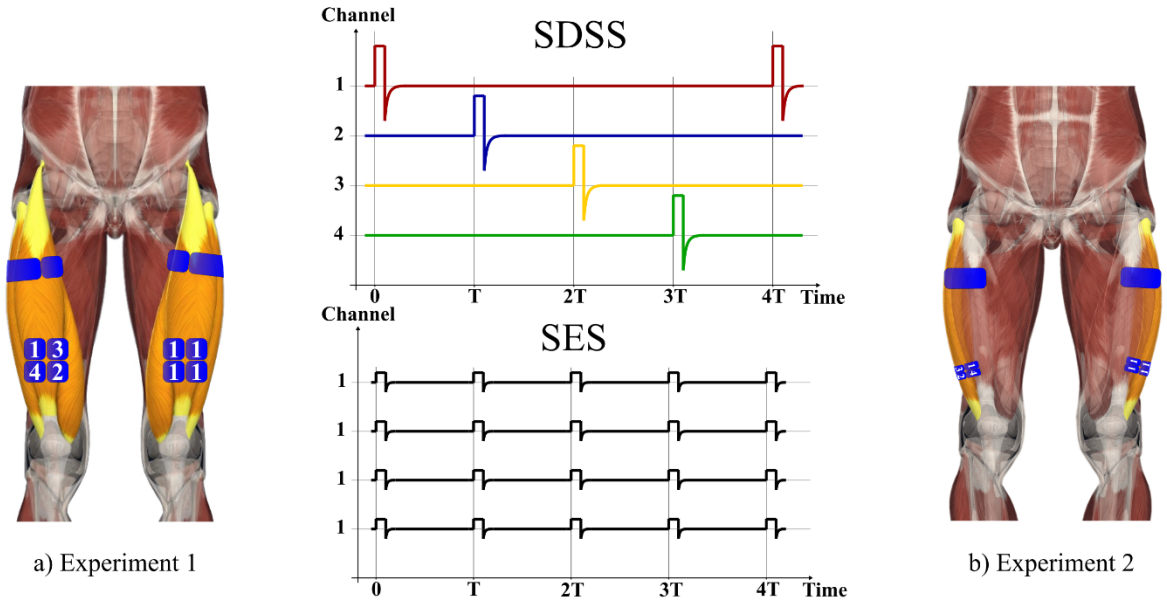

a) Experiment 1

b) Experiment 2

Figure 3.2: Schematics of electrode configurations for Experiment 1 and Experiment 2, together with typical electrical pulse trains for SDSS and SES protocols. In the graphs, electrode channels are labeled on the y-axis versus time (in arbitrary units) on the x-axis. The orange regions in the schematics correspond to the stimulated muscle groups. The proximal electrodes are colored blue while distal electrodes are colored blue and labeled with a number. Colors in the SDSS plots are to remind the reader that different electrodes (regions around the motor point) are activated at different times.

In both Experiment 1 and 2, the described electrode configuration was used for both SDSS and SES. Unlike previous studies that have explored the topic of SDSS, in the SES mode, all four distal electrodes were connected to the cathode of the same stimulation channel effectively forming a single large electrode (indicated in Figure 3.2 using electrode numeration 1,1,1,1). This was done to ensure that the electrode positioning and the area covered by the electrodes remained identical during SES and SDSS. Conversely, in the SDSS mode, each distal electrode was connected to a different output channel of the AFU device, thereby producing the SDSS effect (indicated in Figure 3.2 using electrode numeration 1,2,3,4).

3.2.4 Experimental protocol

All experiments were divided into two types of experimental sessions, one with high-intensity stimulation (order of 130 mA) and the other with moderate-intensity stimulation (order of 70 mA) - the sequence of which was chosen at random for each subject tested. To eliminate the possibility of residual fatigue from previous experimental sessions, a minimum of 48 hours in between them was imposed. For each subject, before the first experimental session, SDSS was randomly assigned to one leg while SES was applied to the other leg. The chosen leg-stimulation arrangement was kept throughout all experimental sessions.

During the experiments, the pulse width was set to 400 μs and the stimulation frequency was 48 Hz for SES and 12 Hz per channel for SDSS (composite frequency of 12 Hz x 4 = 48 Hz). Each experimental session began with determining the high and moderate stimulation intensities for the quadriceps muscle group (Experiment 1) or vastus lateralis muscle (Experiment 2) on a randomly selected leg. High and moderate stimulation intensities were calculated based on the muscle's motor threshold intensity (intensity at which the muscle produces a measurable force) and the force plateau intensity (intensity at which the muscle produces maximal force). Using the SDSS configuration, stimulation pulses were sent with increasing intensity while the output force was measured. Every second, the stimulation intensity was programmatically increased in increments of 5 mA from 0 mA to 130 mA (Experiment 1) or from 0 mA to 100 mA (Experiment 2). If the force plateau was observed, the corresponding intensity was chosen as the high intensity, otherwise, the maximum intensity of 130 mA (Experiment 1) or 100 mA (Experiment 2) was used. The moderate stimulation intensity was calculated as the mean value of the detected motor threshold intensity and the high stimulation intensity. After a 5-minute break, fatigue measurement was carried out by applying the stimulation intensity (high or moderate) chosen for the experimental session using the configuration (SDSS or SES) assigned to the selected leg until the measured force fell under 70% of the maximum produced force (MPF) value.

Subsequently, using the SDSS configuration, high and moderate stimulation intensities were determined for the quadriceps muscle group (Experiment 1) or vastus lateralis muscle (Experiment 2) on the other leg. After a 5-minute break, fatigue measurement was carried out by applying the same stimulation intensity (high or moderate) using the other electrode configuration (SES or SDSS). The entire process was repeated for the other experimental session by switching the stimulation intensity used during the fatigue measurements while maintaining the same leg-stimulation arrangement.

3.2.5 Data analysis

The forces recorded during each fatigue measurement were analyzed using MS Excel (Microsoft Corporation, Redmond, WA, USA) and MATLAB (MathWorks, Natick, MA, USA). Time to fatigue (TTF) was calculated as the time difference from the stimulation onset to the moment the output force fell under 70% of the maximum produced force (MPF). The integral of the produced force over this period was termed force-time integral (FTI), and the ratio of FTI to TTF is given the term average produced force until fatigue (APF). The elicited outcome parameters are TTF, MPF, and APF. Any differences between using SDSS versus SES are calculated at the end of each experimental session using the following equations:

$$\%\mathrm{TTF}_{\mathrm{difference}} = 100 \times \frac{(\mathrm{TTF}_{\mathrm{SDSS}} - \mathrm{TTF}_{\mathrm{SES}})}{\mathrm{TTF}_{\mathrm{SES}}} \tag{3.1}$$

$$\%\mathrm{MPF}_{\mathrm{difference}} = 100 \times \frac{(\mathrm{MPF}_{\mathrm{SDSS}} - \mathrm{MPF}_{\mathrm{SES}})}{\mathrm{MPF}_{\mathrm{SES}}} \tag{3.2}$$

$$\%\mathrm{APF}_{\mathrm{difference}} = 100 \times \frac{(\mathrm{APF}_{\mathrm{SDSS}} - \mathrm{APF}_{\mathrm{SES}})}{\mathrm{APF}_{\mathrm{SES}}}. \tag{3.3}$$

As described in the previous section, the subjects participated in two types of experimental sessions, one with moderate intensity and the other with high intensity. The elicited outcome parameters were then classified into two groups based on the level of intensity for statistical analysis. To check the normality of the data and equivalence of the variance, the Shapiro-Wilk test and F-test were conducted, respectively. If the p-values for both tests were greater than 0.05, the two-tailed paired t-test was employed to identify any differences. Otherwise, the Wilcoxon signed-ranked test was applied. The p-values and d-values (Cohen's d) were used to indicate the significance and effect size of parametric tests. The p-values and r-values (Z-score divided by the square root of sample size) were used for the same purpose in non-parametric tests. In this study, a p-value lower than 0.05 indicates statistical significance.

3.3 Results

3.3.1 Experiment 1

Figure 3.3a and Figure 3.3b depict the fatigue measurements of subject P3 for moderate electrical stimulation intensity (80 mA) and high electrical stimulation intensity (130 mA) conditions. These Figures represent force (N) versus time (sec) graphs. During the first experimental session, the subject underwent high-intensity testing where the left quadriceps muscle group was stimulated using the SES configuration and the right quadriceps muscle group was stimulated with the SDSS configuration. In the subsequent experimental session, the moderate electrical stimulation intensity was tested with the same electrode-leg-stimulation configurations (SES-Left quadriceps muscle group and SDSS-Right quadriceps muscle group). The horizontal black lines and shaded areas under the force-time curve represent TTF and FTI, respectively. Under moderate electrical stimulation intensity conditions, the TTF for SDSS and SES electrode configurations were 20.00 seconds and 11.47 seconds, respectively ($\%TTF_{Difference}$ = 74.37%), whereas, for high electrical stimulation intensity, the TTF for SDSS and SES electrode configurations were 13.18 seconds and 10.34 seconds, respectively ($\%TTF_{Difference}$ = 27.47%). For moderate electrical stimulation intensity, the FTI for SDSS and SES electrode configurations were 636.26 N and 111.01 N, respectively ($\%APF_{Difference}$ = 228.70%). For high electrical stimulation intensity, the FTI for SDSS and SES were 836.03 N and 408.85 N, respectively ($\%APF_{Difference}$ = 60.42%).

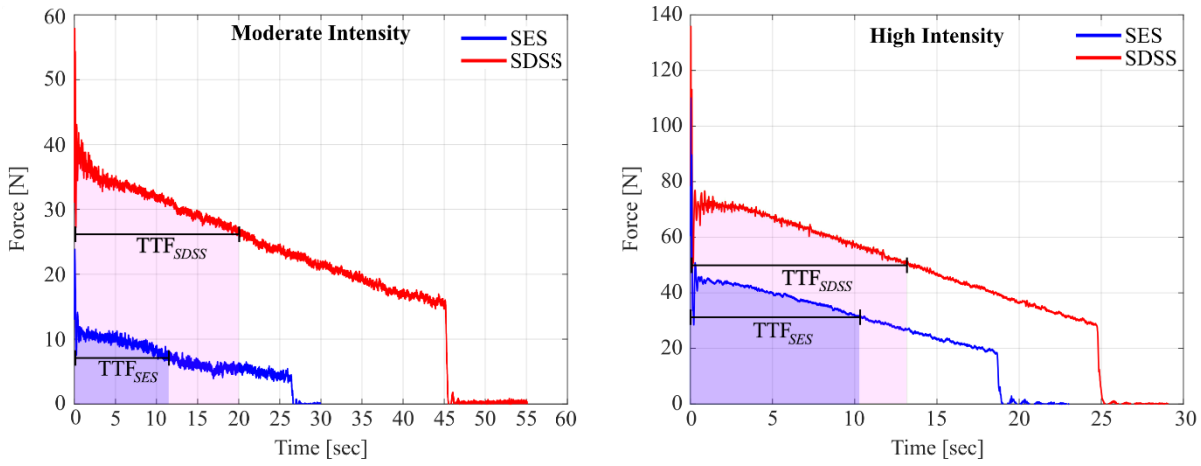

Figure 3.3: Measurements conducted on subject P3 of the force produced by the quadriceps muscle group (Experiment 1) stimulated with a) moderate electrical stimulation intensity (80 mA) and b) high electrical stimulation intensity (130 mA). Forces produced by the quadriceps muscle group stimulated with SDSS and SES electrode configurations are presented with red and blue lines, respectively. Horizontal black lines and shaded areas under the force-time curves represent TTF and FTI, respectively.

Figure 3.4a portrays the $\%TTF_{Difference}$ values for all subjects under moderate (indicated by blue circles) and high (indicated by red circles) electrical stimulation intensity conditions. The $\%TTF_{Difference}$ for moderate electrical stimulation intensity had a median of 118.83%, ranging from 51.90% to 262.44%, while the $\%TTF_{Difference}$ for high electrical stimulation intensity had a median of 40.28%, ranging from 9.84% to 110.28%.

Statistical analysis reveals that the $\%TTF_{Difference}$ for moderate electrical stimulation intensity was significantly larger than that for the high electrical stimulation intensity tests (group mean ± standard deviation, 135.01 ± 71.10% for moderate electrical stimulation intensity and 48.17 ± 32.37% for high electrical stimulation intensity, Figure 3.4b), as determined by paired t_test (p = 0.0065, d = 1.83).

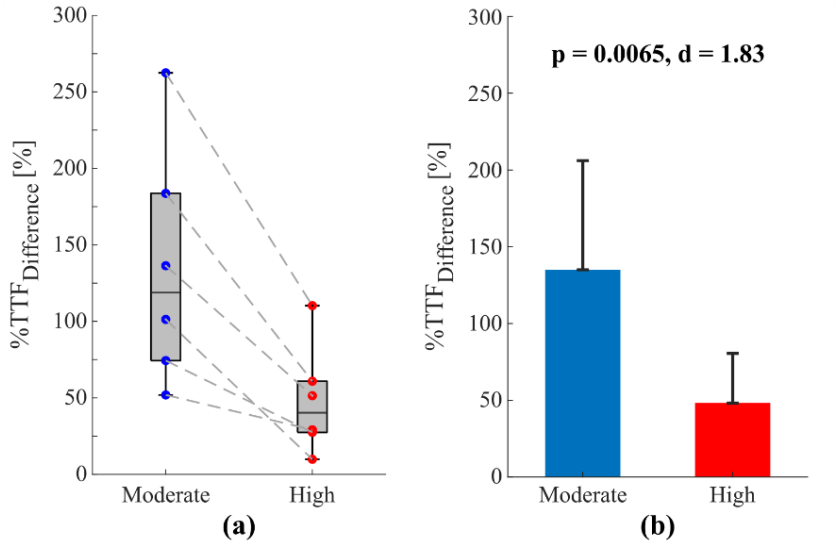

Figure 3.4: Summary of the results from Experiment 1 of $\%TTF_{Difference}$ values for the entire study group under moderate (colored blue) and high (colored red) electrical stimulation intensity conditions. In 3.4 a), the median $\%TTF_{Difference}$ values for the entire study group for moderate and high electrical stimulation tests are provided. The $\%TTF_{Difference}$ results for each subject are presented as a pair of blue (result from moderate electrical stimulation intensity test) and red (result from high electrical stimulation intensity test) circles connected with a dashed line. In 3.4 b) statistical analysis showing the group mean and the standard deviation for moderate and high electrical stimulation intensities is provided.

Figure 3.5a illustrates the $\%MPF_{Difference}$ values for all subjects under moderate (indicated by blue circles) and high (indicated by red circles) electrical stimulation intensity conditions. The $\%MPF_{Difference}$ for moderate electrical stimulation intensity had a median of 151.92%, ranging from 79.28% to 246.92%, whereas the $\%MPF_{Difference}$ for high electrical stimulation intensity had a median of 35.68%, ranging from 0.88% to 66.98%. The $\%MPF_{Difference}$ for moderate electrical stimulation intensity was found to be significantly higher than that for high electrical stimulation intensity (156.19 ± 54.83% for moderate electrical stimulation intensity and 34.95 ± 28.60% for high electrical stimulation intensity, Figure 3.5b), as determined by paired t-test (p = 0.0023, d = 2.32).

Figure 3.6a portrays the $\%APF_{Difference}$ values for all subjects under moderate (indicated by blue circles) and high (indicated by red circles) electrical stimulation intensity conditions. The $\%APF_{Difference}$ for moderate electrical stimulation intensity had a median of 149.73%, ranging from 80.08% to 228.70%, while the $\%APF_{Difference}$ for high electrical stimulation intensity had a median of 35.81%, ranging from 0.08% to 70.33%. The $\%APF_{Difference}$ for moderate electrical stimulation intensity was significantly higher than that for high electrical stimulation intensity (152.40 ± 51.79% for moderate electrical stimulation intensity and 35.48 ± 28.53% for high electrical stimulation intensity, Figure 3.6b), as determined by paired t-test (p = 0.0022, d = 2.35).

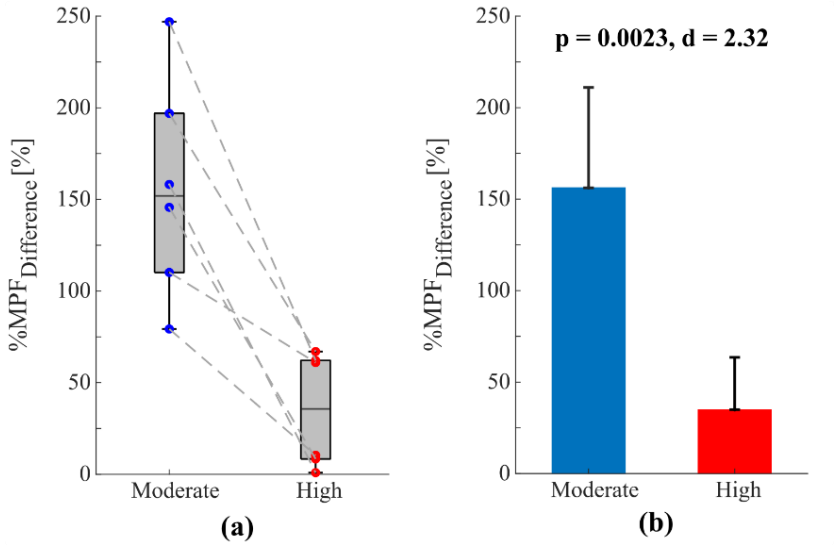

Figure 3.5: Summary of the results from Experiment 1 of $\%MPF_{Difference}$ values for the entire study group under moderate (colored blue) and high (colored red) electrical stimulation intensity conditions. In 3.4 a), the median $\%MPF_{Difference}$ values for the entire study group for moderate and high electrical stimulation tests are provided. The $\%MPF_{Difference}$ results for each subject are presented as a pair of blue (result from moderate electrical stimulation intensity test) and red (result from high electrical stimulation intensity test) circles connected with a dashed line. In 3.4 b) statistical analysis showing the group mean and the standard deviation for moderate and high electrical stimulation intensities is provided.

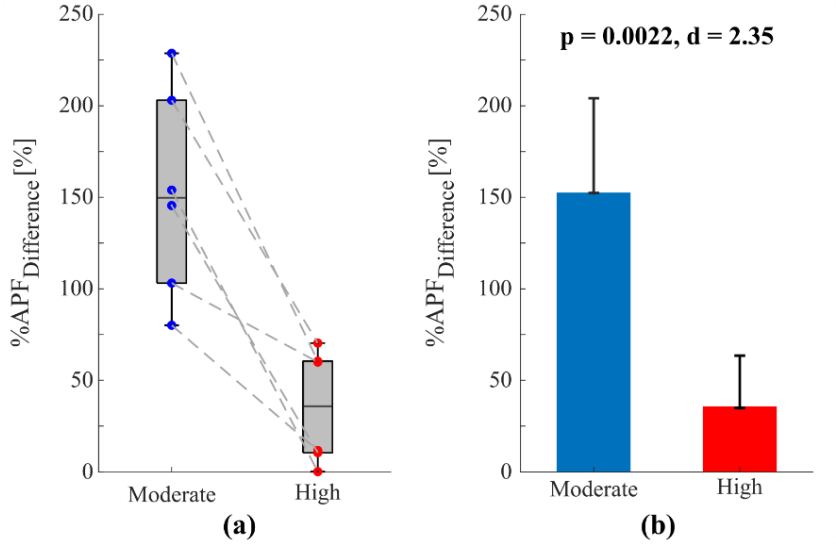

Figure 3.6: Summary of the results from Experiment 1 of $\%APF_{Difference}$ values for the entire study group under moderate (colored blue) and high (colored red) electrical stimulation intensity conditions. In 3.4 a), the median $\%APF_{Difference}$ values for the entire study group for moderate and high electrical stimulation tests are provided. The $\%APF_{Difference}$ results for each subject are presented as a pair of blue (result from moderate electrical stimulation intensity test) and red (result from high electrical stimulation intensity test) circles connected with a dashed line. In 3.4 b) statistical analysis showing the group mean and the standard deviation for moderate and high electrical stimulation intensities is provided.

The values of TTF, MPF, FTI, APF, $\%TTF_{Difference}$, $\%MPF_{Difference}$, and $\%APF_{Difference}$ for moderate and high electrical stimulation intensity with respect to the associated stimulation configuration (SES and SDSS) are shown in Table 3.2.

Table 3.2. The summary of the results from each subject from Experiment 1 conducted on the quadriceps muscle group.

Subj.	[mA]	SDSS				SES				Difference [%]		
		TTF	MPF	FTI	APF	TTF	MPF	FTI	APF	TTF	MPF	APF
P1	70	34.1	43.1	1261	36.9	14.4	20.5	262	18.2	136	110	103
	130	17.3	201.6	3083	178.0	11.4	125.2	1273	111.3	51.4	60.9	59.9
P2	130	17.3	220.9	3312	191.4	15.7	219.1	3012	191.3	9.8	0.88	0.08
	70	24.9	65.2	1410	56.4	12.4	25.3	276	22.2	101	158	154
P3	130	13.2	72.1	836	63.4	10.3	44.5	409	39.5	27.5	62.1	60.4
	80	20.0	37.8	636	31.8	11.5	10.9	111	9.7	74.4	247	229
P4	80	38.0	8.2	275	7.2	10.5	3.3	31	2.9	262	146	145
	130	19.6	23.8	411	20.9	9.3	21.9	177	18.9	110	8.4	10.4
P5	80	27.8	15.5	385	13.9	9.8	8.6	75	7.7	184	79.3	80
	130	14.6	42	543	37	9.1	38.1	302	33.1	61	10.4	11.7
P7	85	10.0	10.6	92	9.2	6.6	3.6	20	3.0	51.9	197	203
	130	7.9	12.5	88	11.1	6.1	7.5	40	6.6	29.1	67	70.3

3.3.2 Experiment 2

Figure 3.7a and Figure 3.7b depict the fatigue measurements of P5 under conditions of moderate electrical stimulation intensity (60 mA) and high electrical stimulation intensity (100 mA). These Figures represent force (N) versus time (sec) graphs. In the initial experimental session, the subject underwent moderate-intensity testing where the left VL was stimulated with the SDSS configuration and the right VL was stimulated using the SES configuration. In the subsequent experimental session, a high-intensity test was conducted with the same electrode-leg-stimulation configuration (SES-Right VL and SDSS-Left VL). The horizontal black lines and shaded areas under the force-time curve represent TTF and FTI, respectively. The TTF values for SDSS and SES electrode configurations under moderate electrical stimulation intensity were 17.90 seconds and 12.65 seconds, respectively, resulting in a $\%TTF_{Difference}$ of 41.50%. At high electrical stimulation intensity, the TTF values for SDSS and SES electrode configurations were 11.96 seconds and 11.22 seconds, respectively, resulting in $\%TTF_{Difference}$ of 6.60%. Regarding FTI, at moderate electrical stimulation intensity, the values for SDSS and SES electrode configurations were 147.03 N and 68.01 N, respectively ($\%APF_{Difference}$ of 52.78%). At high electrical stimulation intensity, the FTI values for SDSS and SES electrode configurations were 246.96 N and 300.87 N, respectively ($\%APF_{Difference}$ of -23.00%).

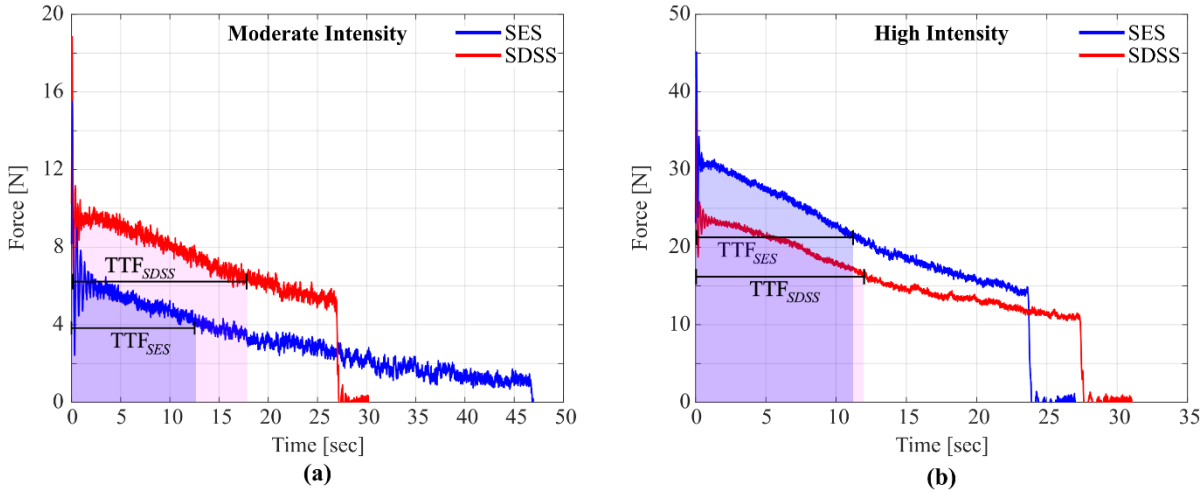

Figure 3.7: Measurements conducted on subject P5 of the force produced by the vastus lateralis muscle stimulated with a) moderate electrical stimulation intensity (60 mA) and b) high electrical stimulation intensity (100 mA). Forces produced by the quadriceps muscle group stimulated with SDSS and SES electrode configurations are presented with red and blue lines, respectively. Horizontal black lines and shaded areas under the force-time curves represent TTF and FTI, respectively.

In Figure 3.8, the $\%TTF_{Difference}$ values for all subjects are presented under conditions of moderate (represented by blue circles) and high (represented by red circles) electrical stimulation intensity. The median $\%TTF_{Difference}$ for moderate electrical stimulation intensity was 39.58%, ranging from -62.17% to 45.59%. For high electrical stimulation intensity, the median $\%TTF_{Difference}$ was -0.80%, ranging from -37.90% to 16.59%. Statistical analysis utilizing the Wilcoxon signed-ranked test revealed no significant difference between $\%TTF_{Difference}$ for moderate and high electrical stimulation intensity ($p = 0.313$, $r = 0.452$).

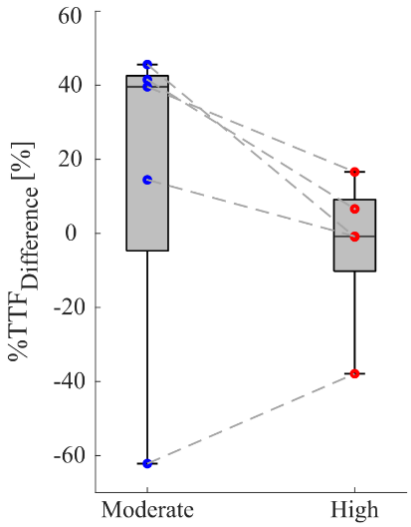

Figure 3.8: Median $\%TTF_{Difference}$ values for the entire study group for moderate and high electrical stimulation tests conducted on the vastus lateralis muscles (Experiment 2) are provided. The $\%TTF_{Difference}$ results for each subject are presented as a pair of blue (result from moderate electrical stimulation intensity test) and red (result from high electrical stimulation intensity test) circles connected with a dashed line.

Figure 3.9a depicts the $\%MPF_{Difference}$ values for all subjects under conditions of moderate (represented by blue circles) and high (represented by red circles) electrical stimulation intensity. The median $\%MPF_{Difference}$ for moderate electrical stimulation intensity was 2.03%, ranging from -51.83% to 98.98%. For high electrical stimulation intensity, the median $\%MPF_{Difference}$ was 8.95%, ranging from -26.72% to 69.64%. The statistical analysis indicated no significant difference between $\%MPF_{Difference}$ for moderate and high electrical stimulation intensity (16.35 ± 54.15% for moderate electrical stimulation intensity and 15.97 ± 39.03% for high electrical stimulation intensity, as shown in Figure 3.9b), as determined by paired t-test ($p = 0.989$, $d = 0.007$).

Figure 3.10a presents the $\%APF_{Difference}$ values for all subjects under moderate (indicated by blue circles) and high (indicated by red circles) electrical stimulation intensity conditions. The $\%APF_{Difference}$ for moderate electrical stimulation intensity had a median of 0.79%, ranging from -51.20% to 72.03%, while $\%APF_{Difference}$ for high electrical stimulation intensity had a median of 6.00%, ranging from -26.21% to 60.65%. Statistical analysis using a paired t-test showed no significant difference between $\%APF_{Difference}$ for moderate and high electrical stimulation intensity (10.85 ± 45.63% for moderate electrical stimulation intensity and 13.61 ± 36.23% for high electrical stimulation intensity, Figure 3.10b) ($p = 0.914$, $d = 0.051$).

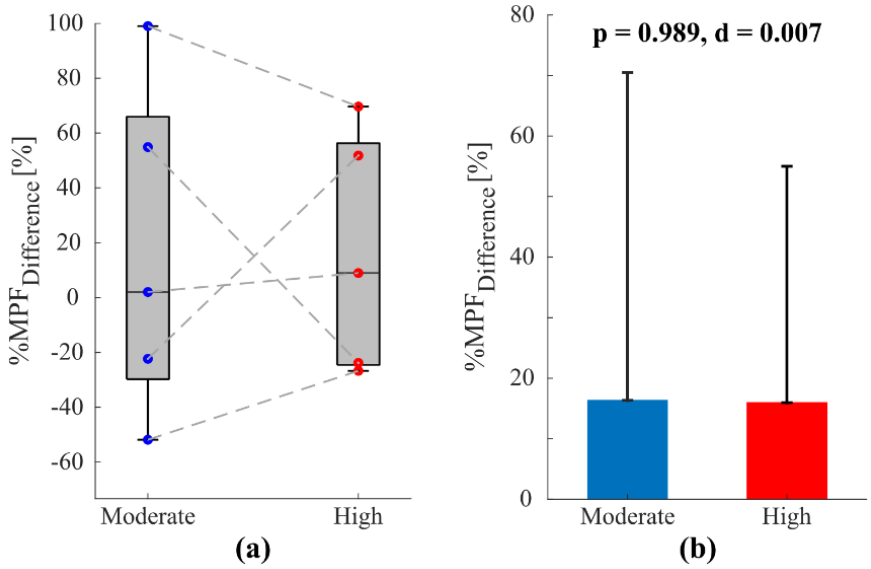

Figure 3.9: Summary of the results from Experiment 2 of $\%MPF_{Difference}$ values for the entire study group under moderate (colored blue) and high (colored red) electrical stimulation intensity conditions. In 3.4 a), the median $\%MPF_{Difference}$ values for the entire study group for moderate and high electrical stimulation tests are provided. The $\%MPF_{Difference}$ results for each subject are presented as a pair of blue (result from moderate electrical stimulation intensity test) and red (result from high electrical stimulation intensity test) circles connected with a dashed line. In 3.4 b) statistical analysis showing the group mean and the standard deviation for moderate and high electrical stimulation intensities is provided.

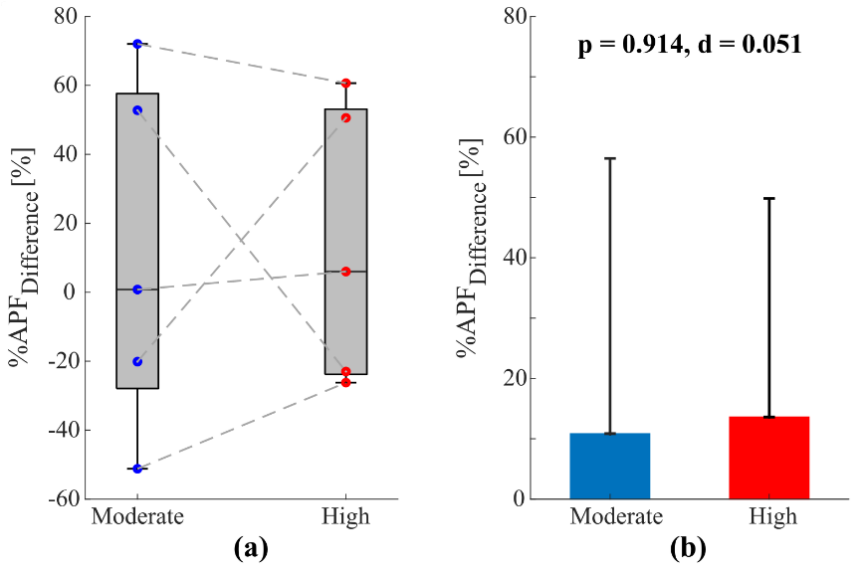

Figure 3.10: Summary of the results from Experiment 2 of $\%APF_{Difference}$ values for the entire study group under moderate (colored blue) and high (colored red) electrical stimulation intensity conditions. In 3.4 a), the median $\%APF_{Difference}$ values for the entire study group for moderate and high electrical stimulation tests are provided. The $\%APF_{Difference}$ results for each subject are presented as a pair of blue (result from moderate electrical stimulation intensity test) and red (result from high electrical stimulation intensity test) circles connected with a dashed line. In 3.4 b) statistical analysis showing the group mean and the standard deviation for moderate and high electrical stimulation intensities is provided.

Table 3.3 provides the values of TTF, MPF, FTI, APF, $\%TTF_{Difference}$, $\%MPF_{Difference}$, and $\%APF_{Difference}$ for moderate and high electrical stimulation intensity, corresponding to the associated stimulation configurations (SES and SDSS).

Table 3.3. The summary of the results from each subject from Experiment 2 conducted on the vastus lateralis muscle.

Subj.	[mA]	SDSS				SES				Difference [%]		
		TTF	MPF	FTI	APF	TTF	MPF	FTI	APF	TTF	MPF	APF
P1	100	9.36	113.2	937	100.0	9.45	74.6	628	66.4	-0.9	51.8	50.6
	60	12.87	29.7	352	27.4	8.84	38.2	303	34.3	45.6	-22	-20
P2	100	13.7	85.6	1063	77.6	13.8	78.6	1011	73.2	-0.8	8.9	6.0
	60	15.3	37.7	495	32.4	13.4	37.0	429	32.1	14.4	2.0	0.8
P3	100	5.2	50.3	219	42.0	8.4	29.7	219	26.1	-38	69.6	60.6
	65	2.8	23.4	49	17.3	7.5	11.8	75	10.0	-62	99.0	72.0
P4	70	13.9	1.8	23.3	1.67	10.0	3.8	34.1	3.4	39.6	-52	-51
	100	10.5	21.7	205	19.5	9.0	29.6	238.7	26.4	16.6	-27	-26
P5	60	17.9	9.4	147	8.2	12.6	6.0	68	5.4	41.5	54.9	52.8
	100	12.0	23.3	247	20.6	11.2	30.6	301	26.9	6.6	-24	-23

3.4 Discussion

In the present study, we assessed the efficacy of spatially distributed sequential stimulation (SDSS) in comparison to the traditional FES using a single electrode stimulation (SES) with respect to the time to fatigue (TTF), maximum produced force (MPF), and average produced force until fatigue (APF) at moderate and high electrical stimulation intensities. The objective of each experimental session was to evaluate the efficacy of SDSS at the chosen stimulation intensity by comparing it to SES applied to the contralateral leg. It is important to note that the described protocol was not designed to directly measure the fatigue-reducing capabilities of SDSS compared to SES. Instead, the purpose was to utilize SES as a reference to ensure a fair comparison of the effectiveness of SDSS across multiple experimental sessions. A common challenge encountered when conducting measurements over multiple days is the variation in the subject's strength, influenced by various physiological factors. By utilizing SES applied to the other leg as a reference, the discrepancies in the subject's strength are largely compensated for, as it can be reasonably assumed that both legs would be similarly affected.

Our research focused on the quadriceps muscle group and the Vastus Lateralis (VL) muscle of subjects with spinal cord injury (SCI). Our findings elucidated that the superior performance of SDSS over SES is considerably compromised for quadriceps muscle group under high-intensity modality. On average, the percentage increase in TTF observed during moderate-intensity stimulation was 2.80-fold greater than the corresponding value observed during high-intensity stimulation. Furthermore, in terms of the percentage increase in MPF and APF, the moderate-intensity modality exhibited a 4.47-fold and 4.3-fold greater increase, respectively, compared to the high-intensity modality. The superior performance of SDSS over SES is generally attributed to the higher current density and the asynchronous recruitment of motor units. Applying the same amount of current to a smaller area creates a higher current density allowing for the resulting electrical fields to reach deeper regions. Asynchronous activation of adjacent motor units at a lower stimulation frequency (12 Hz instead of 48 Hz in this study) allows for longer rest periods for the individual motor units resulting in greater fatigue resistance of SDSS compared to SES. However, higher stimulation intensities generate stronger electrical fields beneath the electrodes, resulting in excessive recruitment of overlapping motor units. Consequently, this situation resembles the configuration of SES, leading to heightened fatigue of the overlapping motor units. To the best of our knowledge, while this phenomenon has been previously observed [69], it has never been investigated directly. Schmoll et al. conducted a study involving SCI individuals performing knee extension tasks and found no significant difference in terms of fatigue resistance between four different distributed stimulation configurations and single electrode stimulation configuration. They postulated that a certain amount of spillover could potentially account for these findings [69]. In a study conducted by Sayenko et al., a similar SDSS configuration to the current work was employed and compared to SES in 2-minute fatiguing isometric tests. They discovered that the mean peak torque during the initial 5 stimulations was not significantly different between SDSS and SES in both able-bodied and SCI individuals [73]. This observation could be attributed to the relatively high stimulation intensities utilized in both protocols, which diminishes the alternating stimulation effect of SDSS.

The primary objective of Experiment 2 was to examine the impact of the high intensity on the efficacy of SDSS compared to SES in individual muscles where the number of accessible motor points is limited, thereby potentially compromising the efficacy of the alternating recruitment strategy. In contrast to the findings from Experiment 1, our results obtained from the Vastus Lateralis muscle did not exhibit a significant difference between moderate and high-intensity modalities in terms of $\%TTF_{Difference}$, $\%MPF_{Difference}$, and $\%APF_{Difference}$. One possible explanation for this outcome could be attributed to the relatively large intensity chosen for the moderate tests. Given the relatively low output force of the Vastus Lateralis muscle and the presence of muscle weakness in individuals with spinal cord injuries (SCI), such intensity selections were inevitable to ensure meaningful stimulation responses. Furthermore, in certain subjects, instances of co-contraction of the Rectus Femoris muscle were observed. This phenomenon may be attributed to the relatively high stimulation intensities used and to the large size of the cathode electrode. The selection of electrode size for the Vastus Lateralis tests requires careful consideration due to the potential for inadvertently stimulating the motor fibers responsible for knee flexion, consequently inducing antagonistic stimulation of the thigh muscles. This delicate and sensitive nature of electrode sizing necessitates precise electrode placement and control to specifically target the intended muscle group and minimize any unintended activation of opposing muscle actions. Conducting further investigations with a larger sample size and repeating the tests using smaller electrodes on a muscle where co-activation of antagonistic muscles is less likely (e.g., Tibialis Anterior) could potentially elucidate the underlying cause for this observed outcome.

In contrast to previous studies [55]–[63], the electrodes employed in both SDSS and SES tests were kept identical in size and shape (4 cathodic electrodes) to prevent inadvertent errors in electrode placement and adherence. To provide further clarification, previous investigations utilized a single large electrode for SES, while employing four smaller electrodes to cover the same area as SES in SDSS. However, the curved edges of the small electrodes used in SDSS result in an unequal overall coverage area compared to the size of the large single electrode used in SES. Additionally, when utilizing a large single electrode, the heterogeneous nature of skin resistance can facilitate the preferential passage of electrical currents through more conductive regions, potentially influencing the outcomes in terms of recruited motor points and subsequently affecting fatigue and force generation. The utilization of four smaller electrodes ensures a uniform distribution of electrical charge among the electrode set. Further investigation is warranted to explore the potential disparities in fatigue and force outcomes between the utilization of four smaller electrodes and a single large electrode during SES. Our future research aims to address this knowledge gap and provide a comprehensive understanding of the implications associated with electrode configuration on fatigue and force generation.

3.5 Conclusion

The study showed that the stimulation intensity has a significant impact on the efficacy of SDSS compared to SES. The superior performance of SDSS over SES is significantly compromised when applying high electrical stimulation intensity to the paralyzed quadriceps muscle groups. The output power increase and the fatigue-reducing ability of SDSS are more pronounced in moderate-intensity conditions than in high-intensity conditions. These findings contribute to the understanding of the mechanisms behind SDSS and form the basis for the assessment of applications of SDSS for performing functional tasks.

4 SDSS Applied to the Paralyzed Quadriceps Muscles while Performing Motor-assisted FES Cycling – a Case series

Abstract

In isometric and isokinetic studies, spatially distributed sequential stimulation (SDSS) was proven to be better than the traditional FES that uses a single electrode stimulation (SES) in terms of fatigue-reducing ability and the power output produced by the muscles. The present case series aims to systematically assess the power output and fatigue-reducing properties of SDSS versus SES applied to the paralyzed quadriceps muscles of subjects performing motor-assisted FES cycling task. Four subjects without lower-limb motor function participated in two multiday experimental sessions. Each experimental session involved two stimulation phases, one with SDSS and one with SES stimulation. The stimulation parameters and the electrode configuration for SDSS and SES were chosen based on the results from the previous chapter. Muscles stimulated with the SDSS setup produced considerably higher overall mean power values in all subjects in all experimental sessions while inducing a similar amount of muscle fatigue. One subject experienced slightly more fatigue while three subjects showed slightly better fatigue resistance with the SDSS setup. The results of the present study strongly suggest that SDSS is superior to SES when applied to paralyzed muscles of subjects performing FES cycling task. Further research should be conducted with more participants in order to achieve statistical significance.

4.1 Introduction

As discussed in Section 1.4, Section 1.6 and Chapter 3 of this thesis, two primary limitations of FES technology are the rapid onset of muscle fatigue and low power output produced by the stimulated muscles. Subsequently in Section 3.1, we have verified that under isometric electrical stimulation of quadriceps muscles, the use of multiple small electrodes over the motor points instead of one large electrode, combined with sequencing of the electrical stimulation pulses to each of the smaller electrodes surrounding the motor points with equivalent overall stimulation of one individual electrode, so-called single electrical setup (SES), the fatigue and power limitations of FES can be improved. This methodology is referred to as spatially distributed sequential stimulation (SDSS) and presumably prevents the entire muscle from being stimulated with every electrical pulse.

Our previous work also revealed that electrical stimulation intensity can have an effect on the level of improvement demonstrated by the SDSS protocol. Improvements were seen to be less dramatic at higher stimulation intensities, which we interpret as a greater overlap of the electrical fields created by each smaller electrode, thereby repeatedly activating a greater number of muscle fibers, negating the local muscle stimulation distribution created by having multiple smaller electrodes.

Despite the fact that some isometric and isokinetic studies have reported either substantial or slight gains in favor of SDSS versus SES, the benefits of performing a functional task such as FES cycling with SDSS are not clear. During these types of activities, the muscles and motor points are constantly moving relative to the electrodes which are attached to the skin surface and this in turn may negate any benefits observed during isometric and less active highly repetitive movements. To the best of our knowledge, only three studies have investigated the effects of SDSS when performing active FES exercise. Ye et al. [74] have reported that SDSS applied to the quadriceps muscles of able-bodied subjects reduced the muscle fatigue while performing FES rowing. The other two studies [45], [70] were conducted on the quadriceps muscle groups of a single SCI subject in preparation for the Cybathlon (i.e., international sporting event for handicapped individuals) FES cycling race. However, the studies report conflicting results. Baptisia et al. [45] demonstrated better performance of SDSS while Ceroni et al. [70] found SES to be superior. That said, both studies involved multiple varying and uncontrolled parameters and Ceroni et al. were investigating four different stimulation strategies, both of which complicate drawing definitive conclusions.

The aim of the present case series was to systematically assess the power output and fatigue-reducing properties of SDSS versus SES applied to the paralyzed quadriceps muscles of subjects without lower-limb motor function, performing a controlled motor-assisted FES cycling task. Our previous isometric study (Chapter 3) allows us to have an in-depth understanding of the influence of the electrode placement and the stimulation parameters on the performance of SDSS. With this knowledge, we have designed a systematic study protocol to determine if SDSS provides similar benefits seen in isometric studies when applied to performing FES cycling exercises. As nearly all FES stationary cycling exercise devices are equipped with motor assistance to help prolong

the exercise experience for individuals who do not have enough strength to cycle only with FES, we have conducted our experiments under motor-assisted conditions. This also helps us to conduct the experiments in a systematic way under constant speed conditions.

4.2 Methods

4.2.1 Subjects

Three adult male subjects with lower-limb motor-complete spinal cord injury and one adult male with multiple sclerosis (MS) participated in the study. The subject with multiple sclerosis (P4) cannot produce voluntary muscle contractions in the lower limbs. All subjects had previous experience with FES of the studied muscles, three of whom had participated in our previous study involving SDSS (Chapter 3). In an effort to mitigate the effects of residual fatigue, all subjects were asked to refrain from using FES for at least 48 hours before each experiment was conducted. The exclusion criteria stipulated that the subjects must not have sustained lower limb fractures within the past year or have open wounds or rashes on the skin surface where the electrodes would be placed. More information about the subjects is provided in Table 4.1 and Table 4.2.

Table 4.1: The demographic and clinical characteristics of subjects with the spinal cord injury.

Subjects	Age	Injury	ASIA	Time after spinal cord injury (years)	Previous FES experience	Current FES training
P1	46	C7-C8	B	11	Yes	No
P2	30	C5-C6	B	6	Yes	Yes
P3	59	C6-C7	A	6	Yes	Yes

Table 4.2: Clinical characteristics of the subject with multiple sclerosis.

Subject	Age	EDDS	MS type	Disease duration (years)	Previous FES experience	Current FES training
P4	38	8	Progressive	11	Yes	No

4.2.2 Measurement instrumentation

The experiments were performed on the instrumented cycling ergometer platform (ICEP) [75]. The wall-mounted platform consists of a modified bicycle frame carrying force-torque measuring pedals, a magnetic ring encoder and a motorized actuator system. The actuator system was designed to assist the subjects with maintaining a constant cycling cadence which can be set using a custom-made LabVIEW program. Each pedal measures all three components (x-y-z axis) of the force and torque applied to their surface, as well as the inclination angle of the pedal in reference to the crank arm. Measured forces, paired with the crank angle data acquired with the ring encoder are saved in a text file for later processing. For more details about the ICEP system, refer to Chapter 2.

Subjects were seated on a modified recumbent tricycle (Carbontrikes, Bandhagen, Sweden) with their legs firmly attached to the force-measuring pedals using modified leg orthoses (Hase Bikes, Waltrop, Germany). The trike was secured to the cycling platform with a retractor system. The distance between the trike and the platform

was measured to ensure an identical sitting position for each subject between the experimental sessions. An illustration of the experimental setup is provided in Figure 4.1.

A PC-controlled 8-channel MotiMove stimulator [48] (3F-Fit Fabricando Faber, Belgrade, Serbia) was used to deliver asymmetric biphasic pulses to the paralyzed quadriceps muscles. The stimulator was synchronized with a crank encoder using a data acquisition card (PCI-6009, National Instruments, Austin, TX, USA). A graphical user interface was implemented to set the stimulation parameters, cycling cadence and the crank angle ranges during which the stimulation was applied. SDSS was created by connecting so-called anti-fatigue unit (AFU) devices (3F-Fit Fabricando Faber, Belgrade, Serbia) to the cathodes of two stimulation channels (one per leg). These AFUs distribute the electrical stimulation to the different electrodes.

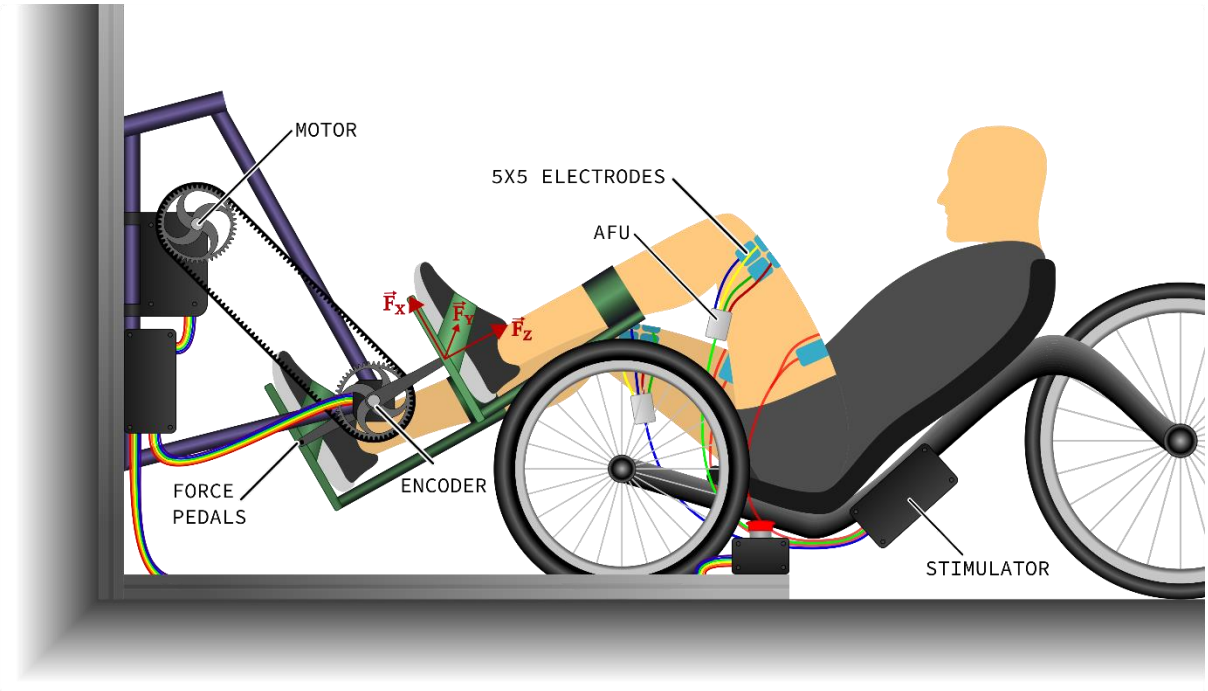

Figure 4.1: Illustration of the experimental setup for the assessment of the power output and fatigue-reducing properties of SDSS versus SES applied to the paralyzed quadriceps muscles of subjects performing motor-assisted FES cycling. The electrode placement and the colors of the wires correspond to the ones used in Figure 4.2. Details concerning the different components and procedures are provided in the text of the manuscript.

4.2.3 Electrode placement

Four self-adhesive surface electrodes (Compex Dura-Stick plus) were placed distally (cathodes) while the reference electrode (anode) was placed proximally over the quadriceps muscle groups. The chosen electrode configuration was identical to the configuration used in the prior isometric study conducted on the quadriceps muscle groups (Section 3.2.3). Before applying the electrodes, the skin was cleaned and proximal and distal motor points of rectus femoris (RF) muscles were found using the measured anatomic landmarks [72]. Motor points

were marked with an indelible marker pen to ensure identical electrode placement across the experimental sessions.

The proximal electrode was made by connecting two electrodes to the anode of the same stimulation channel and thus creating an electrode with an effective surface area of 5 x 14 cm^2. Electrodes used for the anode were a 5 x 5 cm^2 electrode placed on the proximal motor point of RF muscle and a 5 x 9 cm electrode placed laterally, to the side of the 5 x 5 electrode (see Figure 4.2). Distal (cathode) electrodes, with a surface area of 5 x 5 cm^2 each, were placed as close as possible to each other, to form a 2x2 matrix just under the distal motor point of the RF muscle. Positions of the electrodes were confirmed or modified based on visual observations and gentle touch of the muscle contraction resulting from a short train of pulses sent to each electrode separately. In order to minimize fatigue, the pulses used were slightly above the motor threshold. The electrode configuration is illustrated in Figure 4.2.

The described electrode configuration was used for both SDSS and SES. Unlike previous studies that have explored the topic of SDSS, in the SES mode, all four distal electrodes were connected to the cathode of the same stimulation channel effectively making them into one large electrode. This was done to ensure the electrode positioning and the area covered by the electrodes remain absolutely the same during SES and SDSS. In the SDSS mode, each distal electrode was connected to a different output channel of the AFU device.

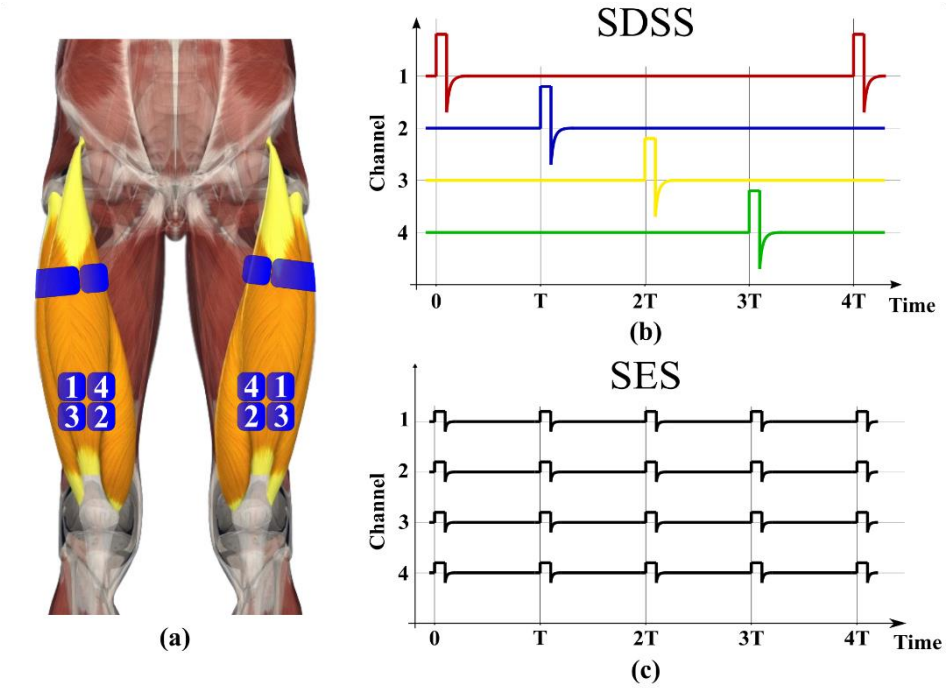

Figure 4.2: (a) An illustration of the electrode configuration used for both SDSS and SES. Stimulated muscle groups are highlighted in orange while the electrodes are colored blue. Distal (cathode) electrodes are labeled in correspondence with the y-axis of the schematics (b) and (c). Schematics represent electrical pulse trains delivered to each electrode (labeled on the y-axis) during four stimulation periods (b) creating the SDSS effect (colors emphasize the fact that different regions of the muscle were stimulated, this study did not investigate the order of which pulses were delivered to the different electrodes), or (c) creating the SES effect.

4.2.4 Stimulation parameters

In our isometric SDSS study (Chapter 3), we found that moderate-intensity SDSS has a more pronounced improvement than high-intensity SDSS in terms of fatigue resistance and power produced. Thus, the electrical stimulation parameters used for SES and SDSS were set identically to the moderate stimulation parameters found in the previous study and were kept constant throughout the experiments. The stimulation pulse width was set to 400 μs and the frequency was 48 Hz for SES and 12 Hz per channel (12 x 4 = 48) for SDSS thus providing a composite frequency of 48 Hz, maintaining coherence in both experimental cases. The moderate stimulation intensity was calculated for each subject as the mean value of their motor threshold and the maximum stimulation intensity restricted to 130 mA. In no case did a subject experience pain during stimulation.

In order to maintain a constant electrical stimulation period for each subject, a crank angle range of 130° for the stimulation period of each set of quadriceps muscles was chosen (note: the motor assistance used is kept at a constant cycling cadence thus ensuring a fixed time-period for the stimulation when the stimulation angle range is fixed). Once the subject is properly positioned, to determine the optimal stimulation patterns (i.e., crank angles for which stimulation is initiated and terminated during the rotation of the crank) that produce the maximum force on the pedals, a comparison between the forces produced during passive cycling (motor-assisted cycling with the cadence of 50 rpm without muscle stimulation) and active cycling (motor-assisted FES cycling at 50 rpm) was made. For active cycling, stimulation pulses of moderate intensity are constantly sent to the muscles over a complete revolution of the crank. We refer to the difference in the force measured between the active and passive cycling over a full revolution as the subject's muscle force profile (MFP) and it represents the forces produced by the stimulated muscle groups on the pedals over the entire crank revolution (more detailed explanation is provided in Section 2.2.2.2). By analyzing the MFP and adhering to the chosen angular range of 130º, the optimal initiation and termination stimulation angles for producing the maximum force from the quadricep muscles is determined (i.e., the 130° angle range was simply overlaid with the MFP for each subject and the intersection of the two were used).

However, to ensure that the muscles are activated at the correct position, the initiation stimulation angle needs to be shifted to compensate for the delay introduced by the system, the electrical stimulator delay and the muscle activation delay. The required angular shift depends on the cycling cadence and it can be calculated using equation 4.1, or it can be directly measured by comparing passive forces and active forces produced by the muscle stimulated between the determined initiation and termination stimulation angles. The required angular shift is the angular difference between the initiation angle and the angle where the muscle produces a noticeable force. The termination angle needs to be compensated only for the delay introduced by the system and the stimulator which can be calculated using equation 4.2.

$$\Delta\theta_i = \frac{(D + D_s + EMD) \times 360}{60}\omega \tag{4.1}$$

$$\Delta\theta_t = \frac{(D + D_s) \times 360}{60}\omega \tag{4.2}$$

where $\Delta\theta$ represents the angular shift [°], EMD is the muscle activation delay [s], D is the delay of the system [s], D_S is the delay of the electrical stimulator [s] and ω is the cycling cadence [rpm]. The required angular shifts were applied to the determined initiation and termination angles to obtain the delay-compensated stimulation pattern. A more detailed description of the method used to determine the optimal stimulation pattern and the delay-compensated pattern is provided in Section 2.2.3 and Section 2.2.4, respectively.

4.2.5 Experimental protocol

Each subject participated in two experimental sessions separated by at least 48h. Within each experimental session, quadriceps muscle groups of both legs were stimulated with SDSS and SES separated by a 15-minute break. To ensure that there was no systematic influence of possible residual fatigue using a certain type of stimulation, the order of stimulation type was chosen at random for the first experimental session and inverted for the second experimental session (i.e., SDSS then SES versus SES then SDSS or SES then SDSS versus SDSS then SES). The cycling cadence was set to 50 rpm.

Preliminary experiments were conducted to ensure equivalent experimental conditions are achieved each day. The stimulation patterns were determined for each subject as described above. To conduct preliminary measurements, we began by determining the moderate stimulation intensity calculated based on the measured motor threshold. Following this step, a 1-minute warm-up (passive cycling) period was carried out. The MFP was then recorded using the calculated moderate intensity, and the optimal stimulation pattern was determined by overlaying the chosen 130° angle range providing the subject's initiation and termination angles for the experiments. After a 10-minute rest period, another 1-minute warm-up was performed followed by the procedure described earlier for measuring the angular shift at a cycling cadence of 50 rpm. The required angular shift was applied and the resulting delay-compensated initiation and termination angles were used throughout the experimental sessions. For each subject, the moderate intensity and the delay-compensated initiation and termination angles were measured before each experimental session to ensure that the sitting and electrode positions were identical between the experimental sessions. A notable difference between the calculated values would indicate that the sitting or electrode position needs to be adjusted.

After a 10-minute break period following the preliminary measurements, the actual experimental session commenced with a 3-minute warm-up phase followed by a 3-minute stimulation phase. During warm-up, the motor passively turned the legs and the electrical stimulation to the muscles was off. The set cycling cadence of 50 rpm was gradually (1 rpm increase per second) achieved in the first minute of warm-up and maintained throughout the rest of the warm-up and stimulation phases (represented by a blue line in Figure 4.3). During the stimulation phase, SES or SDSS was applied to the quadriceps muscle groups while the actuator system, with the motor, assisted with keeping the cadence constant. After a 15-minute break, during which both the motor and the stimulation were off, another 3-minute warm-up and stimulation phases were performed using the stimulation

type that was not applied during the first stimulation phase (SDSS or SES). After at least 48h, the preliminary measurements and the second experimental session were repeated using the inverse order of the stimulation phases. The protocol is illustrated in Figure 4.3.

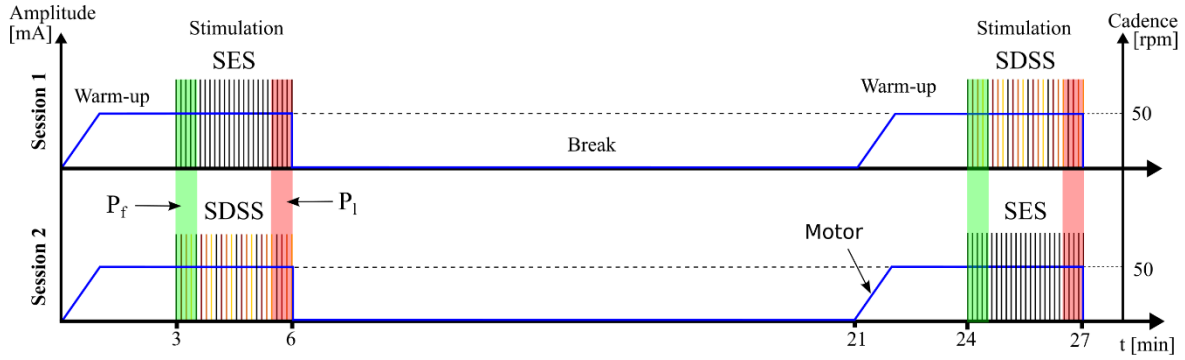

Figure 4.3: An illustration of the experimental protocol. Each subject participated in two experimental sessions involving 3 min warm-up phases, 3 min stimulation phases and a 15-minute break between experimental trials. The x-axis corresponds to the time in minutes. The blue line overlaid on the graph indicates the cadence of the motor assistance, while subsequent vertical lines correspond to electrical stimulation pulses. Vertical colored lines represent SDSS stimulation pulses while the black lines represent SES stimulation pulses. The areas of power produced (P_F) during the first 30 sec are shaded green and red-shaded areas are power produced (P_L) during the last 30 seconds of stimulation.

4.2.6 Data collection and analysis

Power was calculated as the product of the angular velocity, crank arm length and the tangential component of the force (see Figure 2.5) acquired by each pedal. Mean power during each warm-up phase (after the set cadence was reached) was subtracted from the power produced during the subsequent stimulation phase to calculate the power produced only by the electrical stimulated muscles (P). The total mean power (P_m) for each stimulation phase was assessed. As a measure of induced muscle fatigue, a "fatigue index" (FI) was used. Based on the mean power produced in the first (P_F) and last (P_L) 30s of each stimulation phase (Figure 4.3), the fatigue index was calculated according to the following equation:

$$FI = 100 \times \frac{P_F - P_L}{P_F} \ [\%] \tag{4.3}$$

This fatigue index corresponds to the percent muscle fatigue over the 3 min stimulation period, (i.e., FI = 0 means no muscle fatigue while FI = 1 describes completely fatigued muscles.) All data analysis was carried out using Matlab (Mathworks Inc, Natick, MA, USA).

4.3 Results

4.3.1 Overall outcomes

Muscles stimulated with the SDSS setup produced higher overall mean power values for all subjects (an increase of 240% for P1, 88% for P2, 198% for P3 and 116% for P4). The fatigue index indicated slightly better fatigue resistance with SDSS for subjects P1, P3 and P4 but worse for subject P2. The results for each experimental session with all subjects were summarized in Table 4.3. Individual results of the power developed in each experimental session are presented in Figure 4.4, Figure 4.5, Figure 4.6 and Figure 4.7.

Table 4.3. Summary of the results for power produced and the fatigue index of each experimental session along with the overall mean power produced by each subject during both experimental sessions with SDSS and SES stimulations.

Subject	Session	Stim.	P_m [W]	P_F [W]	P_L [W]	FI [%]	Overall power [W]		
							SDSS	SES	%
P1	S1	SES	4.06	10.75	1.80	83.2	10.98	3.23	240
		SDSS	11.80	21.54	6.81	68.4			
	S2	SDSS	10.16	20.14	4.67	76.8			
		SES	2.39	5.92	1.04	82.4			
P2	S1	SDSS	9.65	18.46	5.12	72.2	10.34	5.51	87.8
		SES	4.95	8.24	3.86	53.1			
	S2	SES	6.06	18.49	7.50	59.4			
		SDSS	11.03	17.02	6.82	59.9			
P3	S1	SES	3.61	11.16	0.64	94.3	9.42	3.17	197.6
		SDSS	8.73	16.21	4.65	71.3			
	S2	SDSS	10.11	18.82	4.80	74.5			
		SES	2.72	6.62	1.54	76.8			
P4	S1	SDSS	9.93	21.16	5.46	74.2	11.25	5.22	115.7
		SES	6.03	14.15	3.04	78.5			
	S2	SES	4.40	8.53	3.55	58.4			
		SDSS	12.57	17.63	8.16	53.7			

4.3.2 Individual cases

4.3.2.1 Case 1

Subject P1 had a lesion level C7-C8, AIS B and the injury occurred 11 years prior to the study. The subject had ample experience with FES of the quadriceps muscles as he had participated in the 2016 and 2020 editions of Cybathlon's FES cycling races. Even though not involved in FES strength training at the time of the study, the muscle strength remained high. No co-contractions or muscle spasms were observed or reported by the subject during the measurements. The power produced by the left and right quadriceps muscle groups during the first and the second experimental sessions are shown in Figure 4.4. Stimulation parameters and the results for both experimental sessions are presented in Table 4.4.

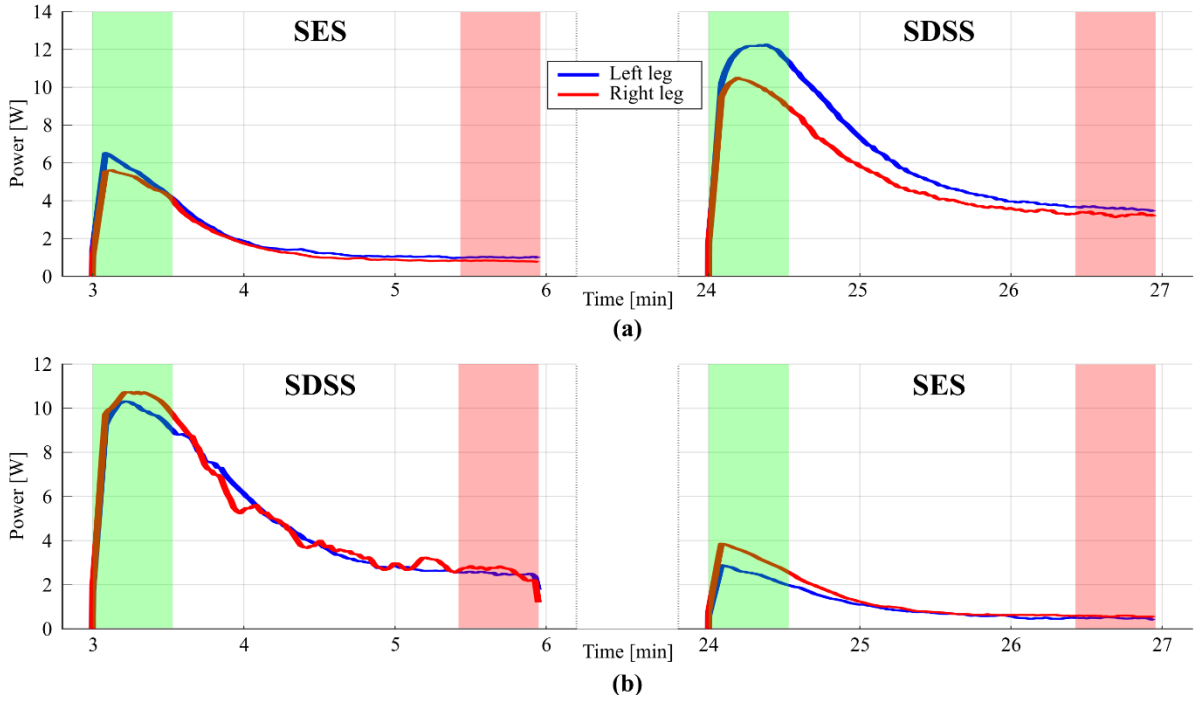

Figure 4.4: Power produced by the subject's P1 left leg (blue) and right leg (red) during each stimulation phase of (a) the first experimental session and (b) the second experimental session. The areas where the power produced during the first (P_F) and the last (P_L) 30 seconds of each stimulation phase are highlighted in green and red, respectively.

Table 4.4. Stimulation intensity and stimulation patterns measured for subject P1 for each experimental session and the results of each stimulation phase presented in chronological order.

Session	Intensity [mA]	Left Angles [º]		Right Angles [º]		Stim.	P_m [W]	P_F [W]	P_L [W]	FI [%]
		Init	Term	Init	Term					
S1	70	198	335	16	153	SES	4.06	10.75	1.80	83.2
						SDSS	11.80	21.54	6.81	68.4
S2	70	194	329	8	143	SDSS	10.16	20.14	4.67	76.8
						SES	2.39	5.92	1.04	82.4

4.3.2.2 Case 2

Subject P2 had a lesion level C5-C6, AIS B and the injury occurred 6 years prior to the study. The subject was undergoing FES-cycling strength training at the time of the study (twice per week). The subject did not perform FES exercise for at least 48 hours before the experimental sessions. Due to the issues with the actuator system, the stimulation intensity used throughout the experimental sessions was lowered from the calculated 70 mA to 60 mA. In both experimental sessions, during the first warm-up phase, spastic leg activations were observed. During the stimulation phases, no muscle spasms were observed or reported by the subject. However, from the power recorded during the first experimental session provided in Figure 4.5 (a), it can be deduced that small spastic contractions occurred. The power produced by the left and right quadriceps muscle groups during

the first and the second experimental sessions are shown in Figure 4.5. Stimulation parameters and the results for both experimental sessions are presented in Table 4.5.

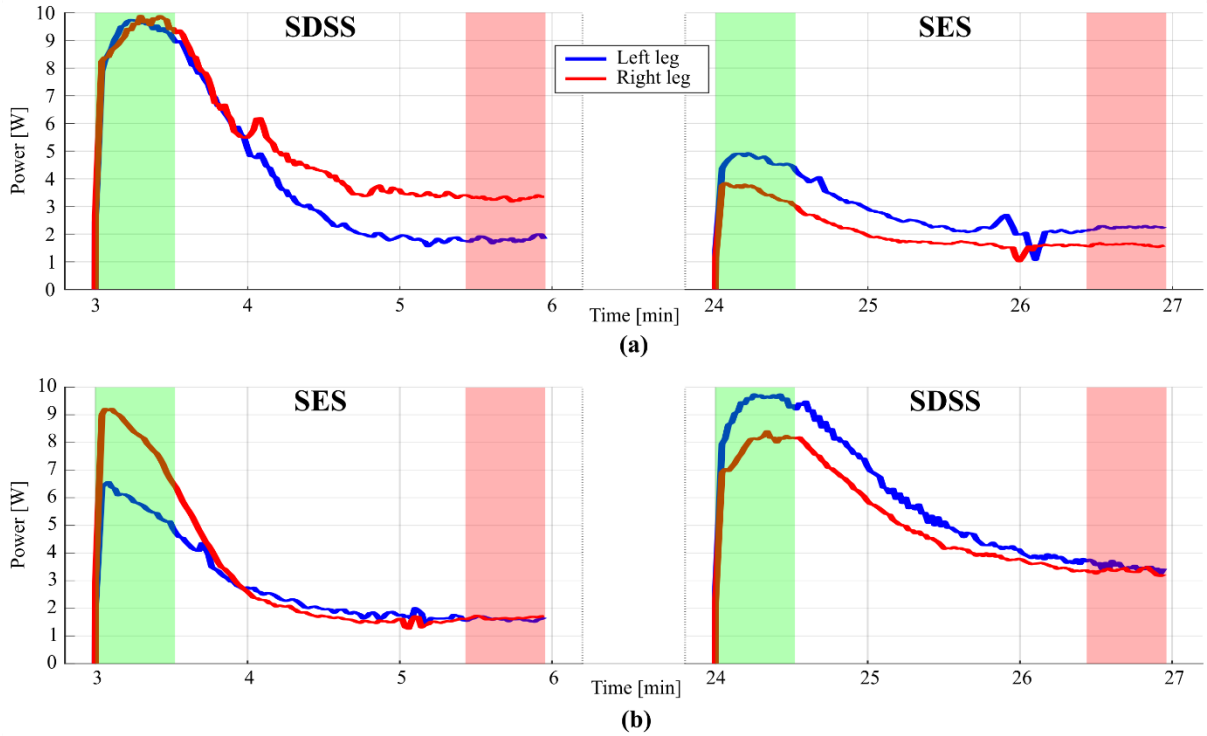

Figure 4.5: Power produced by the subject's P2 left leg (blue) and right leg (red) during each stimulation phase of (a) the first experimental session and (b) the second experimental session. The areas where the power produced during the first (P_F) and the last (P_L) 30 seconds of each stimulation phase are highlighted in green and red, respectively.

Table 4.5. Stimulation intensity and stimulation patterns measured for subject P2 for each experimental session and the results of each stimulation phase presented in chronological order.

Session	Intensity [mA]	Left Angles [º]		Right Angles [º]		Stim.	P_m [W]	P_F [W]	P_L [W]	FI [%]
		Init	Term	Init	Term					
S1	60	190	327	10	147	SDSS	9.65	18.46	5.12	72.2
						SES	4.95	8.24	3.86	53.1
S2	60	193	324	13	144	SES	6.06	18.49	7.50	59.4
						SDSS	11.03	17.02	6.82	59.9

4.3.2.3 Case 3

Subject P3 had a lesion level C6-C7, AIS A and the injury occurred 6 years prior to the study. The subject was undergoing FES-cycling strength training at the time of the study (once per week). The subject did not perform any FES exercise for at least 48 hours before the experimental sessions. No co-contractions or muscle spasms were observed or reported by the subject during the measurements. The power produced by the left and right

quadriceps muscle groups during the first and the second experimental sessions are shown in Figure 4.6. Stimulation parameters and the results for both experimental sessions are presented in Table 4.6.

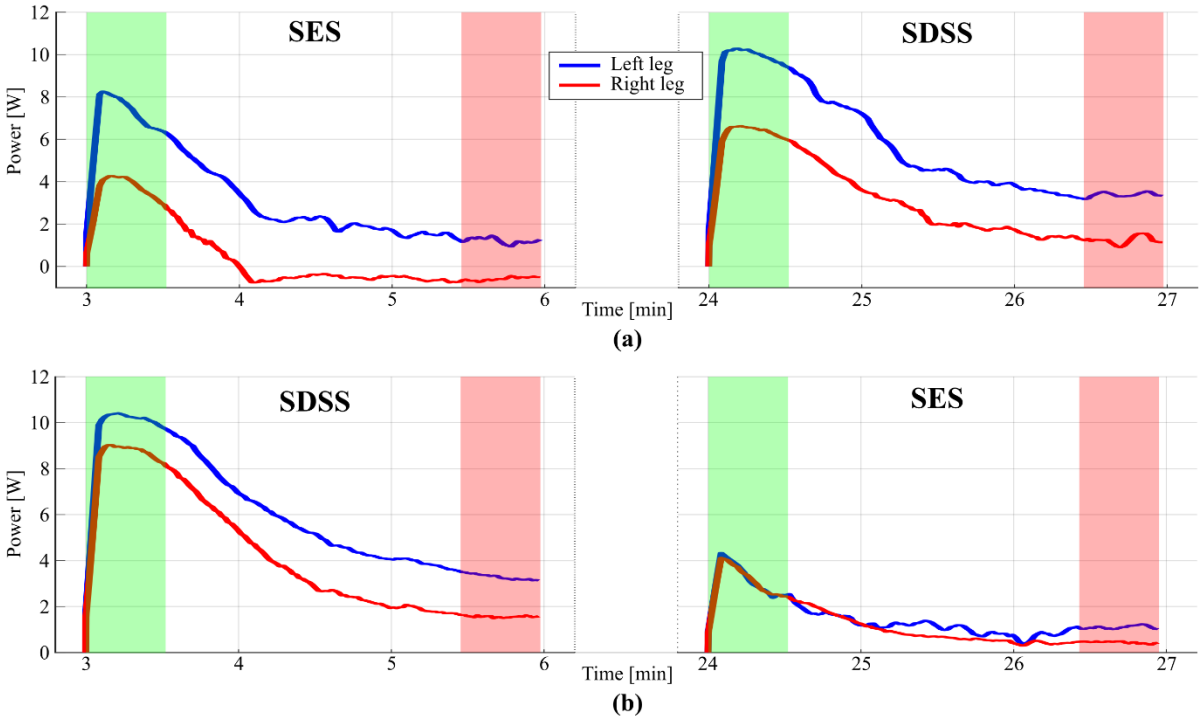

Figure 4.6: Power produced by the subject's P3 left leg (blue) and right leg (red) during each stimulation phase of (a) the first experimental session and (b) the second experimental session. The areas where the power produced during the first (P_F) and the last (P_L) 30 seconds of each stimulation phase are highlighted in green and red, respectively.

Table 4.6. Stimulation intensity and stimulation patterns measured for subject P3 for each experimental session and the results of each stimulation phase presented in chronological order.

Session	Intensity [mA]	Left Angles [º]		Right Angles [º]		Stim.	P_m [W]	P_F [W]	P_L [W]	FI [%]
		Init	Term	Init	Term					
S1	85	145	279	349	123	SES	3.61	11.16	0.64	94.3
						SDSS	8.73	16.21	4.65	71.3
S2	85	143	277	346	120	SDSS	10.11	18.82	4.80	74.5
						SES	2.72	6.62	1.54	76.8

4.3.2.4 Case 4

Subject P4 had multiple sclerosis, an EDDS score of 8. The subject was unable to achieve voluntary muscle contractions in the lower limbs, but some sensory functions remained. The subject had prior experience with FES of the quadriceps muscles but was not involved in FES cycling training at the time of the study. The subject reported a brief spastic activation of the hamstring muscles during the beginning of the second SES stimulation phase. Later analysis showed that the 8-second-long spasm was triggered by the onset of the stimulation. Two

data analyses were conducted, one considering and one disregarding the first 8 seconds of the second SES stimulation phase (results are provided in Table 4.7). In the latter case, the stimulation phase was considered to have begun after the spastic activation of the muscles had been finished, i.e., the stimulation phase was 172 seconds long. The power produced by the left and right quadriceps muscle groups during the first and the second experimental sessions (with discarded spastic muscle activation) are presented in Figure 4.7.

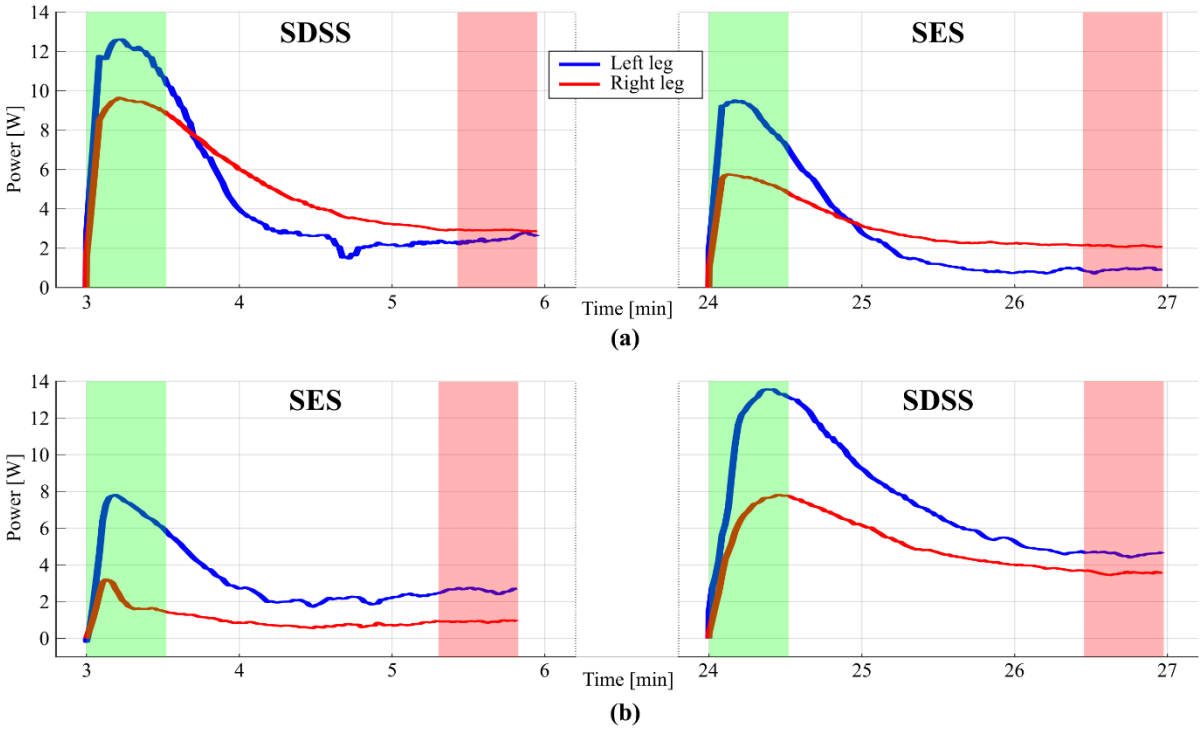

Figure 4.7: Power produced by the subject's P4 left leg (blue) and right leg (red) during each stimulation phase of (a) the first experimental session and (b) the second experimental session. The areas where the power produced during the first (P_F) and the last (P_L) 30 seconds of each stimulation phase are highlighted in green and red, respectively.

Table 4.7. Stimulation intensity and stimulation patterns measured for subject P4 for each experimental session and the results of each stimulation phase presented in chronological order.

Session	Intensity [mA]	Left Angles [°]		Right Angles [°]		Stim.	P_m [W]	P_F [W]	P_L [W]	FI [%]
		Init	Term	Init	Term					
S1	75	165	295	345	115	SDSS	9.93	21.16	5.46	74.2
						SES	6.03	14.15	3.04	78.5
						SES_{SP}	4.54	8.37	3.55	57.5
S2	75	155	285	350	120	SES	4.40	8.53	3.55	58.4
						SDSS	12.57	17.63	8.16	53.7

4.4 Discussion

The goal of the present work was to compare the power output and the fatigue-reducing properties of spatially distributed sequential stimulation versus the traditional single electrode stimulation applied to the paralyzed quadriceps muscle groups of subjects performing motor-assisted FES cycling task. From prior isometric [57], [59], [62], [73], [76] and isokinetic studies [63], [64], [68], better performance of SDSS compared to SES can be expected. However, the only two studies that have compared SDSS to SES with SCI subjects performing FES cycling were reported with contrasting results [45], [70]. Both studies were conducted in preparation for the Cybathlon FES cycling race on the paralyzed quadriceps muscles of a single subject, and in either case was there motor assistance to maintain constant cycling cadence. Although these studies represent a more practical "real-life" test of SDSS application in FES cycling in a racing situation where motor assistance is not allowed, they involve a multitude of varying parameters such as stimulation intensity and cycling cadence which make drawing concrete conclusions more difficult. In that regard, we have designed a protocol to systematically evaluate the efficacy of SDSS versus SES where the number of variables is minimal. Furthermore, our study was designed for FES cycling under exercise and training conditions which have motor-assisted compensation for smooth constant speeds. For instance, stimulation parameters, stimulation time and cycling cadence are kept constant. We also note that an isometric study was conducted to examine the influence of the electrode placement and the stimulation parameters (specifically intensity) on the efficacy of SDSS (Chapter 3). Subsequently, we chose parameters that produced the best results for the present study in order to provide optimal conditions for SDSS. In contrast to the protocol in [45], each experimental session involved both stimulation phases (SES and SDSS) allowing for a direct comparison of the tested stimulation methods, circumventing the common challenge of variations in the subject's strength and seating position over multiday tests.

Under moderate electrical stimulation conditions, quadriceps muscle groups produced considerably more power when stimulated with SDSS compared to SES (from 88% to 240%). This was the outcome of each experimental session, regardless of the subject, the stimulated leg or the order of the stimulation phases (SES then SDSS versus SDSS then SES). When analyzing individual cases, it can be noticed that subject P3 produced negative power with the right leg during a part of the first SES stimulation phase. After closer inspection of the recorded forces, it was observed that the right quadriceps muscle group was completely fatigued, producing little to no force during the crank angle interval where the stimulation was operational. However, during the interval where the muscle was not stimulated, the recorded force did not perfectly match the reference force (force measured during the warm-up phase). We believe that this small discrepancy is most likely caused by a change of position of the leg in reference to the pedal, which appeared as a hindering force that resulted in a negative power value. Another point of discussion is the occurrence of a spastic muscle activation during the second SES stimulation phase of subject's P4 quadriceps muscle groups. After processing the data containing (SES_{SP}) and excluding (SES) the power produced by the spastic activation of the muscles, it was evident that there was no noteworthy difference between P_m, P_F, P_L and FI values (Table 4.7). Thus, it was decided to exclude the first 8 seconds of data from the second SES stimulation phase. There is a possibility that the spastic activity altered the

performance of the muscles. However, it is unlikely that the power produced during the second SES stimulation phase would be augmented to the degree that would impact the overall results of the experiment, especially when considering the results of the first experimental session.

Based on the fatigue index (Table 4.3), one subject experienced slightly more fatigue while three subjects showed slightly better fatigue resistance with SDSS. Coupled with the power produced during the last 30 seconds of each of the stimulation phases P_L, these results suggest that SDSS has better fatigue characteristics than SES. However, further investigation with more subjects is needed to draw statistically supported conclusions.

The overall outcome of the present work was that paralyzed quadriceps muscle groups stimulated with moderate electrical stimulation intensity SDSS produced substantially more power with lower or equal levels of muscle fatigue than the equivalent SES stimulation while performing motor-assisted FES cycling. From the consensus of isometric studies comparing SDSS to SES, better performance of SDSS was expected under the conditions tested. Baptista et al. [45] reported modest benefits of SDSS whereas in the present study, the benefits of SDSS are much greater despite both studies stimulating the same muscle groups with a similar electrode configuration. This result may be due to the contrast in study protocols but the results from Chapter 3 suggest an alternative explanation. In Chapter 3, it was concluded that the efficacy of SDSS drops with the increase in electrical stimulation intensity. Indeed, we used moderate stimulation intensity in Chapter 4 to see if we could favor SDSS over SES during FES cycling conditions. We note, however, Baptista et al. used higher stimulation intensities that were increased as their study progressed. The same reasoning can explain the opposite result (worse performance of SDSS compared to SES) reported by Ceroni et al. [70].

The present study will be carried out with more subjects for statistical relevance. Moreover, using high stimulation intensities when performing FES cycling with SDSS should be investigated as well. Repeating the present study using high stimulation intensities would more rigorously test the performance of SDSS regardless of the stimulation parameters and it would provide new insight into the conclusion reached in Chapter 3.

Additionally, further investigation exploring a more practical use of SDSS applied to FES cycling should be conducted. By using a similar setup in a closed-loop configuration, the output power can be kept constant by altering the stimulation intensity. A protocol design around the aforementioned setup would be similar to most practical uses of FES cycling and it would provide a better assessment of the fatigue characteristics of SDSS. Another important factor for practical use is the electrode placement. Based on previous work (Chapter 3), we have concluded that placing a 2x2 matrix of cathode electrodes just under the distal motor point of the RF muscle is perhaps the optimal electrode configuration for the stimulation of the quadriceps muscle groups. This is supported by the results of the present study and work done by Baptista et al. [45]. However, the exact position for each electrode was found through trial and error. Each electrode was activated separately in order to verify that the muscle achieved a fused contraction. This process requires experience with SDSS and it can take up to 15 minutes which is unreasonable for any clinical or personal use. Further examination of the electrode placement for SDSS applied to FES cycling should be conducted in order to determine more general and simple guidelines for electrode placement.

4.5 Conclusion

The present study demonstrated that, under the right conditions, SDSS can be superior to SES for performing motor-assisted FES cycling. Paralyzed quadriceps muscle groups stimulated with moderate electrical stimulation intensity SDSS produced substantially more power with lower or equal levels of muscle fatigue than the equivalent SES stimulation while performing motor-assisted FES cycling. Further studies should assess the efficacy of SDSS under suboptimal conditions and develop long-term training strategies suitable for clinical use.

5 Knee-angle-based FES cycling control

Abstract

The aim of this work is to address the high price and complexity limitation of FES cycling equipment by separating the stimulation control from the cycling ergometer allowing for the use of any cycling device for FES exercise. A knee-angle-based FES cycling system using a stretch sensor, placed over the knee joint, acquiring the position of the knee, was designed and developed. The system was tested by assessing the forces produced by quadriceps and hamstring muscle stimulation while performing motor-assisted FES cycling on the instrumented cycling ergometer platform. Forces produced by the stimulated muscles were similar for each cycle indicating that the muscles contracted and relaxed at the same crank angles, showing that the system was performing as intended. The present study serves as a proof of concept for using a stretch sensor, instead of the crank encoder, for FES cycling enabling the use of regular cycling ergometers for FES. This will allow for the development of simple and affordable FES cycling systems suitable for home use and thus greatly expand the number of handicapped individuals that will be able to exercise.

5.1 Introduction

Functional Electrical Stimulation (FES) is a method that uses weak electric fields to trigger action potentials, which provoke nerve impulses leading to muscle contractions. When contractions are properly sequenced, the muscle activity can produce movement which has functional outcomes such as: cycling, ambulation, grasp-to-reach and other practical movements. This method is particularly useful to actuate paretic muscles in the physically disabled, allowing them to gain autonomy and improve their health through participation in physical activities. Specific benefits to the patients resulting from this activity are increased cardiovascular fitness, metabolic influences by means of increases in capillary activity and increased glucose metabolism, decrease of muscle atrophy, recovery of bone mass and improvement in range of movement. Of the different possible physical activities available, cycling has emerged as one of the easiest to implement and the cited benefits can be achieved if the patient can practice the activity on a regular basis: 3 sessions of 30-45 minutes a week [21]. For more information on the benefits of FES and FES cycling, refer to Section 1.4 and Section 1.5, respectively.

Currently, the available cycling ergometers are located in hospitals or specialty physical re-education centers. Unfortunately, not all hospitals have FES cycling ergometers and those that do can only be used by patients that are admitted to the hospital. Additionally, the number of Physical re-education centers that have FES equipment is very limited and they require relatively expensive admission fees. Even when facilities exist, another limiting factor for motor-handicapped individuals is transportation to and from the different locations, which, in many cases is simply impossible particularly when they live in an urban environment. This situation means that patients have very few opportunities to practice FES cycling at the levels needed to achieve health benefits. One solution to these problems is to have a home-based unit that allows the patients to exercise in the comfort of their own homes, but regrettably, the current commercially available FES cycling ergometers are difficult to use without having trained personnel for assistance. Furthermore, they require a large amount of space and are extremely expensive to acquire (10-40 k€). Therefore, adapting a cycling ergometer and fitting it with FES equipment would be a viable option to create an inexpensive home-based FES cycling and offer new possibilities for handicapped individuals to exercise.

In most FES cycling ergometers, the stimulation is controlled based on the crank angle using a preset stimulation pattern. The crank angle is acquired with an encoder placed in the crank of the ergometer. Incorporating a crank encoder into an ergometer is often complicated and expensive making it difficult to adapt to existing systems using commercially available ergometers. Separating the stimulation control from the ergometer would allow for the use of any cycling device enabling the development of cheaper FES cycling equipment.

Inertial measurement units (IMUs) were previously used for gait assessment [77], [78], joint angle measurement [79], [80] and, more recently, for FES cycling control based on the angle of the thigh [39], [40], [42], [81] or the knee joint [82], [83] of the patient. Similarly, stretch sensors have been successfully used for gait

analysis [84], [85] and joint angle measurements [86]–[90] showing promising results compared to the benchmark optical technology historically used. Stretch sensors are flexible sensors that change their electrical properties (most notably resistance or capacitance) when stretched. Given that stretch sensors are cheap, simple to use and designed to be incorporated into clothes, they are a suitable candite to be used for knee angle-based stimulation control of FES cycling.

The aim of this work is to examine the possibility of using a stretch sensor for stimulation control during FES cycling. We have designed and tested an FES cycling system as proof of concept. The designed system is easy to use, can be controlled with a laptop or a tablet and it consists of commercially available components (electrical stimulator, ergometer, leg orthosis and stretch sensor). A list of alternative components is provided making the system easily replicable, robust and relatively affordable.

5.2 Materials and Methods

5.2.1 Material

Electronic stretch sensors are devices designed to measure and monitor the deformation or stretching of materials. These sensors utilize electronic components and principles to detect and quantify changes in length, strain, or displacement. They are typically constructed using flexible materials and incorporate various sensing mechanisms such as resistance, capacitance or piezoresistive elements. When the sensor is subjected to stretching or deformation, the sensing mechanism undergoes a change that can be converted into an electrical signal. This signal is then processed and analyzed to provide information about the magnitude and direction of the applied force or strain. Electronic stretch sensors find applications in a wide range of fields including wearable technology, sports and fitness monitoring, robotics, healthcare, and industrial sensing. They offer the advantage of real-time monitoring and precise measurement capabilities, enabling accurate and reliable tracking of mechanical properties and movements in various materials and systems. The processed signal can be further utilized in various applications such as motion tracking, biomechanical analysis, robotic control of wearable objects and medical monitoring systems.

To acquire the angle of the knee joint in a lower limb cycling motion, a capacitive stretch sensor (Leap Technologies, Aabenraa, Denmark) sewn into a knee brace was used (Figure 5.1). The sensor consists of a 10 cm long elastic fabric with two 6 cm long attachment points that can be sewn in or glued to a garment. The capacitance of the sensor correlates with the amount of stretch of the sensor, increasing as the sensor stretches. In order to connect to other devices, the sensor was equipped with an integrated electric circuit (Leap Technologies, Aabenraa, Denmark) converting the input capacitance into an output voltage. The circuit was placed into the attachment point of the sensor (Figure 5.2) and it outputs an analog voltage between 0V to 5V that linearly changes based on the deformation of the sensor.

Figure 5.1: A photograph of a stretch sensor sewn into a knee brace.

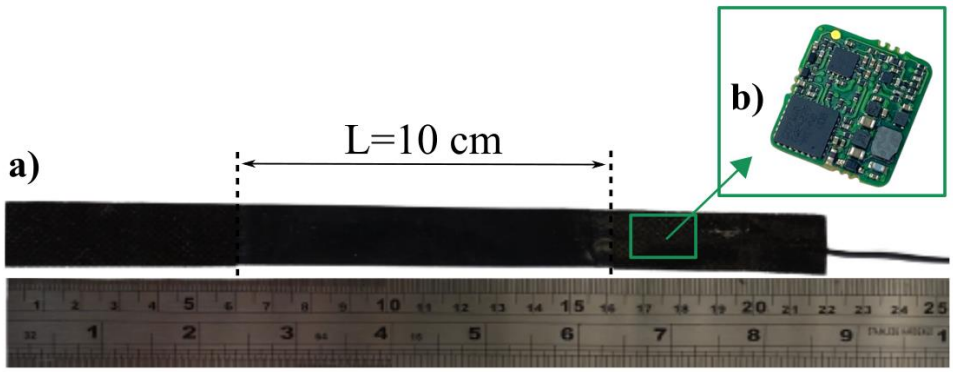

Figure 5.2: a) The capacitive stretch sensor consisting of the 10 cm long elastic fabric and two attachment points are shown with a focus on b) the electric circuit for converting input capacitance into an output voltage.

The sensor is connected to the analog input port of a current-controlled electrical stimulator (MotiMove, 3F-Fit Fabricando Faber, Belgrade, Serbia). The 8-channel stimulator produces asymmetrical biphasic pulses with the following stimulation parameters: pulse amplitude (0–170 mA), pulse width (0–1000 μs) and frequency (0–100 Hz) [48].

5.2.2 Software

In order to communicate with the stimulator and the sensor, graphical user interphase (GUI) was developed using Python 2.7. The GUI (Figure 5.3) allows the user to calibrate the sensor, choose which muscles to stimulate, set start and stop positions for each chosen muscle and set stimulation parameters such as frequency, pulse width and intensity. When set, the stimulation parameters are sent to the stimulator via Bluetooth and stored in the stimulator where the algorithm acquires and processes the sensor data in order to control the stimulation.

5.2.2.1 Calibration

When the knee brace is placed over the knee joint, the material (including the sensor) stretches based on the size of the leg. Additionally, the knee brace can slide or twist on the skin during cycling and therefore change the initial position of the sensor. To compensate for these movements, the sensor is calibrated before and during each rotation. Indeed, with each revolution, the sensor undergoes a maximum and minimum length corresponding to the positional location of the leg. When the leg is totally extended, the sensor is stretched to a minimum position for the particular rotational movement being monitored. When the knee is bent at its minimum angle, the sensor is stretched to its maximum position for the particular rotational movement. These key positions allow us to determine the crank angle when the lower limb muscles are at their critical crank angles for electrical stimulation to produce optimal rotational cycle motion, thus allowing us to calibrate in real time each pedal stroke.

Before setting up the stimulation parameters, the GUI prompts the user to calibrate the sensor by performing one full revolution of the crank, allowing the system to acquire the full range of motion of the knee joint. Maximum (MF) and minimum (ME) values acquired during calibration correspond to the peak knee flexion

and peak knee extension, respectively. These values are saved and used as reference points for the detection of unwanted movement (i.e., change in the initial position) of the sensor during cycling.

5.2.2.2 Stimulation parameters

After the sensor has been calibrated, the stimulation parameters can be set using the GUI (Figure 5.3). The user can select which muscles are stimulated and the start and stop positions for the stimulation of each selected muscle. The start position is selected by placing the leg in the position where the stimulation of the selected muscle should start and pressing the "Start" button. Analogously, the stop position is set and the whole process is repeated for each selected muscle.

Figure 5.3: Snapshot image of the designed graphical user interface (GUI) for the stimulation parameter setup. Four muscles along with the maximum stimulation intensities (in mA) can be selected. Start and stop positions for each muscle can be chosen by placing the leg in the position and clicking the adjacent "Start" or "Stop" button. The horizontal bar in the middle represents the stimulation intensity applied to the muscles as a percentage of the selected maximum stimulation intensity.

5.2.3 Algorithm

Data from the stretch sensor is acquired at 200Hz and processed in real-time to determine if the selected muscles need to be stimulated. The algorithm processing the data consists of three phases:

1. Motion recognition – Determining if the current motion is flexion or extension;
2. Stimulation control – Determining if the current leg position is in the preset range of stimulation;
3. Sensor recalibration – Detecting unwanted sensor sliding/twisting and recalibrating accordingly.

5.2.3.1 Motion recognition

Prior to entering the algorithm, each newly acquired sample is passed through a low-pass filter. For the filtered sample s(n), a gradient is calculated by subtracting a value of the previously acquired sample s(n-1) from the sample s(n). If the gradient is higher than the threshold Th1, the sensor is stretching. If the gradient is lower than the threshold -Th1, the sensor is contracting. Otherwise, the sensor is either not moving or moving extremely slowly which is considered a "neutral" movement. However, the calculated sensor movement can be misleading due to noise or data outliers. To account for this, a direction buffer was introduced. The buffer stores the last seven

movements based on which the direction of the movement (Dir) is determined (similar to the debouncing algorithms used when working with the on/off switches).

As illustrated in Figure 5.4, four motion states can be differentiated based on the Dir variable. While Dir is above the threshold Th2, the sensor is stretching and the knee joint is flexing (Flexion state). When Dir is lower than the threshold -Th2, the sensor is contracting and the knee joint is extending (Extension state). When switching states from Flexion to Extension, the knee joint reaches peak flexion, the sensor is fully stretched and the maximum stretch value is recorded in the Max state. Analogously, when transitioning from Extension to Flexion, the sensor is fully contracted and in the Min state, the minimum stretch value is recorded. The recorded maximum and minimum values of stretch are used in the sensor recalibration phase.

5.2.3.2 Stimulation control

As mentioned in Section 5.2.2, start and stop positions (i.e., initial and final crank angles) for each muscle group are chosen by the user. In the stimulation control phase, the current lower limb motion state (Flexion or Extension) and the newly acquired sample s(n) are used to determine which muscle groups should be stimulated. The muscle is activated if the sample s(n) is in between the start and stop values selected for that muscle and if the motion state is correct (i.e., Extension for left quadriceps (QL) and right hamstring (HR) or Flexion for left hamstring (HL) and right quadriceps (QR)). We note that the quadriceps muscles push the crank away from, while, the hamstring muscles pull the crank toward the rider, to produce the rotational movement.

5.2.3.3 Sensor recalibration

For each 360° rotation of the cycle, the maximum and the minimum values of the stretch sensor are recorded and used to determine if the sensor has moved from the initial position on the knee (i.e., the position of the stretch sensor was used during the initial calibration phase). If in two subsequent cycles, either the maximum or the minimum value deviates by more than 5% from the ME or MF values obtained during the calibration phase, the sensor is considered to be out of position. In that case, the sensor is recalibrated by setting the maximum and minimum values as the new ME and MF values. The start and stop positions (i.e., crank angles) for each selected muscle are proportionally shifted based on the change in the ME and MF values and therefore compensated for the unwanted movement of the sensor. For example, if the new MF value changes the range of motion (MF-ME) by 10%, the start and stop values will be changed by 10% relative to the ME value.

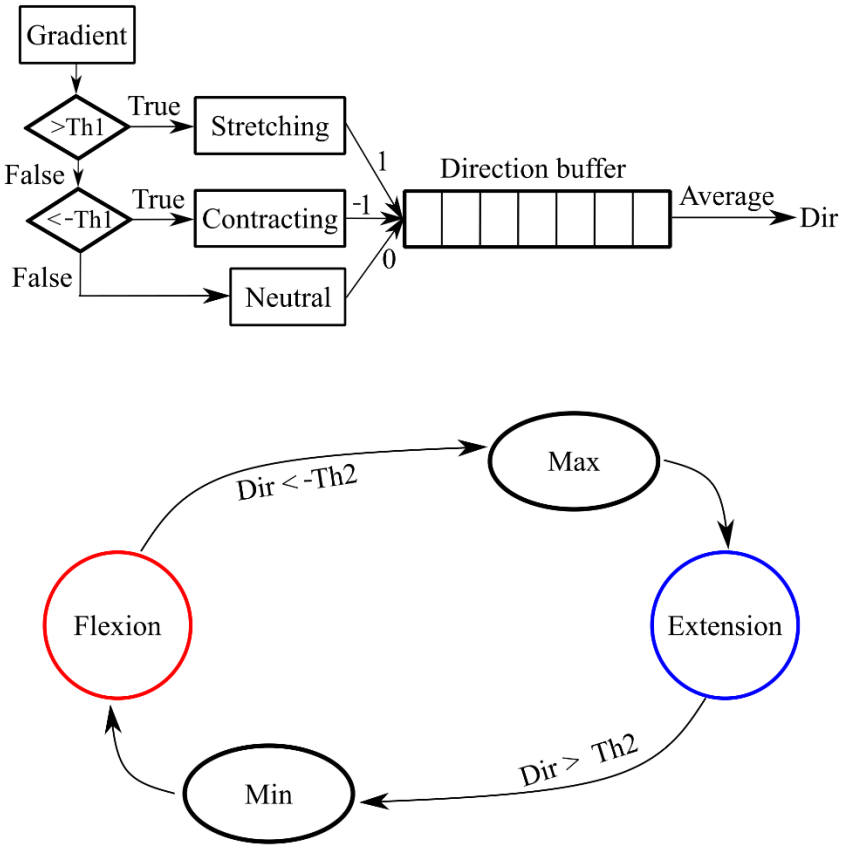

Figure 5.4: The top section of the figure shows the decision algorithm for determining the direction of movement of the sensor based on the calculated gradients and the preset threshold (Th1). The bottom part of the figure illustrates the state machine with Flexion and Extension states in which the selected muscles are stimulated. The states change based on the determined direction of movement of the sensor and the preset threshold (Th2).

5.2.4 Experimental setup

5.2.4.1 Subject

To test and verify the correct operation of the device, one 61-year-old male subject with a motor-complete SCI (lesion level C5-C6, ASIA B) participated in the present study. The injury occurred 9 years prior to the study. The subject had previous experience with FES cycling and as such was able to provide valuable feedback on the ease-of-use and comfort of the device relative to more expensive encoder-based FES devices.

5.2.4.2 Measurement instrumentation

The stretch sensor was tested with respect to an encoder-based system, on a custom-built instrumented cycling ergometer platform [75]. The platform consists of a modified bicycle frame fitted with force/torque measuring pedals, a crank encoder and a motor. The pedals measure all components of the force and torque applied

to their surface while a magnetic ring encoder acquires the crank angle. The cycling cadence can be set from within a custom-made LabVIEW (National Instruments, Austin, TX, USA) graphical interface, with values ranging from 1 rpm to 100 rpm.

5.2.4.3 Experimental Protocol

The subject was seated in his wheelchair with the legs secured to the force-measuring pedals using modified leg orthoses (Hase Bikes, Waltrop, Germany). A knee brace with a sewn-in stretch sensor was placed on the subject's left knee (Figure 5.5). Using one stimulation channel per muscle group, stimulation was delivered through 9 × 5 cm electrodes (Dura-Stick Premium, Chattanooga, UK) located over the motor points of the quadriceps and hamstring muscle groups. Based on the prior experience working with the subject, stimulation parameters for each channel were set to 100 mA intensity, 350 µs pulse width and 40 Hz frequency.

The experiment consisted of an initialization phase followed by two stimulation phases. The stretch sensor was calibrated and the start and stop positions for the stimulation of the quadriceps and hamstring muscles were chosen. The recording portion of the experiment began after the initial 2-minute passive cycling warm-up phase (motor passively turning the legs without electrical stimulation).

The cycling cadence increased from 10 rpm to 50 rpm in steps of 10 rpm. For each cadence, 5 to 10 passive cycles were performed followed by active cycling (motor-assisted FES cycling). In the first phase, active cycling consisted of quadriceps stimulation while in the second phase, both quadriceps and hamstring muscle groups were stimulated.

5.2.4.4 Data processing

During both phases, the output voltage from the stretch sensor was recorded along with the crank angle and the forces exerted on the pedals. The accuracy of the stretch sensor compared to the crank encoder was quantified using the RMS error:

$$RMSE = \sqrt{\frac{1}{n}\sum_{i=1}^{n}\left(\theta_{enc}(i) - \theta(i)\right)^2} \tag{5.1}$$

where θ_{enc} is the crank angle measured by the crank encoder, θ is the crank angle calculated based on the output voltage of the stretch sensor and n is the number of samples acquired during one full cycle. Forces produced by the muscle stimulation is calculated by subtracting the forces produced during passive cycling from the forces produced during active cycling.

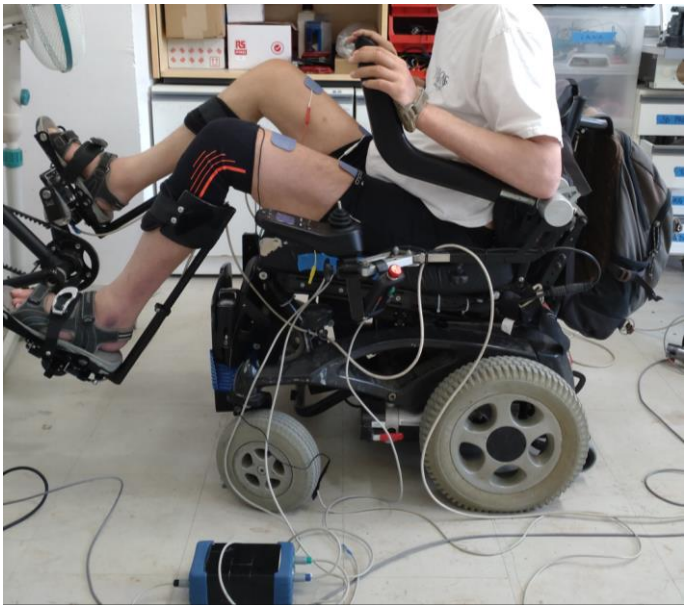

Figure 5.5: Photographic image of the test subject performing motor-assisted FES cycling with the stretch sensor placed on over the left knee.

5.3 Results

In Figure 5.6, the raw output voltage from the stretch sensor (red) and the crank angle (blue) for cycling cadence of (a) 10 rpm, (b) 30 rpm and (c) 50 rpm are presented. RMSE of the filtered output voltage of the stretch sensor was 3°, expressed in the degrees of the crank angle. Figure 5.7 is a representation of the torque produced by the stimulation of the left and the right quadriceps muscles during multiple cycles of knee-angle-based FES cycling. Figure 5.8 provides a graph of the torque produced by the stimulation of the left and the right quadriceps and hamstring muscles during one cycle of knee-angle-based FES cycling.

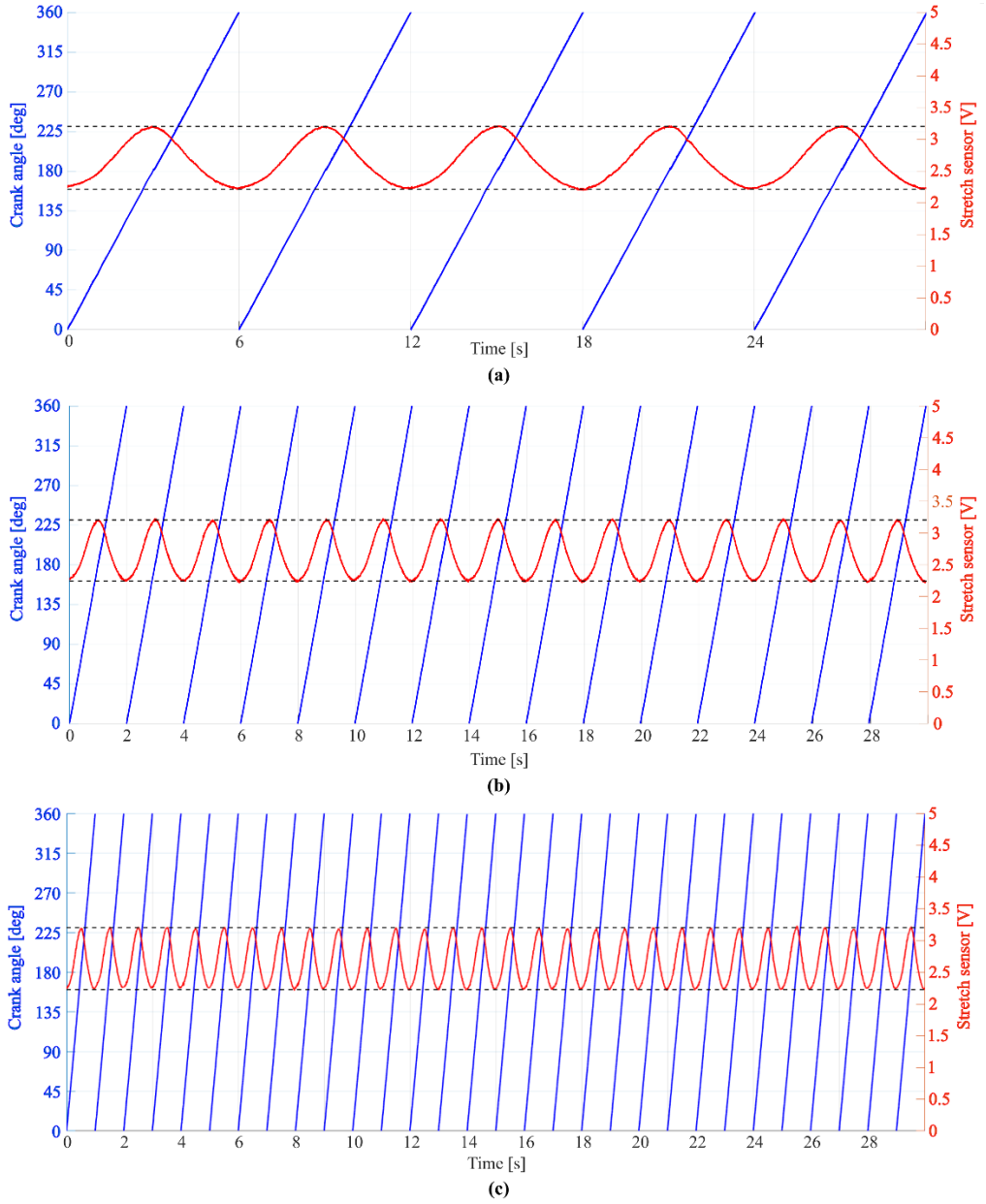

Figure 5.6: The output voltage from the stretch sensor (red) and the crank angle (blue) recorded during motor-assisted cycling at (a) 10 rpm, (b) 30 rpm and (c) 50 rpm. The left y-axis corresponds to the crank angle in degrees while the red y-axis corresponds to the output voltage of the stretch sensor in volts.

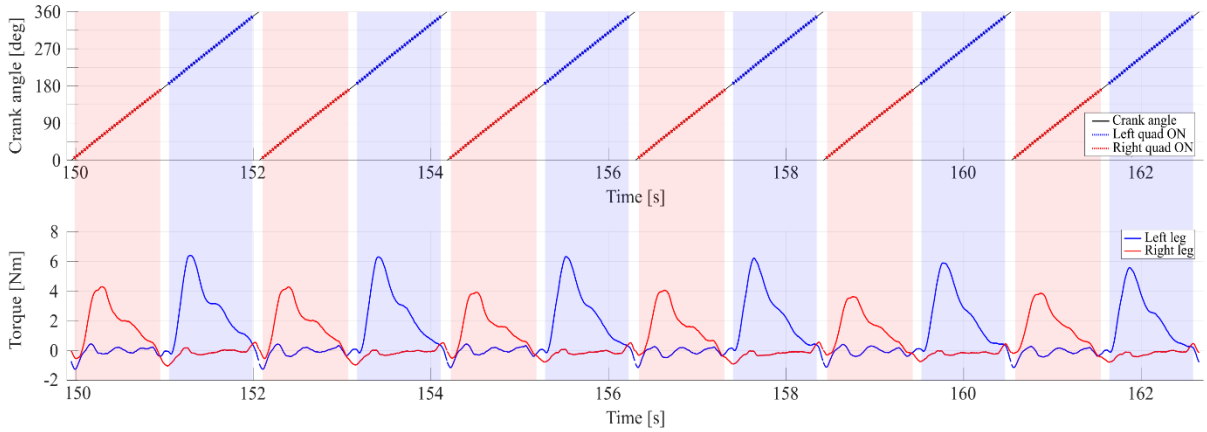

Figure 5.7: The bottom graph represents the torque produced by the stimulated quadriceps muscle groups of the left (blue line) and right (red line) leg during six full revolutions of the crank while performing motor-assisted knee-angle-based FES cycling at 30 rpm. The top graph shows the crank angle (black) in time with the dotted blue and red lines illustrating the crank angle range for the stimulation of the left and right quadriceps, respectively.

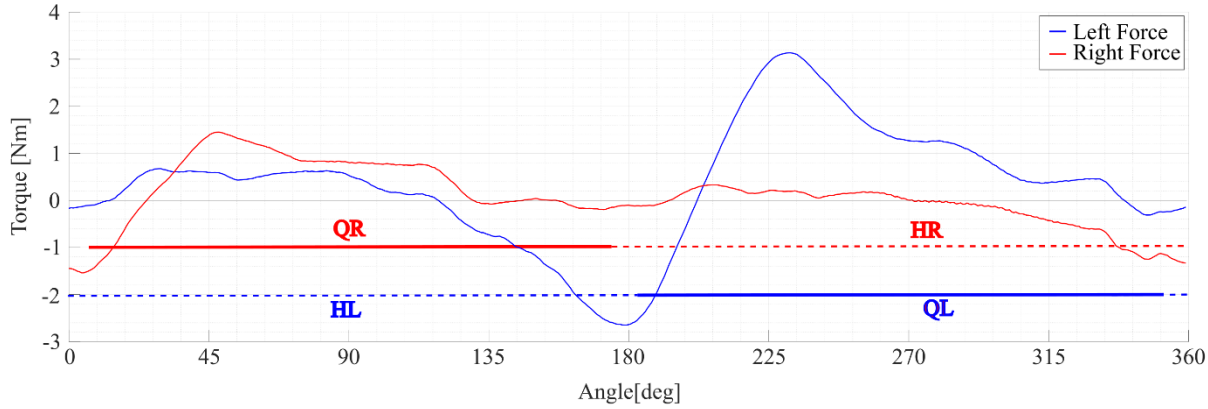

Figure 5.8: Torque produced by the stimulated muscles of the left (blue) and right (red) leg over a full crank revolution. Crank ranges over which the right quadriceps (QR) and left quadriceps (QL) muscle groups are stimulated are marked with a full line while the crank ranges over which the right hamstrings (HR) and left hamstrings (HL) muscle groups are stimulated are marked with a dashed line.

5.4 Discussion

One of the primary aims of this work is to investigate the feasibility of a novel method for the control of FES cycling based on the knee angle acquired with a wearable stretch sensor. The stretch sensor was compared to a high-resolution magnetic, ring crank encoder at different cycling cadences and the system was tested on a laboratory-based instrumented cycling platform.

The calculated RMSE does not exceed 3º showing that the stretch sensor can be used to assess the position of the leg with adequate accuracy for cycling cadences of up to 50 rpm. Forces produced by the stimulated quadriceps muscles (Figure 5.7) are similar for each cycle (i.e., the muscles contract and relax at the same crank angles), showing that the system is performing as intended). However, the stimulation pattern chosen for the hamstring muscles was too long. The stimulation should have stopped before the muscle produced forces resisting the cycling motion (Figure 5.8). This however was not introduced by the use of the stretch sensor and could be corrected with a better choice of the stimulation patterns.

The developed system requires some prior experience or knowledge of FES cycling as the user is expected to set the start and stop positions for the stimulation of each muscle allowing for the setup of custom and more accurate stimulation patterns. However, including a default stimulation pattern based on certain events [39] such as full knee extension or flexion would make the system more accessible for people without FES cycling experience.

Quadriceps muscles produce the majority of the force during FES cycling. Hamstring muscles are also often stimulated in FES cycling as they provide knee flexion. However, since they also provide hip extension, electrode positioning and muscle activation timing are important for achieving the “best” intended movement. Including the stimulation of the gluteal muscles would contribute to cycling and benefit the patient without introducing complexity. Furthermore, setting a default stimulation pattern for gluteal muscles would be straightforward and the electrode positioning would be less crucial than for the hamstring muscle group.

A drawback of the system is that the knee brace holding the stretch sensor does not fit every leg size. Instead, there are four knee brace sizes available. The knee brace needs to be tightly wrapped around the knee so that the sewn-in sensor stretches as the knee flexes or extends. Therefore, for the best fit, the stretch sensor should be attached to the knee brace chosen by the user. However, the stretch sensor could be incorporated into an FES garment equipped with surface electrodes [14], [91] which would allow for FES-cycling with minimal setup requirements from the user.

The present case study serves as a proof of concept for using a stretch sensor, instead of the crank encoders for FES cycling thus allowing for the development of an FES cycling ergometer from any existing cycling device. This allows for the use of regular cycling ergometers for FES cycling which are more widespread, smaller and cheaper compared to the purpose-built FES cycling ergometers. By applying this concept, a simple and affordable

FES cycling system suitable for home use can be built, greatly expanding the number of handicapped individuals that will be able to exercise.

5.5 Low-cost FES cycling options for home use

5.5.1 General description

Figure 5.9 provides an image of a typical low-cost FES cycling system that can be built using our proposed methodology. The patient remains seated in their wheelchair without having to transfer to a separate unit. The cycling ergometer is a typical motorized pedaling system that is designed for home use and there are numerous manufacturers and online stores where these types of devices can be purchased. Similarly, different leg support systems are available and can be chosen to be adapted to each individual's needs depending on size, comfort and level of support required. Once an ergometer and leg supports are acquired, the system can be outfitted with an electrostimulation unit and synchronization element that permits the stimulator to actuate the appropriate leg muscles (quadriceps, hamstrings, glutes) to drive the cycling motion.

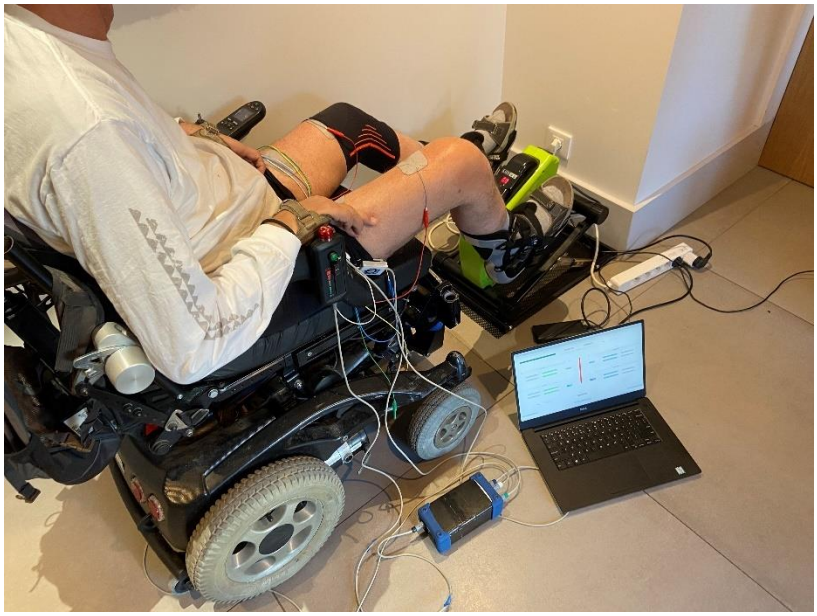

Figure 5.9: A photograph of an individual using a low-cost FES cycling ergometer built with commercially available devices that can be used to exercise in the comfort of their home and rehabilitate paralyzed lower limbs.

5.5.2 Commercially available stimulators

Some commercially available stimulators have recently been suggested by Alam et al. [92] and are listed in Table 5.1. In most cases, the price is not available and one must contact the manufacturer for more details. That said the prices of stimulators have drastically been falling and it is now reasonable to obtain cost-affordable stimulators for individuals. All of the simulators are easily incorporated into the electronics of simple cycling ergometers. If an individual requirement calls for a stimulator classified as a medical device the price of the stimulator will be more costly, however, recent master theses by Derungs et al. [93] and Wang et al. [94] provided

all the information needed to have a reputable electronic manufacturer to produce high-quality safe instruments. Currently, although there exist hundreds of low-cost transcutaneous electrical neurostimulators (TENS) that have been used for years without notable injury to individuals, legislative bodies are restricting the medical device labeling for stimulators that are typically used in FES devices. This unfortunately restricts the availability of FES exercise equipment that is so desperately needed for motor handicapped individuals.

Table 5.1. List of commercial FES electrical stimulators provided by Alam et al.

Name	Company	Country	Approval	Mode	Channels	Power	Price
Biostim-5	Cosyma Inc.	Russia	N/A	Current	5	Battery	N/A
NeoStim-5		USA	N/A	Current	5	Battery	N/A
ARC_{EX}[17]	ONWARD Medical Inc.	Netherlands Switzerland	FDA	Current	4	Battery	N/A
Stimulette r2x	Dr Schuhfried Medizintechnik GmbH	Austria	N/A	Current	2	Line	N/A
SCONE™	SpineX Inc.	USA	FDA	Current	2	Battery	N/A
SCiP				Current	2	Battery	N/A
DS8R	Digitimer Ltd	UK	CE	Current	1	Line	£8,335
OpenXstim		Australia	Un-approved	Voltage	1	Battery	A$66.6

6 Summary and future prospects

The overall aim of this thesis was to address the limitations of functional electrical stimulation (FES) cycling, particularly concerning patients with spinal cord injury (SCI), i.e., to postpone the onset of muscle fatigue and augment the power produced by the paralyzed muscles during FES cycling. Moreover, a novel knee-angle-based control method, combined with off-the-shelf equipment for FES cycling, was proposed in order to make FES cycling exercising more universal and less expensive, and thus more accessible to a greater number of people.

In order to achieve this aim, an instrumented cycling ergometer platform was developed. This platform was equipped with force-torque measuring pedals, a magnetic ring encoder and a motorized assistance system designed to help the subject maintain a constant and smooth cycling cadence. This cycling platform enabled us to systematically assess novel FES cycling strategies. The capabilities of the platform were showcased by allowing us to determine optimal stimulation patterns which were employed in subsequent fundamental electrical stimulation studies. In particular, the platform was used as an indispensable tool to carry out precise studies to investigate the effects of spatially distributed sequential stimulation SDSS (Chapter 4) and variable-frequency trains [95] applied to the paralyzed quadriceps muscles of SCI subjects performing FES lower-limb cycling. In our future studies, this experimental platform will facilitate our work to determine the effects of electrical stimulation intensity variation based on the muscle force profile and/or the optimization of the sitting position of the cyclist while performing FES cycling [96]. However, one major improvement we propose to increase the platform capabilities is to provide a feedback control system for maintaining a preset value of the power produced by the stimulated muscles. Such a system would allow us to conduct a large variety of studies including studies designed to specifically assess fatigue and more closely simulate FES cycling racing conditions. As the platform is height adjustable, another expansion of its capacities is the inclusion of hand cycling. Adapting the pedals to the force-measuring system will introduce the possibility of performing upper-limb FES cycling studies. One open question we wish to answer is: what are the optimal positions of the hands and wrists to better understand which muscles can be used and optimized for competitive hand cycling and rehabilitation of the upper limbs?

In our present studies of isometric and isokinetic movements of the quadriceps muscles, we showed that the use of SDSS postpones the onset of electrically stimulated muscle fatigue and augments the power produced by the stimulated muscles compared to conventional FES that uses single electrode stimulation (SES). First, an isometric study was conducted in order to determine the effects of different stimulation intensities and electrode placements on the efficacy of SDSS. The study showed that the superior performance of SDSS over SES is more significant at moderate electrical stimulation intensities (order of 75 mA) than in high-intensity conditions (130 mA). These findings support the hypothesis that with the increase of the stimulation intensity, the electric fields produced by each SDSS-activated electrode overlap the regions of the other electrodes used, thus activating a greater number of muscle fibers more frequently (as with SES) and diminishing the intended effect of SDSS. However, a similar experiment performed on a single muscle, where the number of accessible motor points is limited (m. vastus lateralis), did not provide a significant difference between the high and moderate electrical stimulation intensities, possibly because of the relatively high intensities chosen for the moderate-intensity

conditions and the co-activation of antagonistic muscle groups. Conducting further investigations with a larger sample size and repeating the tests using smaller electrodes and lower stimulation intensities, on a muscle where co-activation of antagonistic muscles is less likely (e.g., Tibialis Anterior), could potentially further our understanding of SDSS and shed light on this discrepancy. In a future study intended to more fully understand the electric fields created by the surface electrodes during stimulation, particularly in the SDSS configuration, we are developing a method that uses gel birefringence and fluorescently labeled probes to visualize the electrical fields created between the electrodes placed on a physical model of the human leg.

After concluding that SDSS increased the efficacy of the stimulated quadriceps with respect to muscle fatigue and output power under isometric conditions, we tested SDSS versus SES under dynamic muscle cyclic movements. To achieve this, we examined the performance of subjects with paralyzed quadriceps muscles while performing motor-assisted FES cycling. In these tests, we systematically assessed performance under moderate stimulation intensity conditions. In each experimental session, quadriceps muscles stimulated with SDSS produced substantially more power with lower or equal levels of muscle fatigue compared to the equivalent SES stimulation. The study showed that under our test conditions, SDSS can be superior to SES for performing motor-assisted FES cycling but a larger sample size is needed for statistical relevance. Conducting further investigations and exploring a wider range of parameters (i.e., electrode size and placement, stimulation intensity) of SDSS in FES cycling is needed. Furthermore, designing a study using a closed-loop system, where the output power produced by the stimulated muscles is kept at a preset value while changing the stimulation intensity as the muscle fatigues, would provide a better assessment of the fatigue-reducing ability of SDSS under high-intensity racing conditions. Additionally, determining more general and simple guidelines for the electrode placement is necessary to realistically include SDSS in clinical use.

Finally, to address the high price and the complexity of FES exercise equipment, the possibility of using a stretch sensor for acquiring the position of the knee joint, instead of the conventional crank-angle-based system was examined. Combined with off-the-shelf mass-produced equipment, a prototype of a knee-angle-based FES cycling system was developed and tested. The stretch sensor showed adequate accuracy for measuring the angle of the knee joint when performing cycling at cadences up to 50 rpm, and the forces produced by the stimulated quadriceps and hamstring muscle groups of a SCI subject performing motor-assisted FES cycling showed that muscle contraction timing was identical for each cycle indicating that the knee-angle-based FES cycling system can be successfully used. Further improvements can be made by attaching the stretch sensor to an FES garment [91] making the system easier to don by the user. A comparison of the proposed knee-angle-based system using a stretch sensor to a thigh-angle-based system [39] using internal measurement units (IMUs) should be conducted. However, due to “administrative medical device” requirements both systems are inhibited by the price of the electrical stimulators. Further efforts should be made to design less complex, cheaper stimulators suitable for safe nonprofessional home use as already demonstrated by the high number of transcutaneous electrical stimulator (TENS) devices that already exist on the market for more than 30 years.

7 Bibliography

[1] G. J. Tortora and B. Derrickson, *Principles of Anatomy and Physiology*, 15th Editi. New York: Wiley, 2017.

[2] S. C. Rastogi, *Cell and Molecular Biology*. New Age International, 2003.

[3] "Action potential.svg — Wikipédia." https://fr.m.wikipedia.org/wiki/Fichier:Action_potential.svg (accessed Jun. 27, 2023).

[4] J. Ólafsdóttir, "Muscle Responses in Dynamic Events - Volunteer experiments and numerical modelling for the advancement of human body models for vehicle safety assessment," 2017.

[5] B. MacIntosh, P. Gardiner, and A. McComas, "Skeletal muscle : form and function." Human Kinetics, Champaign, IL, 2006.

[6] "Muscle Contraction 3D - YouTube." https://www.youtube.com/watch?v=GrHsiHazpsw&ab_channel=3DBiology (accessed Jun. 29, 2023).

[7] D. A. Jones and J. M. Round, *Skeletal Muscle in Health and Disease: A Textbook of Muscle Physiology*. Manchester University Press, 1990.

[8] "10.4 Nervous System Control of Muscle Tension - Anatomy and Physiology | OpenStax." https://openstax.org/books/anatomy-and-physiology/pages/10-4-nervous-system-control-of-muscle-tension (accessed Jun. 25, 2023).

[9] D. Popović and T. Sinkjaer, *Control of Movement for the Physically Disabled: Control for Rehabilitation Technology*. 2000.

[10] J. E. Mendoza and A. L. Foundas, *Clinical neuroanatomy: A neurobehavioral approach.* New York, NY, US: Springer Science + Business Media, 2008.

[11] E. M. Marcus and S. Jacobson, *Integrated Neuroscience: A Clinical Problem Solving Approach*. Boston: Kluwer Academic Publishers, 2003.

[12] "Spinal Cord Injury Levels & Classification." https://www.sci-info-pages.com/levels-and-classification/ (accessed Jun. 27, 2023).

[13] "Towards concerted efforts for treating and curing spinal cord injury." https://assembly.coe.int/nw/xml/XRef/X2H-Xref-ViewHTML.asp?FileID=9680&lang=EN (accessed Jun. 27, 2023).

[14] C. Marquez-Chin and M. R. Popovic, "Functional electrical stimulation therapy for restoration of motor function after spinal cord injury and stroke: a review," *Biomed. Eng. Online*, vol. 19, no. 1, p. 34, 2020, doi: 10.1186/s12938-020-00773-4.

[15] L. Romera-De Francisco and S. Jimenez-Del Barrio, "Effectiveness of functional electrical stimulation in stroke patients: a systematic review," *Rev. Neurol.*, vol. 63, no. 3, pp. 109–118, Aug. 2016.

[16] J. B. Scally, J. S. Baker, J. Rankin, L. Renfrew, and N. Sculthorpe, "Evaluating functional electrical stimulation (FES) cycling on cardiovascular, musculoskeletal and functional outcomes in adults with

multiple sclerosis and mobility impairment: A systematic review," *Mult. Scler. Relat. Disord.*, vol. 37, p. 101485, 2020, doi: https://doi.org/10.1016/j.msard.2019.101485.

[17] B. Andrews, R. Gibbons, and G. Wheeler, "Development of Functional Electrical Stimulation Rowing: The Rowstim Series," *Artif. Organs*, vol. 41, no. 11, pp. E203–E212, Nov. 2017, doi: https://doi.org/10.1111/aor.13053.

[18] G. Ye, E. P. Grabke, M. Pakosh, J. C. Furlan, and K. Masani, "Clinical Benefits and System Design of FES-Rowing Exercise for Rehabilitation of Individuals with Spinal Cord Injury: A Systematic Review.," *Arch. Phys. Med. Rehabil.*, vol. 102, no. 8, pp. 1595–1605, Aug. 2021, doi: 10.1016/j.apmr.2021.01.075.

[19] N. Kapadia, B. Moineau, and M. R. Popovic, "Functional Electrical Stimulation Therapy for Retraining Reaching and Grasping After Spinal Cord Injury and Stroke.," *Front. Neurosci.*, vol. 14, p. 718, 2020, doi: 10.3389/fnins.2020.00718.

[20] S. Patil, W. Raza, F. Jamil, R. Caley, and R. O'Connor, "Functional electrical stimulation for the upper limb in tetraplegic spinal cord injury: A systematic review," *J. Med. Eng. Technol.*, vol. 39, pp. 1–5, Sep. 2015, doi: 10.3109/03091902.2015.1088095.

[21] J. W. van der Scheer, V. L. Goosey-Tolfrey, S. E. Valentino, G. M. Davis, and C. H. Ho, "Functional electrical stimulation cycling exercise after spinal cord injury: a systematic review of health and fitness-related outcomes.," *J. Neuroeng. Rehabil.*, vol. 18, no. 1, p. 99, Jun. 2021, doi: 10.1186/s12984-021-00882-8.

[22] C. Wiesener *et al.*, "Supporting front crawl swimming in paraplegics using electrical stimulation: A feasibility study," *J. Neuroeng. Rehabil.*, vol. 17, Apr. 2020, doi: 10.1186/s12984-020-00682-6.

[23] J. S. Petrofsky, C. A. Phillips, R. M. Glaser, and H. H. Heaton III, "System and method for treating paralyzed persons," U.S. Patent No. 4,499,900, Feb. 19, 1985.

[24] M. Laubacher, E. A. Aksöz, I. Bersch, and K. J. Hunt, "The road to Cybathlon 2016 - Functional electrical stimulation cycling Team IRPT/SPZ," *Eur. J. Transl. Myol.*, vol. 27, no. 4 SE-FES Cycling/Cybathlon-Case Reports, Dec. 2017, doi: 10.4081/ejtm.2017.7086.

[25] E. Henneman, G. Somjen, and D. O. Carpenter, "Excitability and inhibitability of motoneurons of different sizes," *J. Neurophysiol.*, vol. 28, no. 3, pp. 599–620, May 1965, doi: 10.1152/JN.1965.28.3.599.

[26] A. E. Aksöz, "Optimising Performance in Paraplegic FES-Cycling by Modulating Stimulation Parameters," ETH Zurich A4 - Riener, Robert A4 - Hunt, Kenneth J., 2018.

[27] "List of bicycle types - Wikipedia." https://en.wikipedia.org/wiki/List_of_bicycle_types (accessed Jul. 06, 2023).

[28] "What Are the Different Types of Bicycles? - Bike LVR." https://bikelvr.com/beginners/types-of-bicycles/ (accessed Jul. 06, 2023).

[29] H.-C. Lo, Y.-C. Hsu, Y.-H. Hsueh, and C.-Y. Yeh, "Cycling exercise with functional electrical stimulation improves postural control in stroke patients.," *Gait Posture*, vol. 35, no. 3, pp. 506–510, Mar. 2012, doi: 10.1016/j.gaitpost.2011.11.017.

[30] D. J. Newham and N. de N. Donaldson, "FES cycling," in *Operative Neuromodulation: Volume 1: Functional Neuroprosthetic Surgery. An Introduction*, D. E. Sakas, B. A. Simpson, and E. S. Krames, Eds. Vienna: Springer Vienna, 2007, pp. 395–402.

[31] K. J. Hunt, J. Fang, J. Saengsuwan, M. Grob, and M. Laubacher, "On the efficiency of FES cycling: A framework and systematic review," *Technol. Heal. Care*, vol. 20, no. 5, 2012, doi: 10.3233/THC-2012-

0689.

[32] D. N. Rushton, "Functional Electrical Stimulation and rehabilitation—an hypothesis," *Med. Eng. Phys.*, vol. 25, no. 1, pp. 75–78, 2003, doi: https://doi.org/10.1016/S1350-4533(02)00040-1.

[33] P. H. Peckham and J. S. Knutson, "Functional Electrical Stimulation for Neuromuscular Applications," *Annu. Rev. Biomed. Eng.*, vol. 7, no. 1, pp. 327–360, Jul. 2005, doi: 10.1146/annurev.bioeng.6.040803.140103.

[34] D. B. Popović, "Advances in functional electrical stimulation (FES)," *J. Electromyogr. Kinesiol.*, vol. 24, no. 6, pp. 795–802, 2014, doi: https://doi.org/10.1016/j.jelekin.2014.09.008.

[35] C. Azevedo Coste and P. Wolf, "FES-Cycling at Cybathlon 2016: Overview on Teams and Results," *Artif. Organs*, vol. 42, no. 3, pp. 336–341, Mar. 2018, doi: https://doi.org/10.1111/aor.13139.

[36] R. Riener, "The Cybathlon promotes the development of assistive technology for people with physical disabilities," *J. Neuroeng. Rehabil.*, vol. 13, no. 1, p. 49, 2016, doi: 10.1186/s12984-016-0157-2.

[37] "ANTS Asso - YouTube." https://www.youtube.com/@antsasso5157/videos (accessed Jul. 06, 2023).

[38] A. Metani, L. Popović-Maneski, S. Mateo, L. Lemahieu, and V. Bergeron, "Functional electrical stimulation cycling strategies tested during preparation for the First Cybathlon Competition – a practical report from team ENS de Lyon," *Eur. J. Transl. Myol.*, vol. 27, no. 4 SE-FES Cycling/Cybathlon-Case Reports, Dec. 2017, doi: 10.4081/ejtm.2017.7110.

[39] B. Sijobert, R. Le Guillou, C. Fattal, and C. Azevedo Coste, "FES-Induced Cycling in Complete SCI: A Simpler Control Method Based on Inertial Sensors," *Sensors*, vol. 19, no. 19. 2019, doi: 10.3390/s19194268.

[40] R. Le Guillou *et al.*, "A Novel Framework for Quantifying Accuracy and Precision of Event Detection Algorithms in FES-Cycling," *Sensors*, vol. 21, no. 13. 2021, doi: 10.3390/s21134571.

[41] E. Ambrosini, S. Ferrante, T. Schauer, G. Ferrigno, F. Molteni, and A. Pedrocchi, "An Automatic Identification Procedure to Promote the use of FES-Cycling Training for Hemiparetic Patients," *J. Healthc. Eng.*, vol. 5, p. 163457, 2014, doi: 10.1260/2040-2295.5.3.275.

[42] M. Schmoll, R. Le Guillou, C. Fattal, and C. A. Coste, "OIDA: An optimal interval detection algorithm for automatized determination of stimulation patterns for FES-Cycling in individuals with SCI," *J. Neuroeng. Rehabil.*, vol. 19, no. 1, p. 39, Jan. 2022, doi: 10.1109/TNSRE.2003.819955.

[43] L. Popović Maneski and A. Metani, "FES cycling in persons with paralyzed legs: force feedback for setup and control," in *13th Vienna FES workshop, September 23rd-25th, 2019*, 2019.

[44] C. Fornusek, G. M. Davis, P. J. Sinclair, and B. Milthorpe, "Development of an isokinetic functional electrical stimulation cycle ergometer.," *Neuromodulation*, vol. 7, no. 1, pp. 56–64, Jan. 2004, doi: 10.1111/j.1525-1403.2004.04007.x.

[45] R. S. Baptista *et al.*, "User-centered design and spatially-distributed sequential electrical stimulation in cycling for individuals with paraplegia," *J. Neuroeng. Rehabil.*, vol. 19, no. 1, Dec. 2022, doi: 10.1186/s12984-022-01014-6.

[46] K. J. Hunt *et al.*, "Control strategies for integration of electric motor assist and functional electrical stimulation in paraplegic cycling: utility for exercise testing and mobile cycling," *IEEE Trans. Neural Syst. Rehabil. Eng.*, vol. 12, no. 1, pp. 89–101, 2004, doi: 10.1109/TNSRE.2003.819955.

[47] E. A. Aksöz, M. Laubacher, R. Riener, and K. J. Hunt, "Design of an isokinetic knee dynamometer for

evaluation of functional electrical stimulation strategies," *Med. Eng. Phys.*, vol. 73, pp. 100–106, 2019, doi: https://doi.org/10.1016/j.medengphy.2019.07.010.

[48] L. Popović-Maneski and S. Mateo, "MotiMove: Multi-purpose transcutaneous functional electrical stimulator," *Artif. Organs*, vol. 46, no. 10, pp. 1970–1979, Oct. 2022, doi: 10.1111/AOR.14379.

[49] J. S. Petrofsky, "New algorithm to control a cycle ergometer using electrical stimulation," *Med. Biol. Eng. Comput.*, vol. 41, no. 1, pp. 18–27, 2003, doi: 10.1007/BF02343534.

[50] R. Trumbower and P. Faghri, "Improving pedal power during semireclined leg cycling," *IEEE Eng. Med. Biol. Mag.*, vol. 23, pp. 62–71, Apr. 2004, doi: 10.1109/MEMB.2004.1310977.

[51] H. J. Hermens, B. Freriks, C. Disselhorst-Klug, and G. Rau, "Development of recommendations for SEMG sensors and sensor placement procedures," *J. Electromyogr. Kinesiol.*, vol. 10, no. 5, pp. 361–374, 2000, doi: https://doi.org/10.1016/S1050-6411(00)00027-4.

[52] R. J. Downey, M. Merad, E. J. Gonzalez, and W. E. Dixon, "The Time-Varying Nature of Electromechanical Delay and Muscle Control Effectiveness in Response to Stimulation-Induced Fatigue," *IEEE Trans. Neural Syst. Rehabil. Eng.*, vol. 25, no. 9, pp. 1397–1408, 2017, doi: 10.1109/TNSRE.2016.2626471.

[53] S. Rampichini, E. Cè, E. Limonta, and F. Esposito, "Effects of fatigue on the electromechanical delay components in gastrocnemius medialis muscle," *Eur. J. Appl. Physiol.*, vol. 114, no. 3, pp. 639–651, 2014, doi: 10.1007/s00421-013-2790-9.

[54] S. Zhou, "Acute effect of repeated maximal isometric contraction on electromechanical delay of knee extensor muscle.," *J. Electromyogr. Kinesiol. Off. J. Int. Soc. Electrophysiol. Kinesiol.*, vol. 6, no. 2, pp. 117–127, Jun. 1996, doi: 10.1016/1050-6411(95)00024-0.

[55] M. Pournezam, B. J. Andrews, R. H. Baxendale, G. F. Phillips, and J. P. Paul, "Reduction of muscle fatigue in man by cyclical stimulation," *J. Biomed. Eng.*, vol. 10, no. 2, pp. 196–200, 1988, doi: 10.1016/0141-5425(88)90100-8.

[56] L. Z. Popović and N. M. Malešević, "Muscle fatigue of quadriceps in paraplegics: comparison between single vs. multi-pad electrode surface stimulation," in *Annual International Conference of the IEEE Engineering in Medicine and Biology Society. IEEE Engineering in Medicine and Biology Society. Annual International Conference*, 2009, vol. 2009, pp. 6785–6788, doi: 10.1109/IEMBS.2009.5333983.

[57] N. M. Malešević, L. Z. Popović, L. Schwirtlich, and D. B. Popović, "Distributed low-frequency functional electrical stimulation delays muscle fatigue compared to conventional stimulation," *Muscle and Nerve*, vol. 42, no. 4, pp. 556–562, 2010, doi: 10.1002/mus.21736.

[58] M. J. Decker, L. Griffin, L. D. Abraham, and L. Brandt, "Alternating stimulation of synergistic muscles during functional electrical stimulation cycling improves endurance in persons with spinal cord injury," *J. Electromyogr. Kinesiol.*, vol. 20, no. 6, pp. 1163–1169, Dec. 2010, doi: 10.1016/j.jelekin.2010.07.015.

[59] R. Nguyen, K. Masani, S. Micera, M. Morari, and M. R. Popovic, "Spatially distributed sequential stimulation reduces fatigue in paralyzed triceps surae muscles: a case study.," *Artif. Organs*, vol. 35, no. 12, pp. 1174–1180, 2011, doi: 10.1111/j.1525-1594.2010.01195.x.

[60] D. G. Sayenko, M. R. Popovic, and K. Masani, "Spatially distributed sequential stimulation reduces muscle fatigue during neuromuscular electrical stimulation," in *Proceedings of the Annual International Conference of the IEEE Engineering in Medicine and Biology Society, EMBS*, 2013, pp. 3614–3617, doi: 10.1109/EMBC.2013.6610325.

[61] R. J. Downey, M. J. Bellman, H. Kawai, C. M. Gregory, and W. E. Dixon, "Comparing the Induced

Muscle Fatigue Between Asynchronous and Synchronous Electrical Stimulation in Able-Bodied and Spinal Cord Injured Populations," *IEEE Trans. Neural Syst. Rehabil. Eng.*, vol. 23, no. 6, pp. 964–972, Nov. 2015, doi: 10.1109/TNSRE.2014.2364735.

[62] D. G. Sayenko, R. Nguyen, M. R. Popovic, and K. Masani, "Reducing muscle fatigue during transcutaneous neuromuscular electrical stimulation by spatially and sequentially distributing electrical stimulation sources," *Eur. J. Appl. Physiol.*, vol. 114, no. 4, pp. 793–804, 2014, doi: 10.1007/s00421-013-2807-4.

[63] M. Laubacher, E. A. Aksöz, S. Binder-Macleod, and K. J. Hunt, "Proximally vs distally placed electrodes in a knee extension task Comparison of proximally versus distally placed spatially distributed sequential stimulation electrodes in a dynamic knee extension task," 2016.

[64] M. Laubacher, A. E. Aksöz, R. Riener, S. Binder-Macleod, and K. J. Hunt, "Power output and fatigue properties using spatially distributed sequential stimulation in a dynamic knee extension task," *Eur. J. Appl. Physiol.*, vol. 117, no. 9, pp. 1787–1798, Sep. 2017, doi: 10.1007/s00421-017-3675-0.

[65] A. J. Bergquist, V. Babbar, S. Ali, M. R. Popovic, and K. Masani, "Fatigue reduction during aggregated and distributed sequential stimulation," *Muscle and Nerve*, vol. 56, no. 2, pp. 271–281, Aug. 2017, doi: 10.1002/mus.25465.

[66] M. J. Wiest, A. J. Bergquist, M. G. Heffernan, M. Popovic, and K. Masani, "Fatigue and Discomfort During Spatially Distributed Sequential Stimulation of Tibialis Anterior," *IEEE Trans. Neural Syst. Rehabil. Eng.*, vol. 27, no. 8, pp. 1566–1573, Aug. 2019, doi: 10.1109/TNSRE.2019.2923117.

[67] M. Laubacher *et al.*, "Stimulation of paralysed quadriceps muscles with sequentially and spatially distributed electrodes during dynamic knee extension," *J. Neuroeng. Rehabil.*, vol. 16, no. 1, Jan. 2019, doi: 10.1186/s12984-018-0471-y.

[68] L. De MacEdo Pinheiro, A. C. C. De Sousa, and A. P. L. Bo, "Comparing Spatially Distributed and Single Electrode Stimulation on Individuals with Spinal Cord Injury," in *Annual International Conference of the IEEE Engineering in Medicine and Biology Society. IEEE Engineering in Medicine and Biology Society. Annual International Conference*, Jul. 2020, vol. 2020, pp. 3293–3296, doi: 10.1109/EMBC44109.2020.9176616.

[69] M. Schmoll, R. Le Guillou, D. Lobato Borges, C. Fattal, E. Fachin-Martins, and C. Azevedo Coste, "Standardizing fatigue-resistance testing during electrical stimulation of paralysed human quadriceps muscles, a practical approach," *J. Neuroeng. Rehabil.*, vol. 18, no. 1, Dec. 2021, doi: 10.1186/s12984-021-00805-7.

[70] I. Ceroni *et al.*, "Comparing Fatigue Reducing Stimulation Strategies During Cycling Induced by Functional Electrical Stimulation: a Case Study with one Spinal Cord Injured Subject," in *2021 43rd Annual International Conference of the IEEE Engineering in Medicine & Biology Society (EMBC)*, 2021, pp. 6394–6397, doi: 10.1109/EMBC46164.2021.9630197.

[71] S. Agotici, K. Masani, and P. B. Yoo, "Computational Study on Spatially Distributed Sequential Stimulation for Fatigue Resistant Neuromuscular Electrical Stimulation," *IEEE Trans. Neural Syst. Rehabil. Eng.*, vol. 29, pp. 2578–2586, 2021, doi: 10.1109/TNSRE.2021.3133508.

[72] A. Botter, G. Oprandi, F. Lanfranco, S. Allasia, N. A. Maffiuletti, and M. A. Minetto, "Atlas of the muscle motor points for the lower limb: Implications for electrical stimulation procedures and electrode positioning," *Eur. J. Appl. Physiol.*, vol. 111, no. 10, pp. 2461–2471, 2011, doi: 10.1007/s00421-011-2093-y.

[73] D. G. Sayenko, R. Nguyen, T. Hirabayashi, M. R. Popovic, and K. Masani, "Method to Reduce Muscle Fatigue during Transcutaneous Neuromuscular Electrical Stimulation in Major Knee and Ankle Muscle

Groups," *Neurorehabil. Neural Repair*, vol. 29, no. 8, pp. 722–733, Sep. 2015, doi: 10.1177/1545968314565463.

[74] G. Ye, P. Theventhiran, and K. Masani, "Effect of Spatially Distributed Sequential Stimulation on Fatigue in Functional Electrical Stimulation Rowing," *IEEE Trans. Neural Syst. Rehabil. Eng.*, vol. 30, pp. 999–1008, 2022, doi: 10.1109/TNSRE.2022.3166710.

[75] P. Kajganic, V. Bergeron, and A. Metani, "ICEP: An Instrumented Cycling Ergometer Platform for the Assessment of Advanced FES Strategies," *Sensors*, vol. 23, no. 7, 2023, doi: 10.3390/s23073522.

[76] L. Z. P. Maneski, N. M. Malešević, A. M. Savić, T. Keller, and D. B. Popović, "Surface-distributed low-frequency asynchronous stimulation delays fatigue of stimulated muscles.," *Muscle Nerve*, vol. 48, no. 6, pp. 930–937, 2013, doi: 10.1002/mus.23840.

[77] D. Renggli *et al.*, "Wearable Inertial Measurement Units for Assessing Gait in Real-World Environments ," *Frontiers in Physiology* , vol. 11. 2020, [Online]. Available: https://www.frontiersin.org/articles/10.3389/fphys.2020.00090.

[78] T. Gujarathi and K. Bhole, "GAIT ANALYSIS USING IMU SENSOR," in *2019 10th International Conference on Computing, Communication and Networking Technologies (ICCCNT)*, 2019, pp. 1–5, doi: 10.1109/ICCCNT45670.2019.8944545.

[79] T. McGrath, R. Fineman, and L. Stirling, "An Auto-Calibrating Knee Flexion-Extension Axis Estimator Using Principal Component Analysis with Inertial Sensors.," *Sensors (Basel).*, vol. 18, no. 6, Jun. 2018, doi: 10.3390/s18061882.

[80] T. Seel, J. Raisch, and T. Schauer, "IMU-Based Joint Angle Measurement for Gait Analysis," *Sensors*, vol. 14, no. 4. pp. 6891–6909, 2014, doi: 10.3390/s140406891.

[81] "SensorStim Neurotechnology GmbH." https://www.sensorstim.de/#research (accessed Jul. 16, 2023).

[82] R. Baptista, B. Sijobert, and C. A. Coste, "New Approach of Cycling Phases Detection to Improve FES-Pedaling in SCI Individuals," in *2018 IEEE/RSJ International Conference on Intelligent Robots and Systems (IROS)*, 2018, pp. 5181–5186, doi: 10.1109/IROS.2018.8594162.

[83] C. Wiesener and T. Schauer, "The Cybathlon-RehaBike: Inertial-Sensor-Driven Functional Electrical Stimulation Cycling by Team Hasomed," *IEEE Robot. Autom. Mag.*, vol. PP, p. 1, Nov. 2017, doi: 10.1109/MRA.2017.2749318.

[84] E. Papi, D. Osei-Kuffour, Y. M. A. Chen, and A. H. McGregor, "Use of wearable technology for performance assessment: A validation study," *Med. Eng. Phys.*, vol. 37, no. 7, pp. 698–704, 2015, doi: 10.1016/j.medengphy.2015.03.017.

[85] E. Papi, Y. N. Bo, and A. H. McGregor, "A flexible wearable sensor for knee flexion assessment during gait," *Gait Posture*, vol. 62, no. April, pp. 480–483, 2018, doi: 10.1016/j.gaitpost.2018.04.015.

[86] S. Poomsalood, K. Muthumayandi, and K. Hambly, "Can stretch sensors measure knee range of motion in healthy adults?," *Biomed. Hum. Kinet.*, vol. 11, no. 1, pp. 1–8, 2019, doi: 10.2478/bhk-2019-0001.

[87] H. Nakamoto, T. Yamaji, I. Hirata, H. Ootaka, and F. Kobayashi, "Joint angle measurement by stretchable strain sensor," *J. Ambient Intell. Humaniz. Comput.*, vol. 0, no. 0, pp. 1–6, 2018, doi: 10.1007/s12652-018-0915-z.

[88] Y. Feng *et al.*, "Dynamic Measurement of Legs Motion in Sagittal Plane Based on Soft Wearable Sensors," *J. Sensors*, vol. 2020, 2020, doi: 10.1155/2020/9231571.

[89] B. Huang *et al.*, "Wearable stretch sensors for motion measurement of the wrist joint based on dielectric elastomers," *Sensors (Switzerland)*, vol. 17, no. 12, 2017, doi: 10.3390/s17122708.

[90] J. H. M. Bergmann, S. Anastasova-Ivanova, I. Spulber, V. Gulati, P. Georgiou, and A. McGregor, "An attachable clothing sensor system for measuring knee joint angles," *IEEE Sens. J.*, vol. 13, no. 10, pp. 4090–4097, 2013, doi: 10.1109/JSEN.2013.2277697.

[91] B. Moineau, C. Marquez-Chin, M. Alizadeh-Meghrazi, and M. R. Popovic, "Garments for functional electrical stimulation: Design and proofs of concept," *J. Rehabil. Assist. Technol. Eng.*, vol. 6, p. 2055668319854340, Jan. 2019, doi: 10.1177/2055668319854340.

[92] M. Alam. "An easy-to-build transcutaneous electrical stimulator for spinal cord stimulation therapy," 03 October 2022, PREPRINT (Version 1) available at Research Square: https://doi.org/10.21203/rs.3.rs-2116817/v1

[93] A. Derungs, C. Dietrich, and K. J. Hunt, "A Wireless Functional Electrical Stimulation System.," *Biomed. Tech. (Berl).*, vol. 58 Suppl 1, Aug. 2013, doi: 10.1515/bmt-2013-4022.

[94] H.-P. Wang *et al.*, "A wireless wearable surface functional electrical stimulator," *Int. J. Electron.*, vol. 104, pp. 1–13, Apr. 2017, doi: 10.1080/00207217.2017.1312708.

[95] "Abstracts from the IFESS 2021 conferences," *Artif. Organs*, vol. 46, no. 3, pp. E33–E210, Mar. 2022, doi: https://doi.org/10.1111/aor.14132.

[96] E. Jafari, E. A. Aksoez, P. Kajganic, A. Metani, L. Popovic-Maneski, and V. Bergeron, "Optimization of Seating Position and Stimulation Pattern in Functional Electrical Stimulation Cycling: Simulation Study," in *Annual International Conference of the IEEE Engineering in Medicine and Biology Society. IEEE Engineering in Medicine and Biology Society. Annual International Conference*, 2022, vol. 2022, pp. 725–731.